

Air Pollution Burden Around the World: Distributions, Inequalities, and the Economic Benefits of Clean Air

Preliminary draft

The latest version of this paper is available at this [link](#).

Angelo dos Santos, Oscar Morales, Jere R. Behrman, Emily Hannum, Fan Wang*

October 7, 2025

Abstract

We construct a globally harmonized, high-resolution dataset combining satellite-based aerosol optical depth (AOD) and population data to document global inequalities in air pollution exposure. By weighting pollution by population shares, we provide one of the first comprehensive assessments of how exposure to air pollution by aerosols varies across and within countries and regions. We find large disparities: populations in Asia face average exposure levels more than three times higher than those in Oceania, and within-country inequalities reach up to 359%. Our analysis reveals compounding inequalities—regions with higher pollution also tend to be poorer, with double-ratio metrics indicating that environmental disadvantage amplifies economic inequality. Finally, we provide the first Global Compensating Equivalent Variation (CEV) estimate for clean air, finding that welfare gains from cleaner air exceed 10% of GDP in many highly polluted areas, underscoring the significant economic and social returns from targeted pollution abatement policies.

*[Angelo dos Santos](#): Population Studies Center, University of Pennsylvania, PA, USA; [Oscar Morales](#): Graduate Group in Demography and Department of Economics, University of Pennsylvania, Philadelphia, PA 19104, USA; [Jere R. Behrman](#): Departments of Economics and Sociology and Population Studies Center, University of Pennsylvania, Philadelphia, PA 19104, USA; [Emily Hannum](#): Department of Sociology and Population Studies Center, University of Pennsylvania, PA, USA; [Fan Wang](#): Department of Economics, University of Houston, Houston, Texas, USA. This paper is part of the project "Climate Risk, Pollution, and Childhood Inequalities in Low- and Middle-income Countries," which is supported by National Science Foundation Grant 2230615 (PI: Hannum)

1 Introduction

Exposure to air pollution has increased drastically across all parts of the world over the past two centuries, but it is only within the last few decades that the scientific community has begun to understand the high risk it poses to human health (Gakidou et al. 2017). Exposure to fine particulate matter in particular, especially to PM_{2.5} pollution, has been implicated in the deaths of millions annually and has been found to be negatively associated with cardiovascular health, cognitive development in children, and even economic productivity (Fisher et al. 2021; Fu, Viard, and Zhang 2021; Odo et al. 2023). Despite its dangers, more than half of the global population remains exposed to hazardous annual average PM_{2.5} concentrations exceeding 35 $\mu\text{g}/\text{m}^3$, significantly higher than the annual average of 5 $\mu\text{g}/\text{m}^3$ the World Health Organization considers safe for human health (Pirlea and Huang 2019; Shaddick et al. 2020; World Health Organization 2021). Taking advantage of a suite of globally comprehensive, high-resolution measurements on pollution and demographic characteristics that have become available in recent years, we construct a harmonized data set that allows us to globally identify which population groups at which locations experience disproportionate exposure to pollution. We see this paper as forming a foundation for more holistic analyses of pollution's effects on humans by providing a globally comparative assessment of unequal pollution exposure, decomposed by regions, countries, and sub-national units.

As mentioned earlier, the topic of human exposure to harmful pollutants has gained a lot of attention in recent years. In the social sciences, there exists a growing literature that leverages existing microdata in certain parts of the world to estimate the effects of pollution exposure on outcomes such as labor market productivity, cognitive and cardiovascular health, and educational attainment, but these analyses are rarely global in scope due to data limitations (Brabhukumr et al. 2020; Gakidou et al. 2017; Odo et al. 2023). Moreover, a rich literature exists on how pollution varies across geography and time, but these analyses have often been similarly constrained by the unavailability of a geographical distribution of the population experiencing this variation, a detail critical in understanding how pollution affects humans (Mehta et al. 2016; Tian et al. 2023). As a result, papers in this domain have often been restricted to conducting regional and national comparisons of pollution exposure using an unweighted mean of existing pollution within each geographic unit of study. This can often cloud possible insights on human exposure by allowing for the inclusion of exceptionally clean or dirty areas

of pollution where ultimately no people may reside. Our paper is one of the first to build on this literature by weighing our measures of pollution by population shares to account for areas where actual exposure occurs. We further take the opportunity to compare population distributions over pollution exposure across regions and countries through population-weighted measures of central tendency, and we also develop measures of pollution inequality within the population-weighted pollution distribution of a given region or country.

We base our analysis on gridded high-resolution global data on pollution and population shares from years around 2010, the year around which globally reliable measures of air pollution, GDP per capita and population are available. Our gridded pollution data contains satellite-based measurements of aerosol optical depth (AOD), the degree to which aerosols, like dust, smoke, and pollutants, prevent light from reaching the Earth's surface (Xiong et al. 2020). We use AOD data rather than more modern PM_{2.5} datasets since this form of data is immediately globally comparable by virtue of the same instrument recording each measurement. In contrast, modern PM_{2.5} datasets are often inadequate for country-to-country or region-to-region comparisons due to heterogeneities in measurement methods across regions and countries and biases introduced from highly uneven and sparse coverage of physical monitoring stations over which these measurements are calibrated to. We combine this with gridded population data derived from national censuses and population register data (CIESIN Columbia University 2018). Using this consolidated data set, we compute the relative burden of air pollution by aerosol facing a population in a particular gridded cell by computing the ratio between a cell's pollution level and the global population-weighted mean pollution level across all available cells and subtracting one, yielding a global overview of how areas of the world differs from the global average percentage-wise; we term this measure "excess burden". We then construct discrete, country-specific population distributions by all cells within a country, defined over these computed percentage-difference measures. We take the mean for each of these country-specific distributions to compare average pollution levels across countries. We run the same analysis again, but with global regions as the unit of aggregation rather than countries.

We find considerable global inequalities in population-weighted air pollution by aerosol exposures. The population in Asia, the continent with the highest level of air pollution by aerosols, faces a mean exposure level that is 3.3 times larger than that faced by the population in Oceania, which has the lowest mean exposure among continents. Looking across regions

within continents, we find that in Eastern Asia, the subcontinental region with the highest level of air pollution by aerosols, the population faces a mean exposure level that is 6.0 times larger than that faced by the population in Australia and New Zealand, which have the lowest mean exposure among subcontinental regions.

In terms of inequalities, across continents, population at the 80th percentile of the continental air pollution by aerosol distribution have between 28% (Europe) to 141% (Africa) greater air pollution by aerosol exposures than the population at the 20th percentile. Across subcontinental regions, the population at the 80th percentile of the regional air pollution by aerosol distribution has between 2% to 208% greater air pollution by aerosol exposures than the population at the 20th percentile. Within countries, the population at the 80th percentile of country-specific air pollution by aerosol distributions has between 0% to 359% greater air pollution by aerosol exposures than the population at the 20th percentile.

Our global compounding pollution-GDP inequality analysis reveals significant inequality in air pollution exposure that is bigger than economic inequality, creating a double burden of environmental and economic inequality. By calculating a double-ratio metric—comparing the ratio of air pollution burden (EPB) to the ratio of Gross Domestic Product (GDP) across different quantile groups—our results demonstrate that regions with higher pollution concentrations are often disproportionately poorer. Globally, the double ratios consistently exceed the benchmark where inequality is proportional, ranging from 2 to 12 across different comparisons, with the most extreme disparities found when comparing the 1st and 99th percentiles. This pattern, which signifies compounding inequality, is most acute in Africa, where the double-ratio reaches approximately 15 for the most extreme quantile groups. While Asia shows a relative amelioration of inequality among the extremes, most regions exhibit a convergence toward proportionality as broader population segments are compared. This highlights that the relationship between pollution exposure and economic development is not uniform, but the overall pattern confirms that environmental disadvantage severely compounds economic disadvantage, particularly in developing regions. These compounding inequalities get smaller when using less extreme quantiles.

Finally, we quantify the potential welfare gains of achieving cleaner air using the Compensating Equivalent Variation (CEV), expressed as the percentage of GDP a location would be willing to forgo. The analysis reveals a strong, non-linear relationship where the economic incentives for pollution abatement are overwhelmingly concentrated in the world's most pol-

luted regions. At the national level, countries in highly polluted Asia and Africa show the largest potential gains, with CEV values frequently exceeding 10% of GDP and reaching 15–20% in some locations, which contrasts sharply with the minimal gains in cleaner continents. The subnational level exposes significant intra-national heterogeneity, with intensely polluted local hotspots in Asia and Africa, driving the national averages, with CEV estimates for the most affected units reaching up to 25% of GDP. This intra-country variation underscores that targeted clean air interventions in highly polluted subnational units would yield disproportionately large returns in social welfare and economic benefit.

2 Data and Methods

2.1 Data and aggregation

Air pollution by aerosols as measured by AOD Aerosols are ensembles of suspended particles present in the Earth’s atmosphere. Atmospheric pollution by aerosols is important to human health and well-being because higher amounts of aerosol particles degrade visibility and can also damage health, especially when there is a higher concentration of PM_{2.5} particles that are smaller than 2.5 micrometers (Jacobson 2002). Aerosol Optical Depth (AOD) is a satellite-based measure that captures the composition, size and concentration of aerosols by measuring the magnitude of atmospheric light reflection and absorption across the globe (Lenoble, Remer, and Tanre 2013). Scaled between 0 to 1, an AOD value that is less than 0.1 indicates crystal clear sky and clear satellite to earth surface visibility. In contrast, an AOD value close to 1 indicates very hazy conditions (NASA Earth Observatory 2024).

We use AOD measurements based on images collected by the TERRA satellite with its MODIS instruments (Xiong et al. 2020), and we access the data via the NASA EarthData data collection, using the OpenDAP protocol (Cornillon, Gallagher, and Sgouros 2003). On each day in a particular year, tracking along TERRA’s orbital path across the globe, we download AOD data at a spatial resolution of 3km × 3km and at all available 5 minute temporal resolution units. For each day, this process generates a vector of latitude-, longitude-, and time-specific AOD measurements.

Within each 1° × 1° longitude–latitude grid (cell), we compute average daily AOD values based on the subset of the daily AOD measurement vector that fall within the geographical boundaries of each cell on that day. Repeating this across days during a year, we generate for

each cell, a vector of average daily AOD measurements. During each year, the length of these cell-specific daily average AOD vectors is equal to the number of days in which valid AOD measurements are available for a particular cell. On some days, there might be no cell-specific AOD measurements due to high cloud fraction and invalid reflectance assumptions (Wang et al. 2021) or due to limited overlaps between the cells and the daily orbital path (Xiong et al. 2020).

Using the cell-specific vectors of average daily AOD measurements from a year, we compute annual average AOD exposures for each cell, first averaging over the days in which cell-specific measurements are available, and then separately averaging over all days after complementing the observed averages with interpolated and extrapolated estimates on days without cell-specific measurements. Due to the concentration of missing AOD data in regions with the least population, our population-weighted AOD distributional results based on the raw data and interpolated and extrapolated data are very similar. Our global inequality results presented in the text are based on annual averages of the raw data.¹

Global gridded population data In conjunction with the cell-specific AOD data, we generate cell-specific global population estimates based on the Gridded Population of the World Version 4 (GPWv4) dataset from the Center for International Earth Science Information Network (CIESIN Columbia University 2018). The GPWv4 data contains population statistics from 241 global economies. Data is sourced in most cases from national and local statistical agencies, and when that is not available, sourced from the United Nations.

The gridded GPWv4 data provides total population estimates at 30 arc-second grids ($\sim 1\text{km}$ at the equator), and is globally disaggregated from official population data at the smallest administrative level available. As an illustration, the dataset contains disaggregated population data from 316,461 Brazilian sectors, 43,878 Chinese townships, 5,967 Indian sub-districts, 774 Nigerian local government areas, and 10,535,212 US census blocks. To allow for the calculation population-weighted AOD data, we aggregate the GPWv4 population estimates up to $1^\circ \times 1^\circ$ longitude–latitude grid, which matches up with the resolution of our cell-specific annual average AOD exposures data.

Due to variabilities in census survey and population register data availability, GPWv4 population data are sourced between the years 2001 and 2015, with the center of the calendar year

1. See Appendix Figure E.1 for a visualization of the number of days in 2010 with AOD measurements across global cells.

distribution at around 2010. Specifically, data from 27% of the economies are based on 2010 census and population register data, 62% and 83% of the economies' data come from within one and three years of 2010, and about 8% of the economies have data sourced from outside of four years of 2010. To appropriately match up the time-frame of the population and AOD data, we use cell-specific annual average AOD exposure data in 2010.

Subnational GDP data We complement global measurements of air pollution by aerosols and population with data on the relative levels of economic development as captured by GDP per capita. Specifically, we use national and subnational from the Gridded global datasets for Gross Domestic Product (Kummu, Taka, and Guillaume [2018](#)), which is based on subnational GDP per capita data from Gennaioli et al. ([2013](#)). The GDP per capita values are adjusted for purchasing price parity and based on 2005 international dollars.

Gennaioli et al. ([2013](#)) collected subnational GDP data from 1569 subnational first-level or equivalent administrative units from the largest 110 economies up to 2010. These economies accounted for 97% of global GDP in 2010. Kummu, Taka, and Guillaume ([2018](#)) augmented the dataset with national GDP data from economies without subnational data, filling in missing subnational GDP values by interpolating based on geographically and temporally neighboring data-points around missing values, and extended the dataset time-frame to 2015 by extrapolating based on trends up to 2010.

Considering jointly the temporal availability of AOD, pollution, and GDP data, we use the 2010 subnational and national GDP per capita estimates from Kummu, Taka, and Guillaume ([2018](#)).

2.2 Population weighted distributional statistics for AOD

Population-weighted AOD distributions To analyze population-weighted air pollution by aerosol distributions, we define a discrete distribution of 2010 annual average AOD values over the set of all populated cells, where the cell-specific population mass is determined by GPWv4-based population estimates from around 2010. Specifically, let s_c be the share of global population in cell c , a_c be the average annual AOD at cell c , and C be the set of all gridded cells where $s_c > 0$. The global population-weighted annual average AOD distribution function, which provides the share of global population experiencing lower than a^* levels of annual

average AOD, is equal to:

$$F(a^*) = P(a < a^*) = \sum_{c \in C} s_c \cdot \mathbf{1}\{a_c < a^*\} . \quad (1)$$

To compare aerosol distributions conditional on regional groupings based on supranational, national, and subnational boundaries, we define $C_r \subseteq C$ as the set of populated cells that intersect with the boundary enclosures of supranational, national, or subnational location r . For boundary data, we use national boundary data available in the GPWv4 population dataset (CIESIN Columbia University 2018), and the subnational boundary data embedded in the subnational GDP data from (Kummu, Taka, and Guillaume 2018). The share of population in cell c conditional on location grouping r is $s_{c,r} = \frac{s_c}{(\sum_{\hat{c} \in C_r} s_{\hat{c}})}$, and the locational AOD distribution function is:

$$F_r(a^*) = P_r(a < a^*) = \sum_{c \in C_r} s_{c,r} \cdot \mathbf{1}\{a_c < a^*\} . \quad (2)$$

Given the locational distribution function, we compute key distributional statistics for each location r . The mean and variance of the location r -specific distributions are

$$\begin{aligned} \mu_r &= \sum_{c \in C_r} s_{c,r} \cdot a_c \\ \text{and } \sigma_r^2 &= \sum_{c \in C_r} s_{c,r} \cdot (a_c - \mu_r)^2 . \end{aligned} \quad (3)$$

The global weighted mean is $\mu_{\text{global}} = \sum_{c \in C} s_c \cdot a_c$. In our empirical analysis, we compute global, continental, regional, national, and subnational population weighted annual mean AOD exposures.

Given the discrete mass distribution over cells, the location distribution function $F_r(a^*)$ is not invertible. Hence, we define the τ^{th} percentile of the locational distribution as the minimum a^* value where the share of population in location r with less than a^* level of annual average AOD is greater or equal to $\frac{\tau}{100}$, specifically:

$$\text{percentile}_r(\tau) = \min \left\{ a^* : F_r(a^*) \geq \frac{\tau}{100} \right\} . \quad (4)$$

Discussions in our empirical analysis focus on location-specific 20th and 80th as well as 10th and 90th percentiles, and use relative percentile ratios as an additional measures for within location

distributional variabilities.

Relative exposure and excess burden To measure relative exposures, we compute what we call excess aerosol burden, $e_{c,\hat{r}}$, which is the percentage deviation between cell-specific AOD value a_c and location-specific AOD value average $\mu_{\hat{r}}$:

$$e_{c,\hat{r}} = \frac{a_c - \mu_{\hat{r}}}{\mu_{\hat{r}}} = \frac{a_c}{\mu_{\hat{r}}} - 1 . \quad (5)$$

When \hat{r} includes all global cells, we have $e_{c,\text{global}}$, the global excess aerosol burden. We also divide weighted mean from location r against that of another location \hat{r} :

$$e_{r,\hat{r}} = \frac{\mu_r - \mu_{\hat{r}}}{\mu_{\hat{r}}} = \frac{\mu_r}{\mu_{\hat{r}}} - 1 . \quad (6)$$

When r is a country and \hat{r} includes all global cells, $e_{\text{country},\text{global}}$ is the country-specific excess aerosol burdens relative to the global mean. A global excess aerosol value of 0 indicates that a location has the same AOD measure as the global mean, and a value of 0.5 or -0.5 indicates that a location's AOD measure is 50 percent greater or smaller than the global mean.

As an additional interpretation of the ratio of the weighted means of a subset over a super-set, $e_{r,\text{global}}$ can also be expressed as:

$$e_{r,\text{global}} = \frac{\overbrace{\left(\frac{\left(\sum_{c \in C_r} s_c \right) \cdot \mu_r}{\mu_{\text{global}}} \right)}^{\text{Location } r \text{ pop-weighted pollution share}}}{\underbrace{\left(\sum_{c \in C_r} s_c \right)}_{\text{Location } r \text{ population share}}} - 1 = \frac{\mu_r}{\mu_{\text{global}}} - 1 . \quad (7)$$

A value of 0.5 or -0.5 for $e_{r,\text{global}}$ indicates that location r 's share of global population-weighted air pollution is 50 percent greater or smaller than location r 's share of global population.

AOD and PM_{2.5} As a satellite-based measure of air pollution by aerosols, AOD measurements increase with greater concentrations of atmospheric particles, including PM_{2.5} particles. While our analysis is focused on the distribution of air pollution by aerosols as measured by AOD, to help provide additional interpretation of our AOD results, in our presentation and discussion of results, we provide results both in AOD as well as in estimated AOD-transformed PM_{2.5} scales.

While AOD captures directly visibility experiences, the best-fitting model that maps between atmospheric aerosol measurements and on-the-ground ambient particulate matter exposure experienced by people is parameterized by heterogeneous topological and meteorological circumstances (Chu et al. 2016; Holben et al. 1998; Van Donkelaar et al. 2016; Yang et al. 2019). Overall, atmospheric-based AOD measures have been found to substantively and positively correlate with ground-based aerosol and PM_{2.5} measurements (Bibi et al. 2015; Bright and Gueymard 2019; Chu et al. 2016), and AOD is often used as a predictor of ambient PM_{2.5} exposures with locally and temporally calibrated prediction functions (Chen et al. 2022; Fu et al. 2018; Yang et al. 2019).

To create a globally consistent and transparent scale, we use a global linear model to relate our AOD estimates to existing global estimates of PM_{2.5}. Specifically, we relate the cell-specific annual average AOD values we derived to global gridded estimates of surface PM_{2.5} concentration derived based on models that use satellite-based AOD measures as inputs and ground-based PM_{2.5} data for calibration and model validation (Hammer et al. 2020). Regressing the PM_{2.5} values from Hammer et al. (2020) on our AOD measures, we find that a bivariate linear model with subregion fixed effects provides a reasonable global fit with an R² of 0.78. We obtain similar fit and estimates when we restrict the data to only populated cells or when we use all available cells, and higher polynomial orders do not significantly improve the fit.

In our results discussions, we also compare the AOD-transformed PM_{2.5} measures to the WHO interim targets for particulate matter air pollution.² These targets are used as guidelines for classifying the severity of PM_{2.5} exposures. The WHO guideline recommends lowering annual average exposure levels to less than 35 µg/m³, 25 µg/m³, 15 µg/m³, and 10 µg/m³ as interim targets 1, 2, 3, and 4.

3 Within and across country distributions of air pollution by aerosols

Combining global AOD measures and population data, we present in this section the overall population-weighted global distribution of air pollution by aerosols. In contrast to prior studies on global population-based inequality in ambient air pollution, which have focused on comparing means across regions and countries (Shaddick et al. 2018; Van Donkelaar et al. 2021; Van Donkelaar et al. 2016), we study global inequalities based by conducting comparisons

2. The report can be found here <https://www.who.int/publications/i/item/9789240034228>

within and across region as well as countries.

3.1 Global distributions

Global dispersion map Figure 1 presents a global map of the relative distribution of air pollution by aerosols in Panel (a). The map matches cell-specific AOD to cell locations. The colors correspond to levels of global excess aerosol burdens—darker shades of green (red) represent greater magnitudes of negative (positive) excess burdens.

The map shows that Asia and Africa have relatively higher levels of air pollution by aerosols. Focusing on countries, India, China, and Pakistan stand out as large countries with areas experiencing high levels of excess aerosol burdens. In contrast, Australia, Mexico, and Argentina are also large economies, but have relatively lower levels of excess aerosol burdens. Additionally, there are variations in the within-country heterogeneities of exposures. For example, locations in the southeastern and northwestern regions of China have high excess burdens, but areas in northern and southwestern China have relative lower levels of excess burdens. In contrast, countries within Western Europe and North America tend to have limited variations concentrated around lower levels of excess burdens.

While the world map provides a useful visualization of the global dispersion of air pollution, it does not show the relative population shares facing these heterogeneous burdens across locations.

Population-weighted distributions across continents In Panel (b) of Figure 1, we present continent-specific air pollution distributions that combine the distributions of population and excess aerosol burdens across cells.

Comparing continents at the extremes, the average individual in Asia is 3.32 times more exposed to air pollution by aerosols than the average individual in Oceania. Asia and Oceania have average excess burdens of 0.26 ($\approx 29.10 \mu\text{g}/\text{m}^3$ of PM_{2.5}) and -0.63 ($\approx 8.76 \mu\text{g}/\text{m}^3$ of PM_{2.5}). This means that Asia's and Oceania's global shares of air pollution by aerosols are 26% larger and 63% smaller than their global population shares, respectively.

Africa has the second highest mean exposure with a approximate average PM_{2.5} value of $19.91 \mu\text{g}/\text{m}^3$, followed by Europe and the Americas at $14.32 \mu\text{g}/\text{m}^3$ and $12.11 \mu\text{g}/\text{m}^3$. Oceania is the only continent with average PM_{2.5} reaching WHO interim target 4, which suggests that a considerable share of the world lives in places where air pollution by aerosol exposures are

above recommended healthy condition levels.

In addition to the means, the Panel (b) of Figure 1 also shows heterogeneities in the population-weighted dispersion of excess aerosol burdens within each continent. The Americas, Europe, and Oceania have distributions with relatively limited variabilities. Europe is the most equal continent in the world where population at the 80th percentile of excess aerosol burden are only 28% more exposed than those at the 20th percentile. In contrast, distributions in Africa and Asia are more dispersed. Populations at the 80th percentile of the aerosol distribution are 141% and 109% more exposed than population at the 20th percentile in Africa and Asia, respectively. Further at the tails, the exposure faced by populations at the 90th percentile of the aerosol distribution are 227% and 185% higher than those at the 10th percentile in Africa and Asia, respectively.

3.2 Distributions across and within regions and countries

In this section, we decompose the global air pollution by aerosol distribution into sub-continental region- and nation-specific components. We present the results in continent-specific Figures 3 to 4. In each figure, Panel (a) presents air pollution by aerosol distributions by sub-continental group (e.g., Northern Africa, East Asia), and Panel (b) highlights the 20th and 80th percentiles and means of country-specific distributions. Both results are based on population-weighted cell-level results.

There are substantial differences in means and variabilities across sub-continental regions. In terms of means, Eastern Asia has the highest mean AOD of 0.66 ($\approx 33.68 \mu\text{g}/\text{m}^3$ of PM_{2.5}), which is just below WHO interim target 1. Australia and New Zealand have the lowest mean AOD of 0.11 ($\approx 7.65 \mu\text{g}/\text{m}^3$ of PM_{2.5}), which has reached WHO interim target 4. In terms of variabilities, the ratios of exposure for populations at the 80th to 20th percentiles for sub-continental regions range between 1.02 to 3.08, and the 90th to 10th percentile ratios range between 1.06 to 4.31.

Inequalities within Africa Figure 3 shows air pollution by aerosol distributions across cells in the Eastern, Middle, Northern, Southern, and Western Africa regions as well as the variation in cell-level measurements within the countries that fall under these regions. Results show substantial heterogeneities in within-region aerosol exposures.

Western Africa has the highest average annual AOD at 0.51 ($\approx 26 \mu\text{g}/\text{m}^3$ of PM_{2.5}), almost

reaching WHO interim target 2. Southern Africa has the lowest average annual AOD at 0.14 ($\approx 9.05 \mu\text{g}/\text{m}^3$ of PM_{2.5}), which exceeds WHO interim target 4.

The most populous African country, Nigeria, has an annual average AOD of 0.56 ($\approx 28.98 \mu\text{g}/\text{m}^3$ of PM_{2.5}), which is behind WHO interim target 2. Nigeria's average exposure level corresponds to a global excess aerosol burden of 0.24, meaning that Nigeria's global share of air pollution by aerosols is 24% larger than its population share. Exposure inequalities are significant within Nigeria—Nigerian population at the 80th (90th) percentile of aerosol distribution are 77% (106%) more exposed than those at the 20th (10th) percentile. One of the least populous countries in Africa, Sao Tome and Principe, has an average annual AOD of 0.47 ($\approx 24.65 \mu\text{g}/\text{m}^3$ of PM_{2.5}), just passing WHO interim target 2. In contrast to Nigeria, relative population exposure percentiles are close to 1 due to the small size of the country.

At 0.66 ($\approx 35.18 \mu\text{g}/\text{m}^3$ of PM_{2.5}), the Congolese population faces the highest average annual AOD in Africa, which lags behind WHO interim target 1. Congo's global share of air pollution by aerosols is 53% larger than its population share. Exposure inequalities are limited within Congo—Congolese population at the 80th (90th) percentile of aerosol distribution are 15% (22%) more exposed than those at the 20th (10th) percentile. In contrast, at 0.09 ($\approx 6.42 \mu\text{g}/\text{m}^3$ of PM_{2.5}), the population in Lesotho faces the lowest average annual AOD average in Africa, which significantly surpasses WHO interim target 4. Lesotho's global share of air pollution by aerosols is 81% smaller than its population share. Exposure inequalities are limited except at the far tails within Lesotho—the Lesothoan population at the 80th (90th) percentile of aerosol distribution are 0% (40%) more exposed than those at the 20th (10th) percentile.

Inequalities within Americas Figure 5 shows air pollution by aerosol distributions for countries in the Caribbean, Central America, Northern America, and South America. Compared to Africa and Asia, distributions in regions in the Americas have limited variabilities.

South America has the highest average annual AOD at 0.22 ($\approx 12.93 \mu\text{g}/\text{m}^3$ of PM_{2.5}). Central America has the lowest average annual AOD at 0.19 ($\approx 11.65 \mu\text{g}/\text{m}^3$ of PM_{2.5}). All regions in the Americas, on average, have reached WHO interim targets 3.

The most populous country in the Americas, the United States of America, has an annual average AOD of 0.19 ($\approx 11.67 \mu\text{g}/\text{m}^3$ of PM_{2.5}), close to reach WHO interim target 4. The US's average exposure level corresponds to a global excess aerosol burden of -0.56, meaning

that the US's global share of air pollution by aerosols is 56% smaller than its population share. Exposure inequalities are important but limited in the US—Americans population at the 80th (90th) percentile of aerosol distribution are 36% (71%) more exposed than those at the 20th (10th) percentile. One of the least populous countries in the Americas, Saint Lucia, has an average annual AOD of 0.21 ($\approx 12.49 \mu\text{g}/\text{m}^3$ of PM_{2.5}). Relative population exposure percentiles is equal to 1 in Saint Lucia.

At 0.34 ($\approx 18.55 \mu\text{g}/\text{m}^3$ of PM_{2.5}), Colombian population face the highest average annual AOD in the Americas, which is behind WHO interim target 3. Colombia's global share of air pollution by aerosols is 24% smaller than its population share. Exposure inequalities are important but limited within Colombia—Colombian population at the 80th (90th) percentile of aerosol distribution are 28% (55%) more exposed than those at the 20th (10th) percentile. In contrast, at 0.10 ($\approx 7.27 \mu\text{g}/\text{m}^3$ of PM_{2.5}), population in Chile face the lowest average annual AOD in the Americas, which achieves WHO interim target 4. Chile's global share of air pollution by aerosols is 77% smaller than its population share.

Inequalities within Asia Figure 2 shows air pollution by aerosol distributions for countries in Central, Eastern, Southeastern, Southern, and Western Asia. Results show substantial heterogeneities in within-region and within-country aerosol exposures.

Eastern Asia has both the highest average levels of exposure and variabilities in exposures, and Central Asian has the lowest. Eastern Asia has an average annual AOD of 0.66 ($\approx 33.68 \mu\text{g}/\text{m}^3$ of PM_{2.5}). Eastern Asian population at the 80th percentile of aerosol distribution are 158% more exposed than those at the 20th percentile, and its population at the 90th percentile of aerosol distribution are 223% more exposed than those at the 10th percentile. Central Asia has an average annual AOD of 0.36 ($\approx 19.49 \mu\text{g}/\text{m}^3$ of PM_{2.5}), reaching WHO interim target 3. Central Asia's population at the 80th (90th) percentile of aerosol distribution are 64% (110%) more exposed than those at the 20th (10th) percentile.

The most populous Asian country, China, has an annual average AOD of 0.7 ($\approx 35.58 \mu\text{g}/\text{m}^3$ of PM_{2.5}), which is behind WHO interim target 1, indicating very hazardous levels of average air pollution by aerosols. China's average exposure level corresponds to a global excess aerosol burden of 0.55, meaning that China's global share of air pollution by aerosols is 55% larger than its population share. Exposure inequalities are large within China—the Chinese population at the 80th (90th) percentile of aerosol distribution are 111% (216%) more exposed than those

at the 20th (10th) percentile. One of the least populous countries in Asia, Qatar, has an average annual AOD of 0.60, which is similar to the level in China. Relative population exposure percentiles are equal to 1 due to the geographical confines of Qatar.

In Asia, populations in Kuwait and East Timor are at the opposite ends of the air pollution by aerosol exposure spectrum. Both countries' relative within country exposure percentiles are close to 1. At 0.99 ($\approx 49.06 \mu\text{g}/\text{m}^3$ of PM_{2.5}), the Kuwaiti population faces the highest average annual AOD in Asia, which is substantially behind WHO interim target 1. In contrast, at 0.17 ($\approx 10.74 \mu\text{g}/\text{m}^3$ of PM_{2.5}), East Timor population have the lowest average annual AOD in Asia, almost reaching WHO interim target 4. In terms of global excess aerosol burdens, Kuwait's share of global ambient air pollution by aerosol is 118% larger than its global population share, and East Timor's air pollution share is 60% less than its population share.

Inequalities within Europe Figure 4 shows air pollution by aerosol distributions for countries in Eastern, Northern, Southern, and Western Europe. Compared to Africa and Asia, distributions in European regions have limited variabilities.

Eastern Europe has the highest average annual AOD at 0.28 ($\approx 15.53 \mu\text{g}/\text{m}^3$ of PM_{2.5}), just reaching WHO interim target 3. Southern Europe has the lowest average annual AOD at 0.21 ($\approx 12.51 \mu\text{g}/\text{m}^3$ of PM_{2.5}), exceeding interim target 3.

The most populous European country, Russia, has an annual average AOD of 0.29 ($\approx 16.39 \mu\text{g}/\text{m}^3$ of PM_{2.5}), which is behind WHO interim target 3. Russia's average exposure level corresponds to a global excess aerosol burden of -0.34, meaning that Russia's global share of air pollution by aerosols is 34% smaller than its population share. Exposure inequalities are significant within Russia—Russian population at the 80th (90th) percentile of aerosol distribution are 67% (130%) more exposed than those at the 20th (10th) percentile. One of the least populous countries in Europe, Iceland, has an average annual AOD of 0.21 ($\approx 12.68 \mu\text{g}/\text{m}^3$ of PM_{2.5}), close to reaching WHO interim target 4. Despite its limited population, there are exposure variabilities in Iceland due to its large geography—Icelandic population at the 80th (90th) percentile of aerosol distribution are 39% (49%) more exposed than those at the 20th (10th) percentile.

Russia has the highest average annual AOD in Europe. In contrast, at 0.15, population in Norway face the lowest average annual AOD in Europe. Norway's global share of air pollution by aerosols is 65% smaller than its population share. Exposure inequalities are limited but

present in Norway—Norwegian population at the 80th (90th) percentile of aerosol distribution are 21% (31%) more exposed than those at the 20th (10th) percentile.

Inequalities within Oceania Figure 6 shows air pollution by aerosol distributions for countries in Oceania, which has a small number of countries dominated in population by Australia, Papua New Guinea, and New Zealand. Melanesia has the highest average annual AOD at 0.20 ($\approx 12 \mu\text{g}/\text{m}^3$ of PM_{2.5}), which is just above WHO interim target 4. As a region, Australia and New Zealand have the lowest average annual AOD at 0.11 ($\approx 7.65 \mu\text{g}/\text{m}^3$ of PM_{2.5}), which exceeds WHO interim target 4. Compared to the rest of the world, all populated cells in Oceania have relative low levels of air pollution by aerosol exposures.

4 Air pollution and GDP per capita inequalities

In this section, we examine the existence of compounding inequality factors affecting subnational units worldwide. Our analysis focuses on the intersection of two critical dimensions of inequality: first, income inequality, measured by GDP per capita in 2010; and second, inequality in exposure to air pollution, measured by a pollution-weighted Aerosol Optical Depth (AOD) index calculated for each subnational unit.

To integrate these two dimensions into a unified measure, we compute a ratio of ratios. This double-ratio is defined as the Excess Pollution Burden (EPB) quantile ratio divided by the GDP quantile ratio. This measure reveals the extent to which inequality in air pollution exposure between quantile groups exceeds (or falls short of) the corresponding income inequality between the same groups. Its purpose is to document the prevalence of compounding inequalities globally, identifying regions where severely unequal pollution burdens coincide with high income inequality.

We calculate the EPB quantile ratio by dividing the EPB of the upper quantile units by the EPB of the lower quantile units. Similarly, the GDP quantile ratio is the average GDP per capita in the upper EPB quantile group divided by the average GDP per capita in the lower EPB quantile group. We calculate this double-ratio across five paired quantile thresholds: below 1st–above 99th (1p tails), below 5th–above 95th (5p tails), below 10th–above 90th (10p tails), below 20th–above 80th (20p tails), and median–below median (50p tails). Figure 7 shows the distribution of EPB and GDP with vertical lines distinguishing the quantile groups described

above.

Figure 8 presents the results of this double-ratio calculation for the different quantile pairs, illustrating the global distribution (8a) and continental distributions (8b). The figures show how these ratios behave by comparing extreme quantile ratios and the all-distribution ratio.

The dashed 45-degree line in the figure represents a critical threshold where the inequality in pollution burden is exactly proportional to the inequality in income. For any quantile group above this line, the EPB ratio exceeds the GDP ratio. This signifies a state of compounding inequality, where the most polluted regions are also disproportionately poorer, suffering from a double burden of environmental and economic disadvantage. On the other hand, points falling below the line indicate a relative amelioration of inequality. While a pollution disparity exists, it is partially counterbalanced by a reverse income inequality, meaning the more polluted regions are relatively more affluent. Thus, the line serves as a benchmark to guide our analysis. The further above the dashed line a point lies, the more severe the compounding disadvantage faced by a particular quantile group. For ratios below it, air pollution inequality is not a relative compounding inequality factor for a specific group.

The results plotted in Figure 8a reveal a consistent pattern across different quantile thresholds. The relationship shows that subnational units in the upper air pollution exposure quantiles experience substantially higher pollution concentrations relative to those in lower quantiles, with double ratios ranging from approximately 2 to 12 across the different percentile comparisons. The 1p tails, which compare below 1st to above 99th percentiles, show the most extreme disparities, which alleviates towards the 50p tails, median comparisons, indicating a more moderate but still significant inequalities.

At the continental level, the results plotted in Figure 8b reveal substantial regional heterogeneity in the pollution-income inequality relationship. Africa exhibits the most pronounced disparities, particularly within the most extreme quantile groups, where double-ratio values reach approximately 15. This indicates severe compounding inequalities, as a high pollution burden strongly coincides with economic disadvantage. In contrast, Asia demonstrates an opposite pattern for these extreme groups, showing an amelioration of inequality where pollution disparity is less pronounced relative to the observed income inequality. However, as the quantile group definition is expanded to be less extreme, a convergence toward the 45-degree dashed line is observable across all regions. This convergence indicates that disparities in pollution exposure and income become more proportional when comparing broader seg-

ments of the population, rather than just the extremes. The continental analysis confirms that the relationship between pollution exposure and economic development is not uniform, with developing regions experiencing the most acute compounding effects. Overall, the pattern indicates that subnational areas with higher pollution burdens generally have lower economic standing, creating a double burden of environmental and economic inequality that is most severe in Africa.

5 Social welfare gains of clean air

To estimate the social welfare implications of these disparities, we employ a Consumption Equivalent Variation (CEV) approach based on a utility function that incorporates both consumption and the disutility from pollution.

$$U(C, P) = C - \exp(\Lambda) \cdot \frac{P^{1+\epsilon}}{1+\epsilon}$$

To recover values of Λ and ϵ we use the MRS definition below :

$$MRS_{P,C} = \frac{U_P}{U_C} = -\exp(\Lambda) \cdot P^\epsilon$$

Applying the \ln function to recover the willingness to pay for variations in Pollution.

$$\ln(-MRS_{P,C}) = -WTP = \Lambda + \epsilon \cdot \ln(P)$$

To recover values for Λ and ϵ , we use a very simple approach. We use Guo, Wang, and Zhang 2020 and Freeman et al. 2019 willingness to pay information to recover these parameters by solving a system of two equations and two unknowns. We translate currency values to 2010 USD and Pollution values to PM2.5 levels.

After recovering the utility parameters, WE can calculate the CEV values by solving the

following for C^* and $P = 0$ such that:

$$\begin{aligned} U(C^*, 0) &= U(C, P) \\ C^* &= C - \exp(\Lambda) \cdot \frac{P^{1+\epsilon}}{1+\epsilon} \\ \frac{C^* - C}{C} &= CEV = -\frac{\exp(\Lambda) \cdot \frac{P^{1+\epsilon}}{1+\epsilon}}{C} \end{aligned}$$

The CEV indicates how much a country or subnational unit would be willing to forgo from its GDP per capita to achieve clean air.

Figure 9 presents the results of the estimated CEVs for national and subnational units. The y-axis reflects the CEV, which quantifies the potential welfare gains from achieving cleaner air, expressed as a percentage of GDP that a country would be willing to forgo. The analysis reveals a strong, non-linear relationship where the potential welfare gains are greatest in the most polluted areas. At the national level, shown in Figure 9a, countries in Asia and Africa, which exhibit the highest mean PM2.5 concentrations, show the largest potential gains, with CEV values frequently exceeding 10% of GDP and approaching 15-20% in some cases. Nations in Europe and Oceania show minimal CEV values as their pollution levels are low.

Figure 9b shows the subnational level and confirms the central trends described for national units, while highlighting significant intra-national heterogeneity. The more granular analysis reveals that the substantial national-level gains in Asia and Africa are driven by intensely polluted local hotspots, where CEV estimates for the most affected subnational units can reach up to 25% of GDP. This granular view also shows that even within generally cleaner continents like the Americas and Europe, specific localities with higher pollution levels exhibit moderate but non-trivial CEV values, which are masked in the national averages.

The national and subnational CEVs demonstrate that the economic and welfare incentives for pollution abatement are concentrated in the world's most polluted regions, particularly within specific subnational units in Asia and Africa. The heterogeneity of the subnational CEV underscores that interventions in these nations would yield disproportionately large returns in social welfare.

6 Discussion and Conclusion

In this paper, using data from 2010—the most recent year around which reliable granular global population, air pollution by aerosol, and GDP per capita data are jointly available—we document the global relative distribution of air pollution by aerosols, compound air pollution-income inequalities, and benefit gains of clean air across and within regions and countries.

Our focus on population-weighted distribution of air pollution contrasts with much of the focus in the scientific literature on climate change, which focuses largely on the distribution of climatic burden across locations, with relatively little attention to the relative population exposures to climatic burdens across and within locations (Mehta et al. 2016; Tian et al. 2023). This paper follows recent works that have combined global gridded population with air pollution data (Shaddick et al. 2018; Van Donkelaar et al. 2021; Van Donkelaar et al. 2016), which have generally focused on analyzing variabilities in regional and national means as well as aggregate distributions for large supra-national groupings. In contrast, our population-weighted analysis decomposes the overall global population-weighted air pollution by aerosol distribution into both across and within-region and country components.

This paper makes three key contributions to the literature on air pollution distribution. First, this is one of the first studies to document the global distribution of air pollution using population-weighted exposure, and the first using AOD as a pollution measure. Second, we are the first to investigate compounding air pollution exposure and income inequalities across global regions by leveraging granular subnational data and an accurate population weighting scheme. Third, we provide the first welfare benefit analysis for achieving clean air standards at the subnational level.

There are limitations to our analysis. First, our analysis is centered around one year. While it would be of great interest to compare changes over time, the population census and register data we rely on are from different years centered around 2010 (CIESIN Columbia University 2018), and the subnational GDP dataset we use only has data up to 2010 (Gennaioli et al. 2013) and requires extrapolation to extend the dataset to later years (Kummu, Taka, and Guillaume 2018). Second, there are trade-offs between the granularity of cells at which we merge population and air pollution by aerosol data and the precision and availability of cell-specific averages. We use $1^\circ \times 1^\circ$ longitude-latitude grid, which reduces the precision of our population-weighted air pollution by aerosol estimates for smaller countries, but improves the number of

raw satellite-based measurements we can draw on to measure air pollution by aerosol exposures for each cell. Third, rather than using climate models to transform AOD to particulate matter measurements (Hammer et al. 2020), for transparency and to reduce the number of intermediately estimating and approximation layers between raw satellite data measurements and inputs for empirical analysis, we use AOD-based measures directly to assess the global distribution of air pollution by aerosols. We present results in AOD levels and in units of relative global excess aerosol burdens. Given the importance of particulate matter to human health, we also provide approximately translated PM_{2.5} values to facilitate the interpretation of our AOD-based results.

The results suggest the existence of pollution inequalities across locations over the globe, with the Asian population facing the highest average exposure, followed by populations in Africa, Europe, the Americas, and Oceania. At the continental extremes, Asia's global shares of air pollution by aerosols are 26% larger than its population share, but Oceania's is 63% smaller. We find that the Americas, Europe, and Oceania have distributions with relatively limited variabilities. Europe is the most equal continent in the world, with population at the 80th percentile of air pollution by aerosol exposure, only 28% more exposed than those at the 20th percentile. In contrast, in Africa and Asia, populations at the 80th percentile of the air pollution by aerosol distribution are 141% and 109% more exposed than the population at the 20th percentile, respectively. Across subcontinental regions, the percentage increases in exposure between the 80th and 20th percentiles range from 2% to 208%. This range widens further from 0% to 359% when we condition further on within-country air pollution by aerosol distributions.

Finally, our compounding inequality analysis and the welfare findings demonstrate that air pollution is not only a profound global health challenge but also a significant driver of compounding economic disadvantage, with parts of the distribution on air pollution exposure facing compounding inequalities in air pollution and GDP. Additionally, the welfare gains of clean air are concentrated in specific, highly polluted subnational units in Africa and Asia. This evidence strongly motivates targeted policy interventions that address this environmental and economic injustice simultaneously.

References

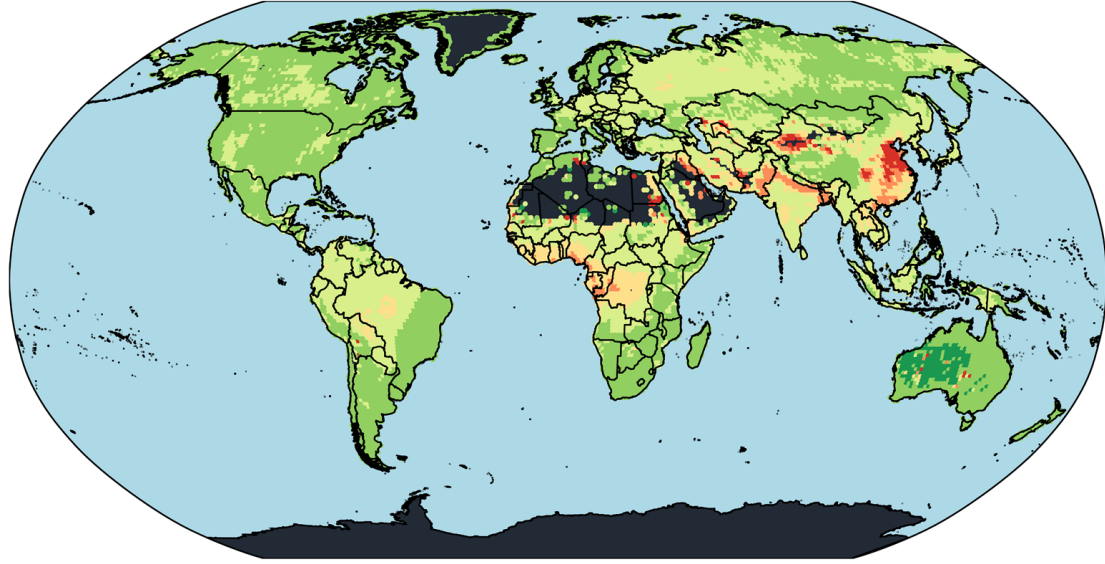
- Bibi, Humera, Khan Alam, Farrukh Chishtie, Samina Bibi, Imran Shahid, and Thomas Blaschke. 2015. "Intercomparison of MODIS, MISR, OMI, and CALIPSO Aerosol Optical Depth Retrievals for Four Locations on the Indo-Gangetic Plains and Validation Against AERONET Data." *Atmospheric Environment* 111 (June 1, 2015): 113–126. <https://doi.org/10.1016/j.atmosenv.2015.04.013>.
- Brabhukumr, Ajith, Prabhjot Malhi, Khaiwal Ravindra, and PVM Lakshmi. 2020. "Exposure to Household Air Pollution During First 3 Years of Life and Iq Level Among 6–8-Year-Old Children in India—a Cross-Sectional Study." *Science of The Total Environment* 709:135110.
- Bright, Jamie M., and Christian A. Gueymard. 2019. "Climate-Specific and Global Validation of MODIS Aqua and Terra Aerosol Optical Depth at 452 AERONET Stations." *Solar Energy* 183 (May 1, 2019): 594–605. <https://doi.org/10.1016/j.solener.2019.03.043>.
- Chen, Youliang, Dan Li, Hamed Karimian, Shiteng Wang, and Shuwei Fang. 2022. "The Relationship Between Air Quality and MODIS Aerosol Optical Depth in Major Cities of the Yangtze River Delta." *Chemosphere* 308 (Pt 2): 136301. <https://doi.org/10.1016/j.chemosphere.2022.136301>.
- Chu, Yuanyuan, Yisi Liu, Xiangyu Li, Zhiyong Liu, Hanson Lu, Yuanan Lu, Zongfu Mao, et al. 2016. "A Review on Predicting Ground PM_{2.5} Concentration Using Satellite Aerosol Optical Depth." *Atmosphere* 7, no. 10 (October): 129. <https://doi.org/10.3390/atmos7100129>.
- CIESIN Columbia University. 2018. *Gridded Population of the World, Version 4 (GPWv4): Basic Demographic Characteristics, Revision 11*. Palisades, New York. <https://doi.org/10.7927/H46M34XX>.
- Cornillon, P., J. Gallagher, and T. Sgouros. 2003. "OPeNDAP: Accessing Data in a Distributed, Heterogeneous Environment." *Data Science Journal* 2:164–174. <https://doi.org/10.2481/dsj.2.164>.
- Fisher, Samantha, David C Bellinger, Maureen L Cropper, Pushpam Kumar, Agnes Binagwaho, Juliette Biao Koudenkpo, Yongjoon Park, et al. 2021. "Air Pollution and Development in Africa: Impacts on Health, the Economy, and Human Capital." *The Lancet Planetary Health* 5 (10): e681–e688.
- Freeman, Richard, Wenquan Liang, Ran Song, and Christopher Timmins. 2019. "Willingness to Pay for Clean Air in China." *Journal of Environmental Economics and Management* 94 (March): 188–216. <https://doi.org/10.1016/j.jeem.2019.01.005>.
- Fu, Disong, Xiangao Xia, Jun Wang, Xiaoling Zhang, Xiaojing Li, and Jianzhong Liu. 2018. "Synergy of AERONET and MODIS AOD Products in the Estimation of PM_{2.5} Concentrations in Beijing." *Scientific Reports* 8, no. 1 (July 5, 2018): 10174. <https://doi.org/10.1038/s41598-018-28535-2>.
- Fu, Shihe, V Brian Viard, and Peng Zhang. 2021. "Air Pollution and Manufacturing Firm Productivity: Nationwide Estimates for China." *The Economic Journal* 131 (640): 3241–3273.
- Gakidou, Emmanuela, Ashkan Afshin, Amanuel Alemu Abajobir, Kalkidan Hassen Abate, Cristiana Abbafati, Kaja M Abbas, Foad Abd-Allah, et al. 2017. "Global, Regional, and National Comparative Risk Assessment of 84 Behavioural, Environmental and Occupational, and Metabolic Risks or Clusters of Risks, 1990–2016: A Systematic Analysis for the Global Burden of Disease Study 2016." *The Lancet* 390 (10100): 1345–1422.
- Gennaioli, Nicola, Rafael La Porta, Florencio Lopez-de-Silanes, and Andrei Shleifer. 2013. "Human Capital and Regional Development." *The Quarterly Journal of Economics* 128, no. 1 (February 1, 2013): 105–164. <https://doi.org/10.1093/qje/qjs050>.

- Guo, Dong, Anyi Wang, and Alice Tianbo Zhang. 2020. "Pollution Exposure and Willingness to Pay for Clean Air in Urban China." *Journal of Environmental Management* 261 (May): 110174. <https://doi.org/10.1016/j.jenvman.2020.110174>.
- Hammer, Melanie S, Aaron van Donkelaar, Chi Li, Alexei Lyapustin, Andrew M Sayer, N Christina Hsu, Robert C Levy, et al. 2020. "Global Estimates and Long-Term Trends of Fine Particulate Matter Concentrations (1998–2018)." *Environmental Science & Technology* 54 (13): 7879–7890.
- Holben, B. N., T. F. Eck, I. Slutsker, D. Tanré, J. P. Buis, A. Setzer, E. Vermote, et al. 1998. "AERONET—A Federated Instrument Network and Data Archive for Aerosol Characterization." *Remote Sensing of Environment* 66, no. 1 (October 1, 1998): 1–16. [https://doi.org/10.1016/S0034-4257\(98\)00031-5](https://doi.org/10.1016/S0034-4257(98)00031-5).
- Jacobson, Mark Z. 2002. *Atmospheric Pollution: History, Science, and Regulation*. Cambridge: Cambridge University Press. <https://doi.org/10.1017/CBO9780511802287>.
- Kummu, Matti, Maija Taka, and Joseph HA Guillaume. 2018. "Gridded Global Datasets for Gross Domestic Product and Human Development Index Over 1990–2015." *Scientific data* 5 (1): 1–15.
- Lenoble, Jacqueline, Lorraine Remer, and Didier Tanre. 2013. *Aerosol Remote Sensing*. Springer Science & Business Media, February 11, 2013.
- Mehta, Manu, Ritu Singh, Ankit Singh, Narendra Singh, and Anshumali. 2016. "Recent Global Aerosol Optical Depth Variations and Trends — a Comparative Study Using MODIS and MISR Level 3 Datasets." *Remote Sensing of Environment* 181 (August 1, 2016): 137–150. <http://doi.org/10.1016/j.rse.2016.04.004>.
- NASA Earth Observatory. 2024. "Aerosol Optical Depth." Aerosol Optical Depth. https://earthobservatory.nasa.gov/global-maps/MODAL2_M_AER_OD.
- Odo, Daniel B, Ian A Yang, Sagnik Dey, Melanie S Hammer, Aaron van Donkelaar, Randall V Martin, Guang-Hui Dong, et al. 2023. "A Cross-Sectional Analysis of Long-Term Exposure to Ambient Air Pollution and Cognitive Development in Children Aged 3–4 Years Living in 12 Low-and Middle-Income Countries." *Environmental Pollution* 318:120916.
- Pirlea, Florina, and Wendy Ven-dee Huang. 2019. "The Global Distribution of Air Pollution," September 12, 2019. <https://datatopics.worldbank.org/world-development-indicators/stories/the-global-distribution-of-air-pollution.html>.
- Shaddick, Gavin, Matthew L Thomas, Heresh Amini, David Broday, Aaron Cohen, Joseph Frostad, Amelia Green, et al. 2018. "Data Integration for the Assessment of Population Exposure to Ambient Air Pollution for Global Burden of Disease Assessment." *Environmental science & technology* 52 (16): 9069–9078.
- Shaddick, Gavin, Matthew L Thomas, Pierpaolo Mudu, Giulia Ruggeri, and Sophie Gumi. 2020. "Half the World's Population Are Exposed to Increasing Air Pollution." *NPJ Climate and Atmospheric Science* 3 (1): 23.
- Tian, Xiaomin, Chaoli Tang, Xin Wu, Jie Yang, Fengmei Zhao, and Dong Liu. 2023. "The Global Spatial-Temporal Distribution and EOF Analysis of AOD Based on MODIS Data During 2003–2021." *Atmospheric Environment* 302 (June 1, 2023): 119722. <https://doi.org/10.1016/j.atmosenv.2023.119722>.
- Van Donkelaar, Aaron, Melanie S Hammer, Liam Bindle, Michael Brauer, Jeffery R Brook, Michael J Garay, N Christina Hsu, et al. 2021. "Monthly Global Estimates of Fine Particulate Matter and Their Uncertainty." *Environmental Science & Technology* 55 (22): 15287–15300.
- Van Donkelaar, Aaron, Randall V Martin, Michael Brauer, N Christina Hsu, Ralph A Kahn, Robert C Levy, Alexei Lyapustin, et al. 2016. "Global Estimates of Fine Particulate Mat-

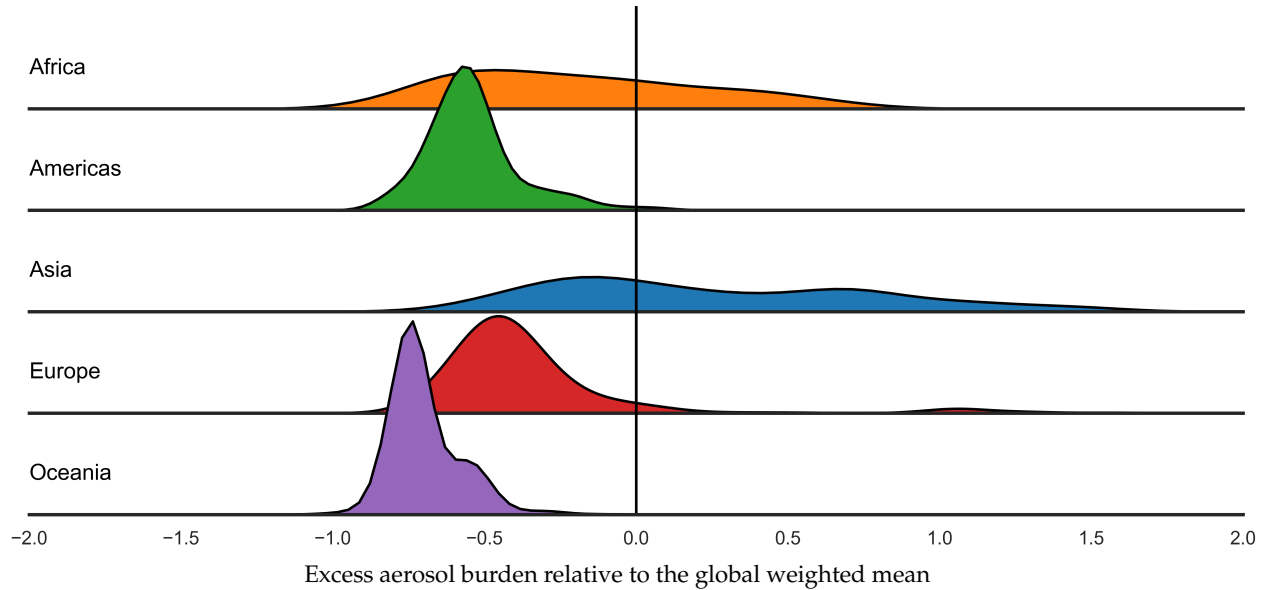
- ter Using a Combined Geophysical-Statistical Method with Information from Satellites, Models, and Monitors." *Environmental science & technology* 50 (7): 3762–3772.
- Wang, Qingxin, Dongsheng Du, Siwei Li, Jie Yang, Hao Lin, and Juan Du. 2021. "Comparison of Different Methods of Determining Land Surface Reflectance for AOD Retrieval." *Atmospheric Pollution Research* 12, no. 8 (August 1, 2021): 101143. <https://doi.org/10.1016/j.apr.2021.101143>.
- World Health Organization. 2021. "WHO Global Air Quality Guidelines: Particulate Matter (PM_{2.5} and PM₁₀), Ozone, Nitrogen Dioxide, Sulfur Dioxide and Carbon Monoxide," <https://www.who.int/publications/i/item/9789240034228>.
- Xiong, Xiaoxiong, Emily J. Aldoretta, Amit Angal, Tiejun Chang, Xu Geng, Daniel O. Link, Vincent V. Salomonson, et al. 2020. "Terra MODIS: 20 Years of on-Orbit Calibration and Performance." *Journal of Applied Remote Sensing* 14, no. 3 (August): 037501. <https://doi.org/10.1117/1.JRS.14.037501>.
- Yang, Qianqian, Qiangqiang Yuan, Linwei Yue, Tongwen Li, Huanfeng Shen, and Liangpei Zhang. 2019. "The Relationships Between PM_{2.5} and Aerosol Optical Depth (AOD) in Mainland China: About and Behind the Spatio-Temporal Variations." *Environmental Pollution* 248 (May 1, 2019): 526–535. <https://doi.org/10.1016/j.envpol.2019.02.071>.

Figure 1: Continental population-weighted distribution of air pollution by aerosols, 2010

(a) 1° cell ($1^\circ \times 1^\circ$ longitude–latitude grid) as the unit of observation map



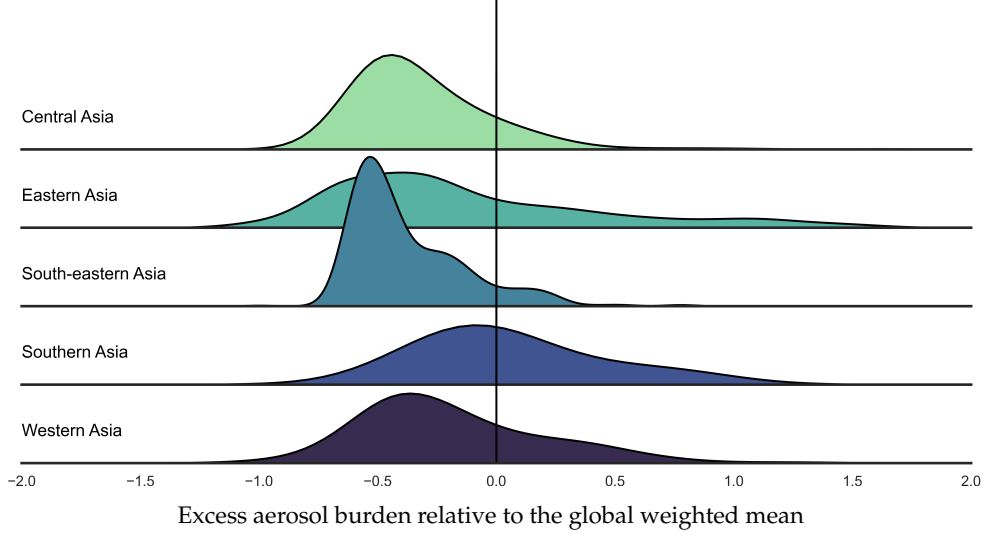
(b) 1° cell as the unit of observation (weighted by cell-population), by regions



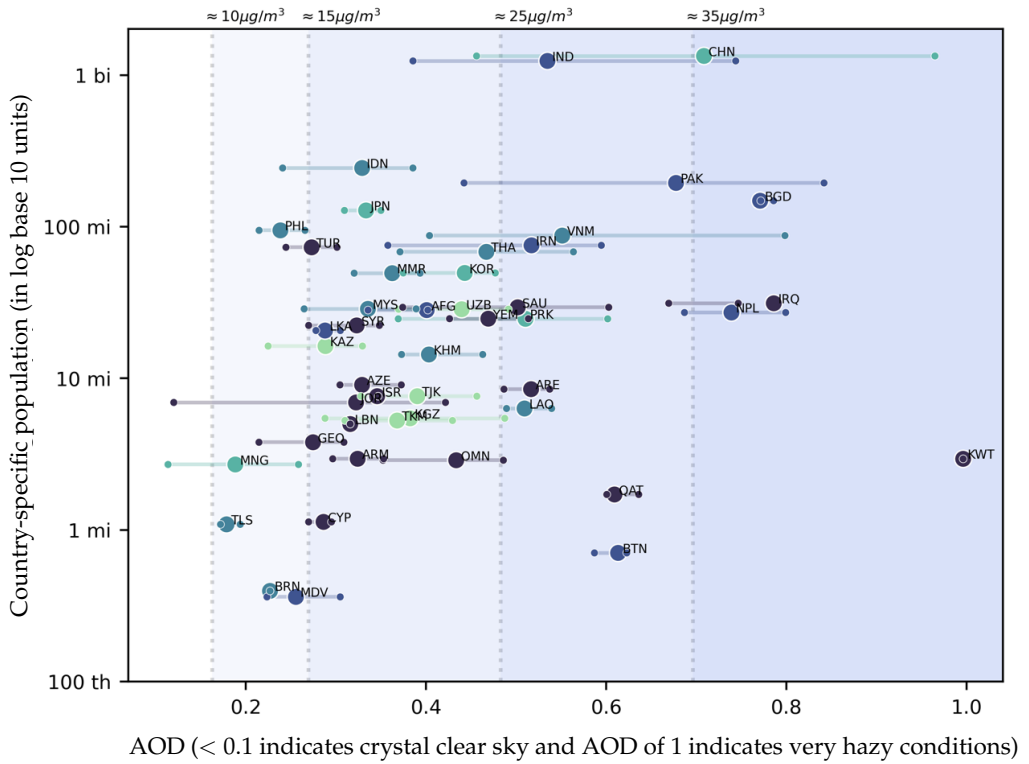
Notes: The panels present the global relative distribution of air pollution by aerosols as measured by Aerosol Optical Depth (AOD). We compute annual average AOD for each 1° cell. The map in Panel (a) matches cell-specific AOD to cell locations. The distribution in Panel (b) uses cell-specific AOD, weighted by cell-specific population estimates. The y-axis in Panel (b) shows cell population weighted density approximations. The colors in Panel (a) and x-axis in Panel (b) correspond to what we call global excess population-pollution burden (EPB): A value of 0.5 (-0.5) indicates that a cell's AOD measure is 50 percent greater (smaller) than the global weighted mean. In Panel (b), darker shades of green (red) correspond to greater magnitudes of negative (positive) excess burdens.

Figure 2: Asian population-weighted distribution of air pollution by aerosols, 2010

(a) 1° cell as the unit of observation (weighted by cell-population), by sub-regions



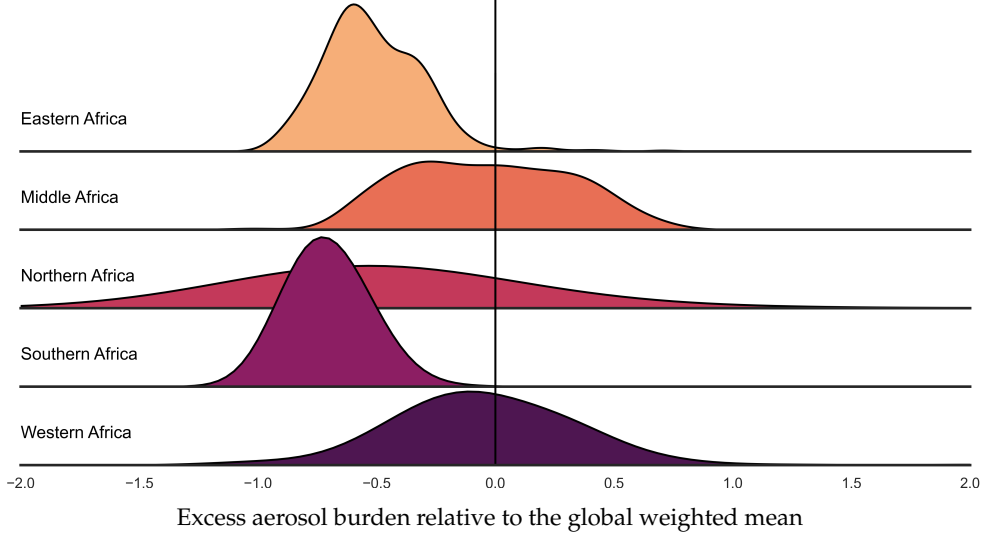
(b) Country-specific distributional ranges: P20 (left-dot), mean (center-dot), P80 (right-dot)



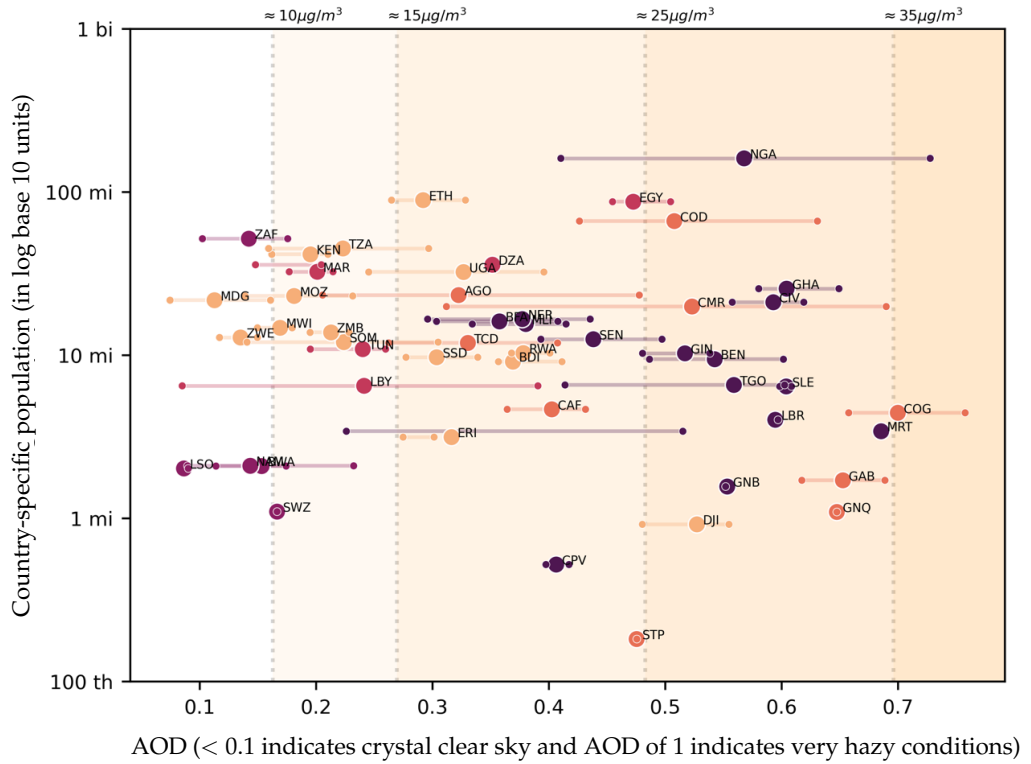
Notes: The panels present the Asian distribution of air pollution by aerosols as measured by Aerosol Optical Depth (AOD). We compute annual average AOD for each 1° cell. Panel (b) lines mark the 20th percentile, mean, and the 80th percentile of a country's AOD distribution, computed based on the distribution of AOD and population across cells corresponding to each country. In Panel (a), the y-axis shows cell population weighted density approximations. The x-axis in Panel (a) corresponds to levels of excess population-pollution burden (EPB), a value of +50% (-50%) indicates that a cell's AOD measure is 50 percent greater (smaller) than the global population-weighted mean. The x-axis in Panel (b) is in AOD units and tick-labels show AOD values. The vertical dashed lines corresponding to PM 2.5 thresholds in $\mu\text{g}/\text{m}^3$ units according to WHO interim targets (ITs). Background color corresponds to the IT ranges, with darker colors indicating lower air quality thresholds.

Figure 3: African population-weighted distribution of air pollution by aerosols, 2010

(a) 1° cell as the unit of observation (weighted by cell-population), by sub-regions



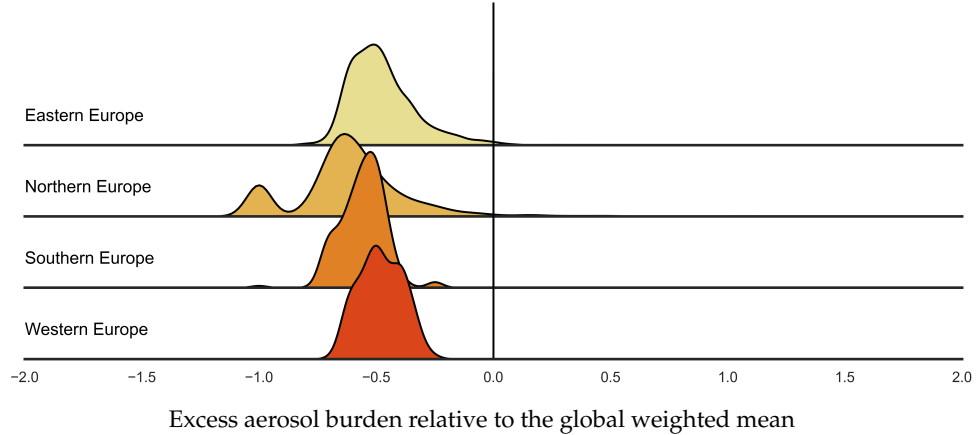
(b) Country-specific distributional ranges: P20 (left-dot), mean (center-dot), P80 (right-dot)



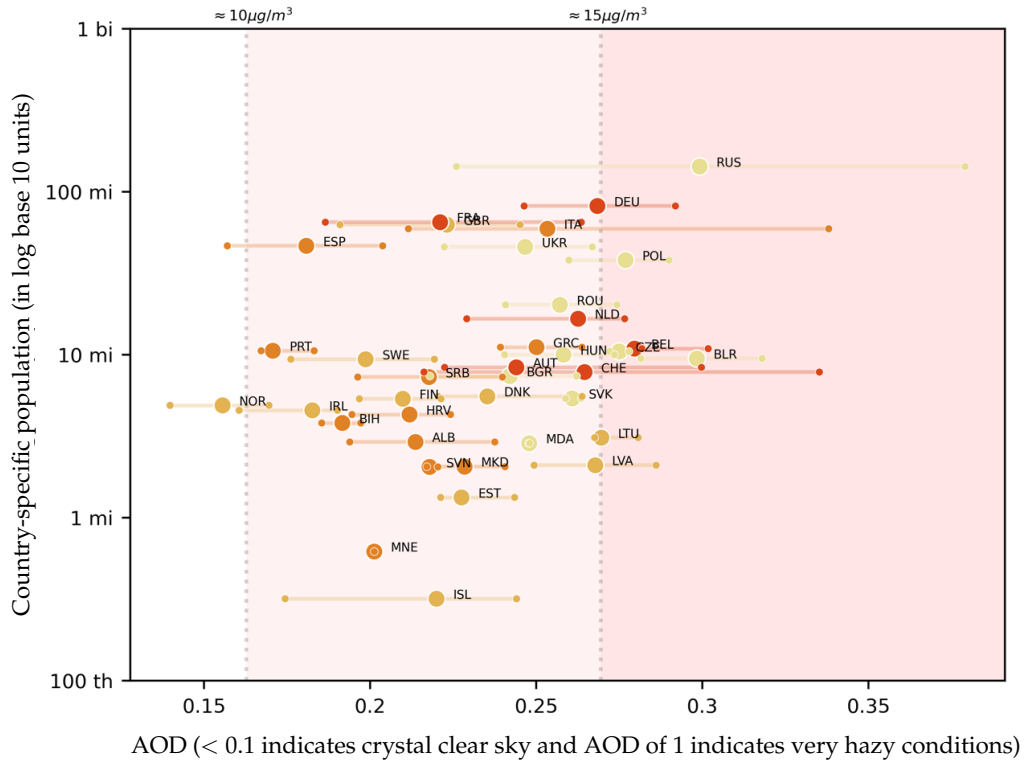
Notes: The panels present the African distribution of air pollution by aerosols as measured by Aerosol Optical Depth (AOD). We compute annual average AOD for each 1° cell. Panel (b) lines mark the 20th percentile, mean, and the 80th percentile of a country's AOD distribution, computed based on the distribution of AOD and population across cells corresponding to each country. In Panel (a), the y-axis shows cell population weighted density approximations. The x-axis in Panel (a) corresponds to levels of excess population-pollution burden (EPB), a value of +50% (-50%) indicates that a cell's AOD measure is 50 percent greater (smaller) than the global population-weighted mean. The x-axis in Panel (b) is in AOD units and tick-labels show AOD values. The vertical dashed lines corresponding to PM 2.5 thresholds in $\mu\text{g}/\text{m}^3$ units according to WHO interim targets (ITs). Background color corresponds to the IT ranges, with darker colors indicating lower air quality thresholds.

Figure 4: European population-weighted distribution of air pollution by aerosols, 2010

(a) 1° cell as the unit of observation (weighted by cell-population), by sub-regions



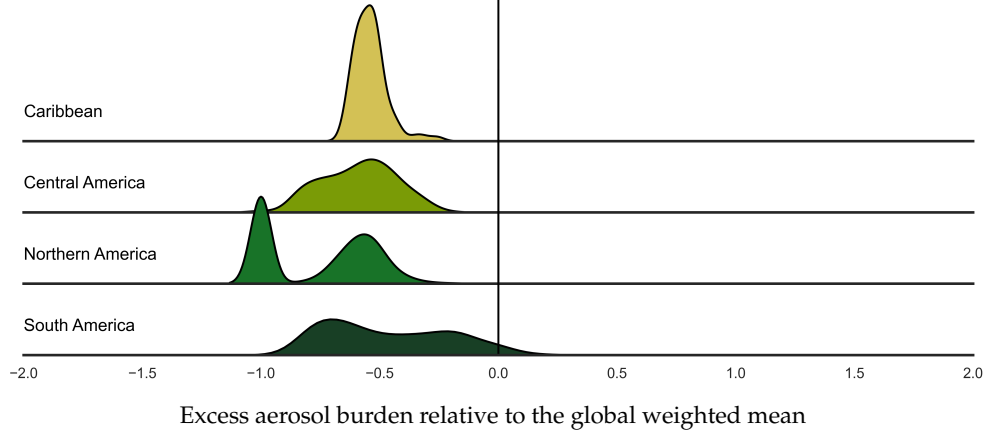
(b) Country-specific distributional ranges: P20 (left-dot), mean (center-dot), P80 (right-dot)



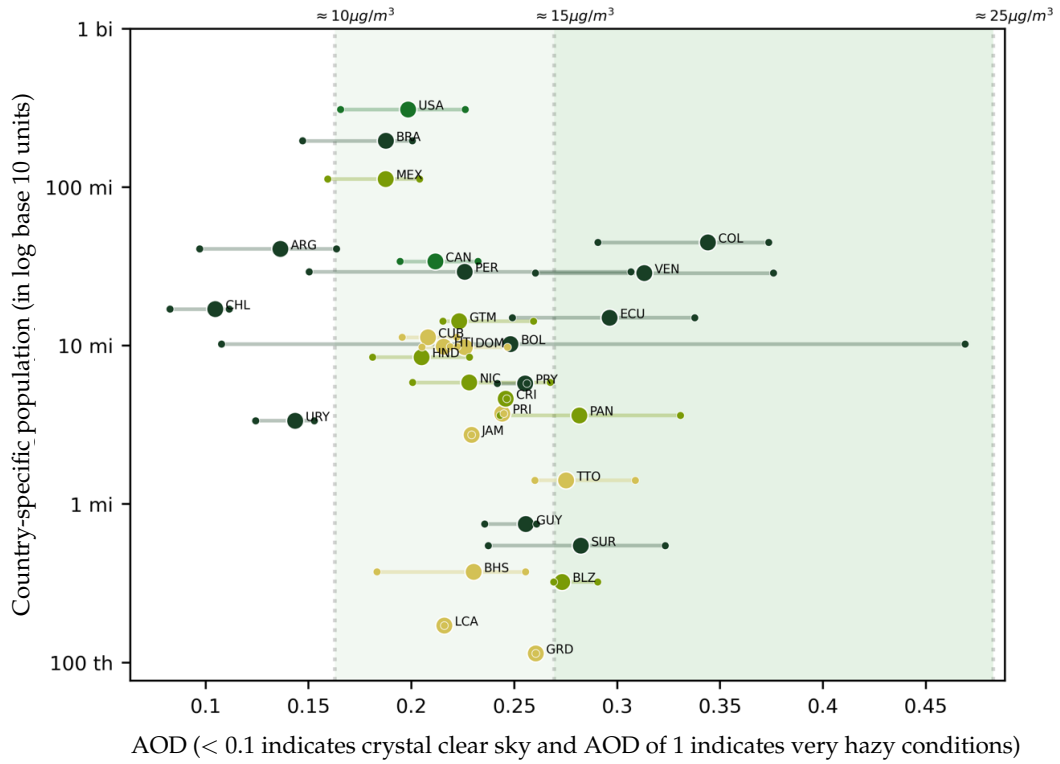
Notes: The panels present the European distribution of air pollution by aerosols as measured by Aerosol Optical Depth (AOD). We compute annual average AOD for each 1° cell. Panel (b) lines mark the 20th percentile, mean, and the 80th percentile of a country's AOD distribution, computed based on the distribution of AOD and population across cells corresponding to each country. In Panel (a), the y-axis shows cell population weighted density approximations. The x-axis in Panel (a) corresponds to levels of excess population-pollution burden (EPB), a value of +50% (-50%) indicates that a cell's AOD measure is 50 percent greater (smaller) than the global population-weighted mean. The x-axis in Panel (b) is in AOD units and tick-labels show AOD values. The vertical dashed lines corresponding to PM 2.5 thresholds in $\mu\text{g}/\text{m}^3$ units according to WHO interim targets (ITs). Background color corresponds to the IT ranges, with darker colors indicating lower air quality thresholds.

Figure 5: American population-weighted distribution of air pollution by aerosols, 2010

(a) 1° cell as the unit of observation (weighted by cell-population), by sub-regions



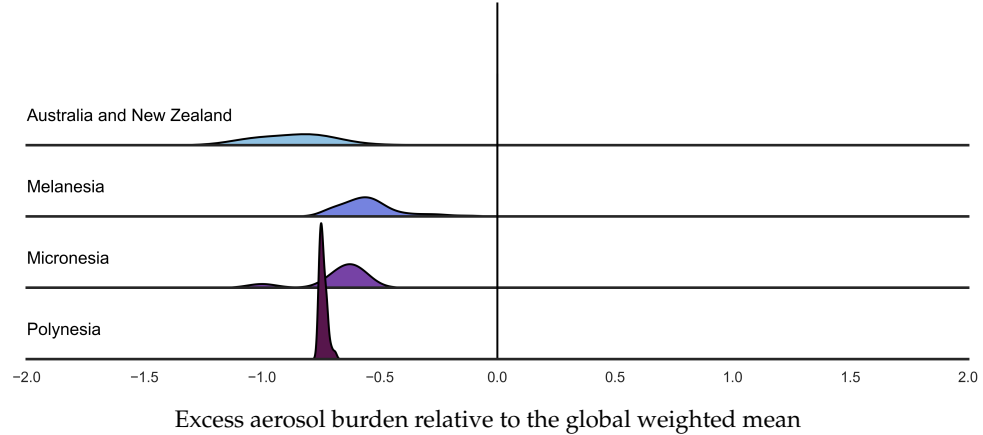
(b) Country-specific distributional ranges: P20 (left-dot), mean (center-dot), P80 (right-dot)



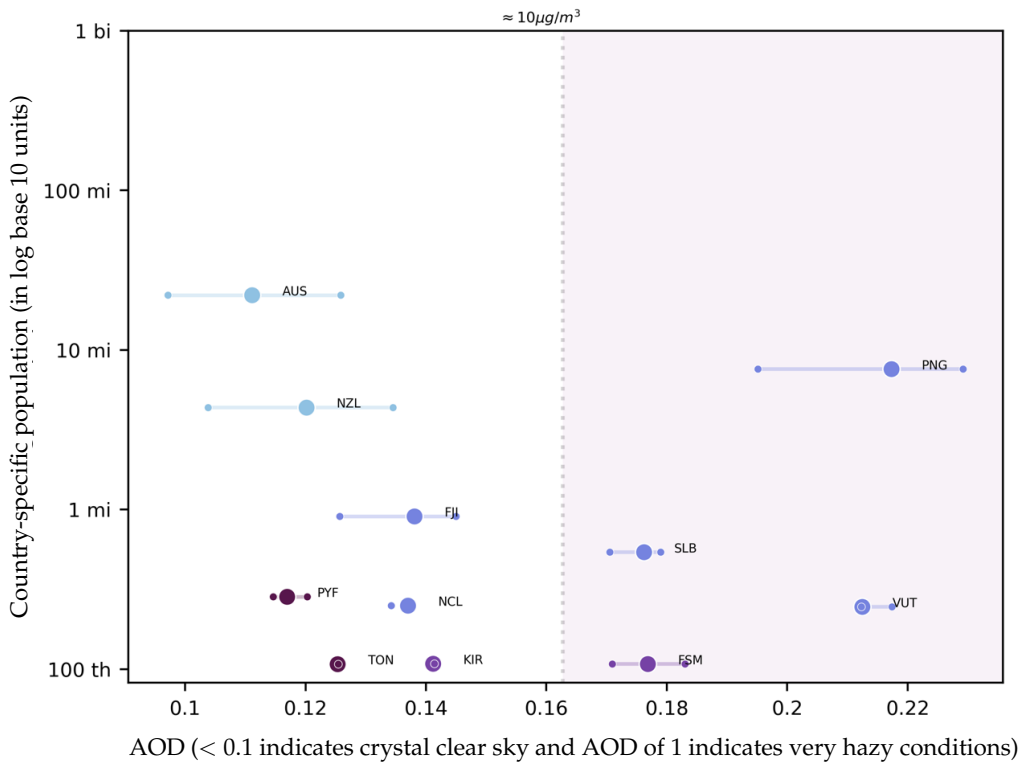
Notes: The panels present the American distribution of air pollution by aerosols as measured by Aerosol Optical Depth (AOD). We compute annual average AOD for each 1° cell. Panel (b) lines mark the 20th percentile, mean, and the 80th percentile of a country's AOD distribution, computed based on the distribution of AOD and population across cells corresponding to each country. In Panel (a), the y-axis shows cell population weighted density approximations. The x-axis in Panel (a) corresponds to levels of excess population-pollution burden (EPB), a value of +50% (-50%) indicates that a cell's AOD measure is 50 percent greater (smaller) than the global population-weighted mean. The x-axis in Panel (b) is in AOD units and tick-labels show AOD values. The vertical dashed lines corresponding to PM 2.5 thresholds in $\mu\text{g}/\text{m}^3$ units according to WHO interim targets (ITs). Background color corresponds to the IT ranges, with darker colors indicating lower air quality thresholds.

Figure 6: Oceanian population-weighted distribution of air pollution by aerosols, 2010

(a) 1° cell as the unit of observation (weighted by cell-population), by sub-regions

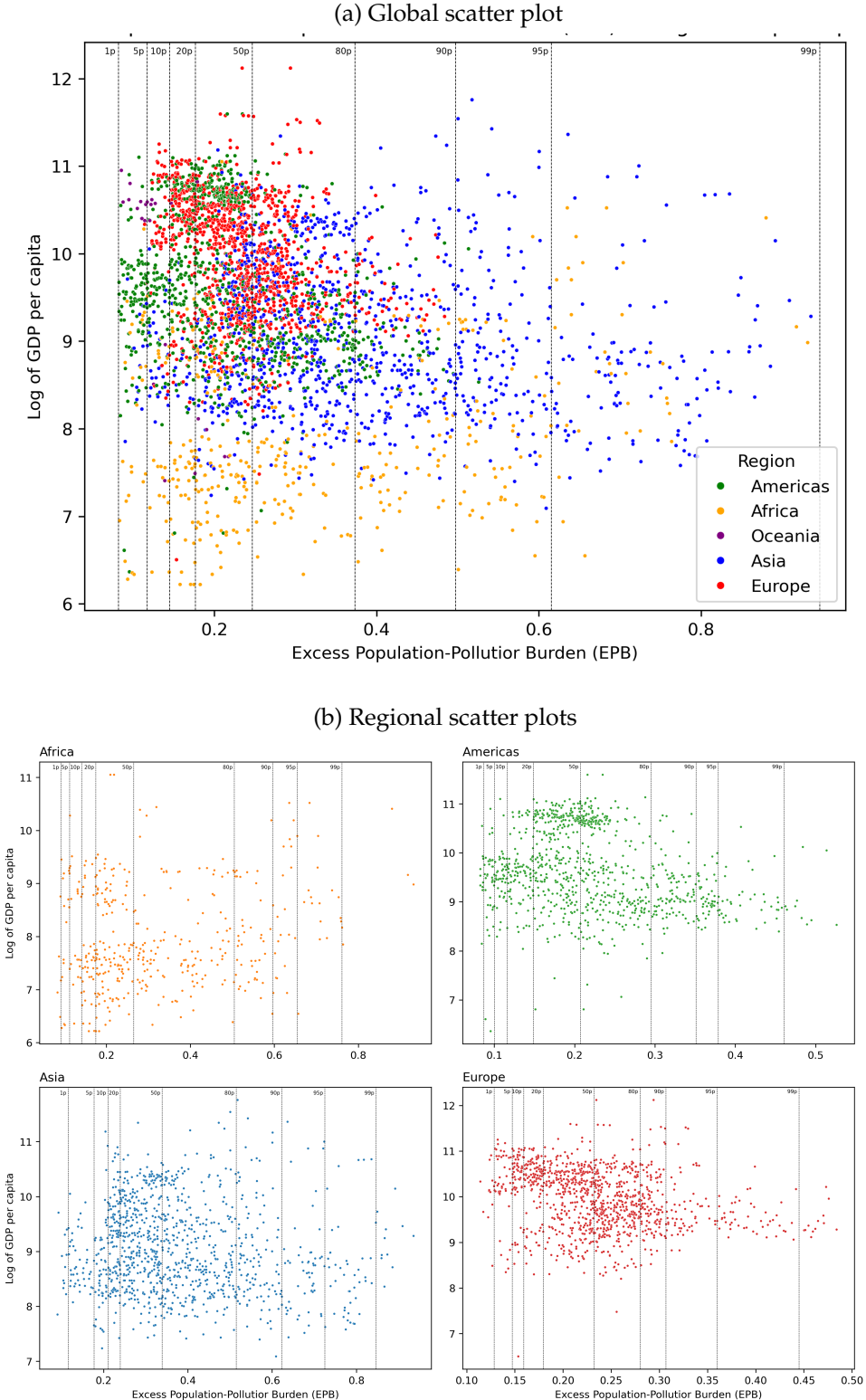


(b) Country-specific distributional ranges: P20 (left-dot), mean (center-dot), P80 (right-dot)



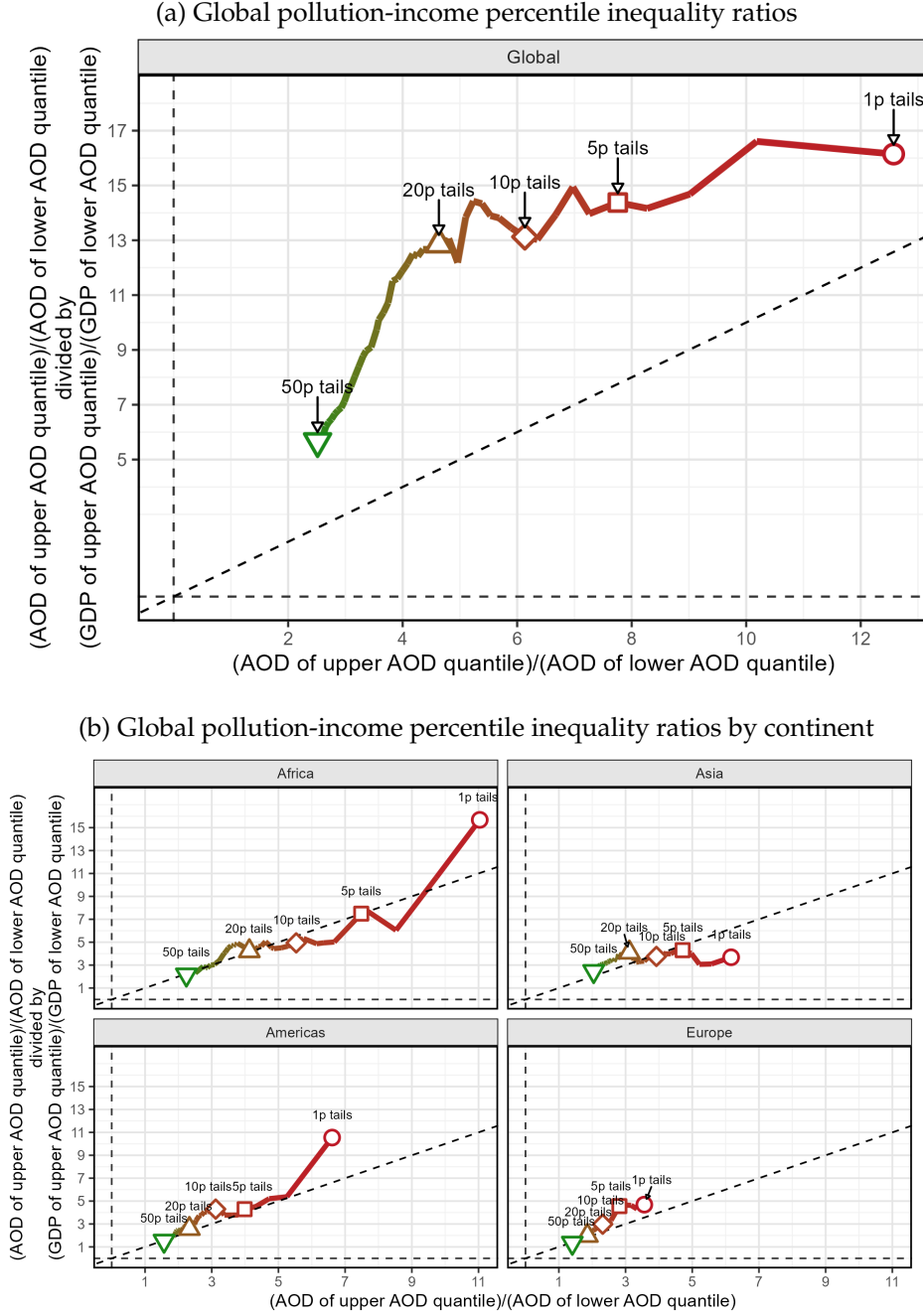
Notes: The panels present Oceanian distribution of air pollution by aerosols as measured by Aerosol Optical Depth (AOD). We compute annual average AOD for each 1° cell. Panel (b) lines mark the 20th percentile, mean, and the 80th percentile of a country's AOD distribution, computed based on the distribution of AOD and population across cells corresponding to each country. In Panel (a), the y-axis shows cell population weighted density approximations. The x-axis in Panel (a) corresponds to levels of excess population-pollution burden (EPB), a value of +50% (-50%) indicates that a cell's AOD measure is 50 percent greater (smaller) than the global population-weighted mean. The x-axis in Panel (b) is in AOD units and tick-labels show AOD values. The vertical dashed lines corresponding to PM 2.5 thresholds in $\mu\text{g}/\text{m}^3$ units according to WHO interim targets (ITs). Background color corresponds to the IT ranges, with darker colors indicating lower air quality thresholds.

Figure 7: Excess Population-Pollution Burden and Log of GDP per capita scatterplot



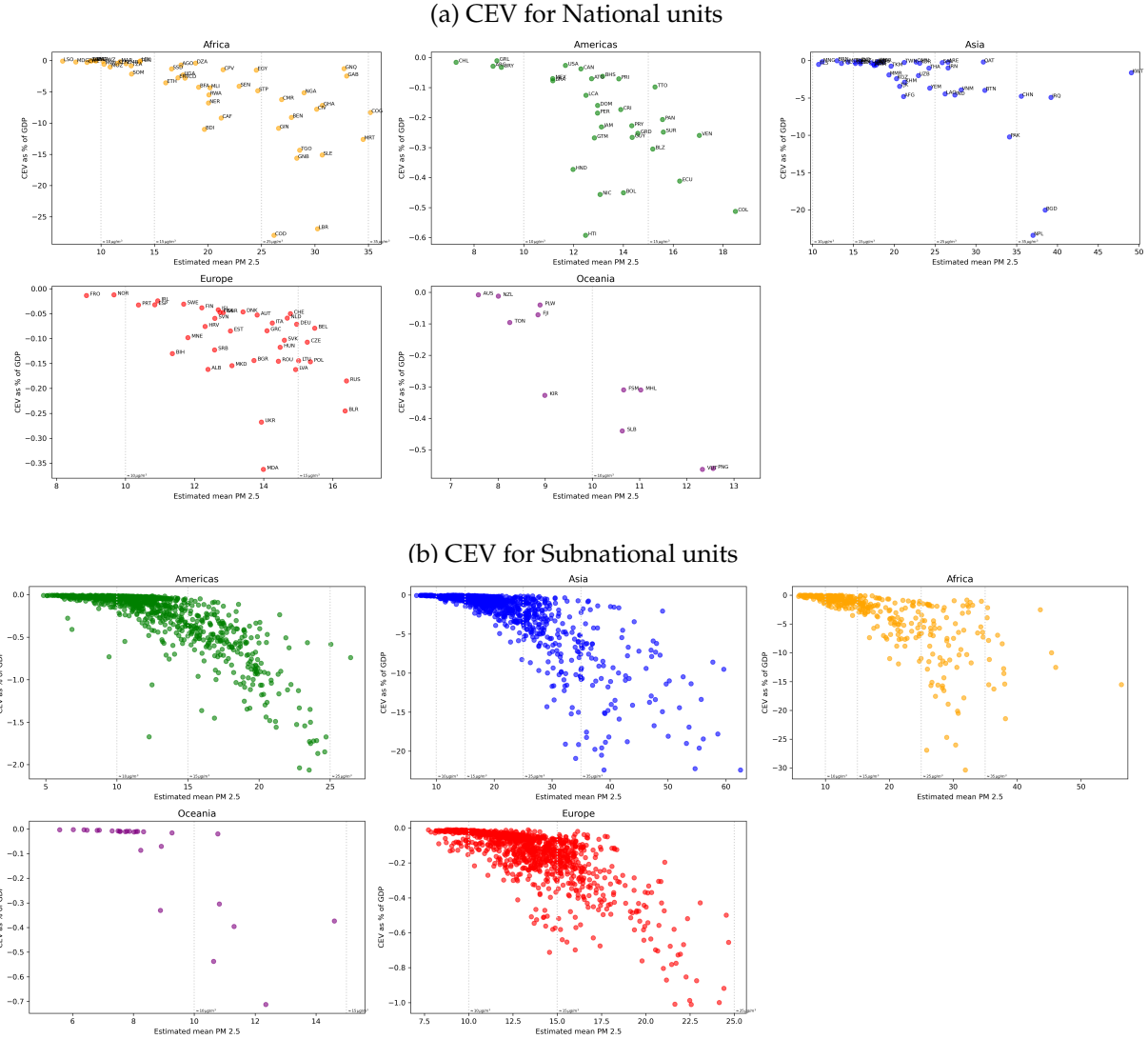
Notes: The plots above plot the subnational units distribution of Excess pollution and its Log of GDP relations. Panel ?? presents the global distributions with different colors by region, and Panel ?? shows regional scatterplots separately. X-axis corresponds to our measure of population-weighted excess burden of pollution (EPB). Y-axis is the log of subantional GDP per capita. Vertical lines indicates pollution burden 1st, 5th, 10th, 20th, 50th, 80th, 90th, 95th, and 99th quantiles. These quantiles are used in Figure 8 to calculate the compound ratio of pollution and GDP inequality.

Figure 8: Compounding inequality pollution-income percentile ratios across subnational units



Notes: These panels present the ratio of Pollution-Income percentile ratios. Panel 8a shows the ratios for the global distribution quantiles, and Panel 8b plots these quantile ratios by continent. The figure uses a double-ratio measure, where the X-axis is defined as the GDP Ratio—the ratio of the average GDP per capita in the upper AOD quantile group to the average GDP per capita in the lower AOD quantile group. The Y-axis is the Double Ratio, calculated as the AOD Ratio (Numerator) divided by the GDP Ratio (Denominator), where the AOD Ratio is the AOD of the upper quantile divided by the AOD of the lower quantile. This double-ratio is defined across five paired AOD quantiles: below 1st- above 99th, below 5th - above 95th, below 10th - above 90th, below 20th - above 80th, and above median-below median.

Figure 9: Consumption Equivalent Variation (CEV) estimations by region



Notes: These panels shows our estimation of the Consumption Equivalent Variation (CEV) for units across continents. Panel 9a shows countries by continents, and Panel 9b plots subunits in each continent. CEV is calculate using the net consumption utility function. X-axis corresponds to PM 2.5 estimates using out linear transformation. Y-axis plots the CEV for each unit. The vertical dashed lines corresponding to PM 2.5 thresholds in $\mu\text{g}/\text{m}^3$ units according to WHO interim targets (ITs). Background color corresponds to the IT ranges, with darker colors indicating lower air quality thresholds. .

Table 1: Regional population-weighted air pollution by aerosol (AOD) distributions: mean, excess population-pollution burden (EPB), interquintile and interdecile ranges and ratios.

Geographical units	Mean (EPB)	Percentile ranges		Percentile ratios	
		Interquintile =	Interdecile =	80th to	90th to
		80th - 20th	90th - 10th	20th	10th
Panel A: World					
Africa	0.37 (-18%)	0.35 = 0.54 - 0.19	0.47 = 0.63 - 0.16	2.78	4.01
Americas	0.21 (-54%)	0.08 = 0.24 - 0.16	0.16 = 0.30 - 0.14	1.56	2.23
Asia	0.57 (+25%)	0.44 = 0.79 - 0.35	0.63 = 0.92 - 0.29	2.25	3.18
Europe	0.25 (-44%)	0.08 = 0.29 - 0.21	0.12 = 0.31 - 0.19	1.36	1.68
Oceania	0.14 (-70%)	0.08 = 0.18 - 0.10	0.12 = 0.21 - 0.09	1.76	2.24
Panel B: Africa					
Eastern Africa	0.24 (-47%)	0.16 = 0.32 - 0.16	0.22 = 0.36 - 0.14	1.95	2.64
Middle Africa	0.46 (+ 2%)	0.31 = 0.62 - 0.31	0.39 = 0.65 - 0.26	2.02	2.54
Northern Africa	0.37 (-20%)	0.26 = 0.46 - 0.20	0.34 = 0.51 - 0.17	2.33	2.94
Southern Africa	0.14 (-69%)	0.08 = 0.18 - 0.10	0.10 = 0.19 - 0.09	1.73	2.10
Western Africa	0.52 (+14%)	0.29 = 0.67 - 0.38	0.41 = 0.73 - 0.32	1.76	2.27
Panel C: The Americas					
Caribbean	0.23 (-51%)	0.05 = 0.25 - 0.20	0.06 = 0.26 - 0.20	1.24	1.31
Central America	0.2 (-57%)	0.06 = 0.23 - 0.17	0.12 = 0.26 - 0.14	1.37	1.79
Northern America	0.2 (-56%)	0.06 = 0.23 - 0.17	0.09 = 0.24 - 0.15	1.34	1.67
South America	0.22 (-52%)	0.16 = 0.31 - 0.15	0.25 = 0.36 - 0.11	2.13	3.17
Panel D: Asia					
Central Asia	0.37 (-20%)	0.17 = 0.44 - 0.27	0.26 = 0.49 - 0.23	1.64	2.10
Eastern Asia	0.67 (+46%)	0.59 = 0.96 - 0.37	0.73 = 1.05 - 0.32	2.59	3.24
South-eastern Asia	0.37 (-19%)	0.21 = 0.46 - 0.25	0.33 = 0.55 - 0.22	1.85	2.46
Southern Asia	0.57 (+26%)	0.37 = 0.77 - 0.40	0.45 = 0.80 - 0.35	1.95	2.27
Western Asia	0.39 (-14%)	0.25 = 0.51 - 0.26	0.43 = 0.67 - 0.24	1.95	2.73
Panel E: Europe					
Eastern Europe	0.28 (-38%)	0.06 = 0.30 - 0.24	0.16 = 0.38 - 0.22	1.28	1.74
Northern Europe	0.22 (-52%)	0.07 = 0.25 - 0.18	0.10 = 0.27 - 0.17	1.36	1.58
Southern Europe	0.22 (-53%)	0.08 = 0.25 - 0.17	0.13 = 0.29 - 0.16	1.45	1.80
Western Europe	0.25 (-45%)	0.06 = 0.28 - 0.22	0.10 = 0.30 - 0.20	1.28	1.51
Panel F: Oceania					
Australia & New Zealand	0.11 (-75%)	0.03 = 0.13 - 0.10	0.04 = 0.13 - 0.09	1.30	1.58
Melanesia	0.21 (-55%)	0.04 = 0.22 - 0.18	0.09 = 0.24 - 0.15	1.23	1.67
Micronesia	0.16 (-66%)	0.02 = 0.16 - 0.14	0.04 = 0.18 - 0.14	1.10	1.33
Polynesia	0.12 (-73%)	0.01 = 0.13 - 0.12	0.01 = 0.13 - 0.12	1.02	1.06

Note: Table statistics are computed based on the distribution of AOD and population across cells ($1^\circ \times 1^\circ$ longitude-latitude grid). The interpretation of AOD is that < 0.1 indicates crystal clear sky and AOD of 1 indicates very hazy conditions. For excess population-pollution burden (EPB), a value of +50% (-50%) indicates that a geographical unit's AOD measure is 50 percent greater (smaller) than the global population-weighted mean.

ONLINE APPENDIX

Air Pollution Burden Around the World: Distributions, Inequalities, and the Economic Benefits of Clean Air

Angelo dos Santos, Oscar Morales, Jere R. Behrman, Emily Hannum, Fan Wang

A Method

A.1 Air pollution measures

Population-weighted AOD distributions To analyze population-weighted air pollution by aerosol distributions, we define a discrete distribution of annual average AOD values for 2010 on the set of all populated cells, where the mass of the cell-specific population is determined by population estimates based on GPWv4 from around 2010. Specifically, let s_c be the share of the global population in cell c , a_c be the average annual AOD in cell c , and C be the set of all gridded cells where $s_c > 0$. The global population-weighted annual average AOD distribution function, which provides the share of global population experiencing lower than a^* levels of annual average AOD, is equal to:

$$F(a^*) = P(a < a^*) = \sum_{c \in C} s_c \cdot \mathbf{1}\{a_c < a^*\} . \quad (8)$$

To compare aerosol distributions conditional on regional groupings based on supranational, national, and subnational boundaries, we define $C_r \subseteq C$ as the set of populated cells that intersect with the boundary enclosures of the supranational, national or subnational location r . For boundary data, we use national boundary data available in the GPWv4 population dataset (CIESIN Columbia University 2018), and the subnational boundary data embedded in the subnational GDP data from (Kummu, Taka, and Guillaume 2018). The share of population in cell c among population within location grouping r is $s_{c,r} = \frac{s_c}{(\sum_{\hat{c} \in C_r} s_{\hat{c}})}$, and the distribution function of the location-specific AOD is:

$$F_r(a^*) = P_r(a < a^*) = \sum_{c \in C_r} s_{c,r} \cdot \mathbf{1}\{a_c < a^*\} . \quad (9)$$

Given the location-specific distribution function, we compute the mean exposure for each

location r :

$$\mu_r = \sum_{c \in C_r} s_{c,r} \cdot a_c . \quad (10)$$

The global weighted mean is $\mu_{\text{global}} = \sum_{c \in C} s_c \cdot a_c$. In our empirical analysis, we compute global, continental, regional, national, and subnational population weighted annual mean AOD exposures.

Given the discrete mass distribution over cells, the location-specific distribution function $F_r(a^*)$ is not invertible. Hence, we define the τ^{th} percentile of the location-specific distribution as the minimum a^* value where the share of population in location r with less than a^* level of annual average AOD is greater or equal to $\frac{\tau}{100}$, specifically:

$$\text{percentile}_r(\tau) = \min \left\{ a^* : F_r(a^*) \geq \frac{\tau}{100} \right\} . \quad (11)$$

Discussions in our empirical analysis focus on location-specific 20th and 80th as well as 10th and 90th percentiles, and use relative percentile ratios as a key measure for within-location distributional variabilities.

Relative exposure and excess burden To measure relative exposures, we compute what we call excess aerosol burden: $e_{c,\hat{r}}$ is the excess aerosol burden of cell c with respect to location \hat{r} , and it measures the percentage deviation between cell-specific AOD value a_c and location-specific AOD value average $\mu_{\hat{r}}$:

$$e_{c,\hat{r}} = \frac{a_c - \mu_{\hat{r}}}{\mu_{\hat{r}}} = \frac{a_c}{\mu_{\hat{r}}} - 1 . \quad (12)$$

When \hat{r} includes all global cells, we have $e_{c,\text{global}}$, the cell-specific global excess aerosol burden.

We also compute $e_{r,\hat{r}}$, which is the excess aerosol burden of location r with respect to location \hat{r} , where \hat{r} (e.g., continent) encompasses r (e.g., countries within continent). Specifically, we compute the percentage deviation between the population-weighted mean exposure from location r and location \hat{r} :

$$e_{r,\hat{r}} = \frac{\mu_r - \mu_{\hat{r}}}{\mu_{\hat{r}}} = \frac{\mu_r}{\mu_{\hat{r}}} - 1 . \quad (13)$$

When r includes all cells within a country and \hat{r} includes all global cells, $e_{\text{country},\text{global}}$ provides

the country-specific excess aerosol burden relative to the global mean. If $e_{\text{country},\text{global}} = 0$, a country's mean exposure level is the same as the global mean. A value of 0.5 or -0.5 for $e_{\text{country},\text{global}} = 0$ indicates that a country's population-weighted AOD measure is 50 percent greater or smaller than the global population-weighted mean.

Importantly, excess aerosol burden also captures the percentage deviation between the share of ambient pollution that a population group is exposed to and the share of population they account for. Specifically, $e_{r,\hat{r}}$ can also be expressed as:

$$e_{r,\text{global}} = \frac{\frac{\text{Location } r \text{ global pop-weighted pollution share}}{\left(\frac{(\sum_{c \in C_r} s_c) \cdot \mu_r}{\mu_{\text{global}}} \right)}}{\frac{\text{Location } r \text{ global population share}}{\left(\sum_{c \in C_r} s_c \right)}} - 1 = \frac{\mu_r}{\mu_{\text{global}}} - 1. \quad (14)$$

Because the term $(\sum_{c \in C_r} s_c) \cdot \mu_r$ appears in both the numerator and the denominator, it cancels out. A value of 0.5 or -0.5 for $e_{r,\text{global}}$ indicates that location r 's share of global population-weighted air pollution is 50 percent greater or smaller than location r 's share of global population.

AOD and PM_{2.5} As a satellite-based measure of air pollution by aerosols, AOD measurements increase with greater concentrations of atmospheric particles, including PM_{2.5} particles. While our analysis is focused on the distribution of air pollution by aerosols as measured by AOD, to assist with the interpretation of the magnitudes of AOD results, in the presentation and discussion of our AOD results, we match measured AOD values to approximate ranges of PM_{2.5} values.

While AOD captures directly visibility experiences, the best-fitting model that maps between atmospheric aerosol measurements and on-the-ground ambient particulate matter exposure experienced by people is parameterized by heterogeneous topological and meteorological circumstances (Chu et al. 2016; Holben et al. 1998; Van Donkelaar et al. 2016; Yang et al. 2019). Overall, atmospheric-based AOD measures have been found to substantively and positively correlate with ground-based aerosol and PM_{2.5} measurements (Bibi et al. 2015; Bright and Gueymard 2019; Chu et al. 2016), and AOD is often used as a predictor of ambient PM_{2.5} exposures with locally and temporally calibrated prediction functions (Chen et al. 2022; Fu et al. 2018; Yang et al. 2019).

To create a globally consistent and transparent scale, we use a global linear model to relate our AOD estimates to existing global estimates of PM_{2.5}. Specifically, we relate the cell-specific annual average AOD values we derived to global gridded estimates of surface PM_{2.5} concentration derived based on models that use satellite-based AOD measures as inputs and ground-based PM_{2.5} data for calibration and model validation (Hammer et al. 2020). Regressing the PM_{2.5} values from Hammer et al. (2020) on our AOD measures, we find that a bivariate linear model with subregion fixed effects provides a reasonable global fit with an R² of 0.78. We obtain similar fit and estimates when we restrict the data to only populated cells or when we use all available cells, and higher polynomial orders do not significantly improve the fit.

In our results discussions, we also compare the AOD-transformed PM_{2.5} measures to the WHO interim targets for particulate matter air pollution.^{A.1} These targets are used as guidelines for classifying the severity of PM_{2.5} exposures. The WHO guideline recommends lowering annual average exposure levels to less than 35 µg/m³, 25 µg/m³, 15 µg/m³, and 10 µg/m³ as interim targets 1, 2, 3, and 4.

Within and across country distributions of air pollution by aerosols Combining global AOD measures and population data, we present in this section the overall population-weighted global distribution of air pollution by aerosols. In contrast to prior studies on global population-based inequality in ambient air pollution, which have focused on comparing means across regions and countries (Shaddick et al. 2018; Van Donkelaar et al. 2021; Van Donkelaar et al. 2016), we study global inequalities by conducting comparisons within and across regions as well as countries.

A.2 Consumption Equivalent Variation (CEV)

Different units of measurement Suppose we have measurements of willingness to pay at some base units, the observed units for the first study are \hat{C}_1 and \hat{P}_1 as well as \hat{C}_2 and \hat{P}_2 . And the relationship between these and our units of interest C and P is:

A.1. The report can be found here <https://www.who.int/publications/i/item/9789240034228>

$$\hat{C}_1 = \gamma_1 \cdot C$$

$$\hat{P}_1 = \rho_{01} + \rho_1 \cdot P$$

$$\hat{C}_2 = \gamma_2 \cdot C$$

$$\hat{P}_2 = \rho_{02} + \rho_2 \cdot P$$

Where $\gamma_1, \rho_1, \gamma_2$, and ρ_2 are conversion factors.

The utility function, in our units of interest, is:

$$U(C, P) = G \left(C - \exp(\Lambda) \cdot \frac{P^{1+\epsilon}}{1+\epsilon} \right)$$

Replacing C and P with \hat{C}_1/γ_1 and \hat{P}_1/ρ_1 , we have:

$$U(\hat{C}_1, \hat{P}_1) = G \left(\frac{\hat{C}_1}{\gamma_1} - \exp(\Lambda) \cdot \frac{\left(\frac{\hat{P}_1 - \rho_{01}}{\rho_1} \right)^{1+\epsilon}}{1+\epsilon} \right)$$

Alternatively, replacing C and P with \hat{C}_2/γ_2 and \hat{P}_2/ρ_2 , we have:

$$U(\hat{C}_2, \hat{P}_2) = G \left(\frac{\hat{C}_2}{\gamma_2} - \exp(\Lambda) \cdot \frac{\left(\frac{\hat{P}_2 - \rho_{02}}{\rho_2} \right)^{1+\epsilon}}{1+\epsilon} \right)$$

The marginal rate of substitution between pollution and consumption, in the units of \hat{C}_j and \hat{P}_j , is:

$$MRS_{\hat{P}_j, \hat{C}_j} = \frac{\frac{\partial U}{\partial \hat{P}_j}}{\frac{\partial U}{\partial \hat{C}_j}} = \frac{\frac{\partial U}{\partial P} \cdot \frac{\partial P}{\partial \hat{P}_j}}{\frac{\partial U}{\partial C} \cdot \frac{\partial C}{\partial \hat{C}_j}} = \frac{\frac{\partial U}{\partial P} \cdot \frac{1}{\rho_j}}{\frac{\partial U}{\partial C} \cdot \frac{1}{\gamma_j}} = \frac{\frac{\partial U}{\partial P}}{\frac{\partial U}{\partial C}} \cdot \frac{\gamma_j}{\rho_j} = MRS_{C, P} \cdot \frac{\gamma_j}{\rho_j}$$

Hence, the log of negative one times the marginal rate of substitution in the units of \hat{C}_j and

\hat{P}_j is:

$$\begin{aligned}\log(-MRS_{\hat{P}_j, \hat{C}_j}) &= \log(-MRS_{C, P}) + \log\left(\frac{\gamma_j}{\rho_j}\right) \\ &= \Lambda + \epsilon \cdot \log(P) + \log\left(\frac{\gamma_j}{\rho_j}\right) \\ &= \left(\Lambda + \log\left(\frac{\gamma_j}{\rho_j}\right)\right) + \epsilon \cdot \log\left(\frac{\hat{P}_j - \rho_{0j}}{\rho_j}\right)\end{aligned}$$

Now, suppose we have two sets of measurements on willingness to pay as well as pollution levels, in the units of \hat{C}_1 and \hat{P}_1 as well as \hat{C}_2 and \hat{P}_2 . We can update the equations we had earlier to:

$$\begin{aligned}\log\left(\frac{\Delta_{\hat{C}_1}^*}{\Delta_{\hat{P}_1}}\right) &= \left(\Lambda + \log\left(\frac{\gamma_1}{\rho_1}\right)\right) + \epsilon \cdot \log\left(\frac{\hat{P}_1 - \rho_{01}}{\rho_1}\right) \\ \log\left(\frac{\Delta_{\hat{C}_2}^*}{\Delta_{\hat{P}_2}}\right) &= \left(\Lambda + \log\left(\frac{\gamma_2}{\rho_2}\right)\right) + \epsilon \cdot \log\left(\frac{\hat{P}_2 - \rho_{02}}{\rho_2}\right)\end{aligned}$$

Given these two equations and two unknowns, we can solve for Λ and ϵ as before. The solution is:

$$\begin{aligned}\epsilon &= \frac{\log\left(\frac{\Delta_{\hat{C}_1}^*}{\Delta_{\hat{P}_1}}\right) - \log\left(\frac{\Delta_{\hat{C}_2}^*}{\Delta_{\hat{P}_2}}\right) + \log\left(\frac{\gamma_2/\rho_2}{\gamma_1/\rho_1}\right)}{\log\left(\frac{\hat{P}_1 - \rho_{01}}{\rho_1}\right) - \log\left(\frac{\hat{P}_2 - \rho_{02}}{\rho_2}\right)} \\ \Lambda &= \log\left(\frac{\Delta_{\hat{C}_1}^*}{\Delta_{\hat{P}_1}}\right) - \epsilon \cdot \log\left(\frac{\hat{P}_1 - \rho_{01}}{\rho_1}\right) - \log\left(\frac{\gamma_1}{\rho_1}\right)\end{aligned}$$

Where \hat{P}_1 and \hat{P}_2 are the pollution levels at which the willingness to pay measurements were made, these can be the mid-point pollution levels, as discussed earlier.

Going from data to estimates of Λ and ϵ with different units of measurements Suppose we have the following measurements. For PM10, we have two sets of willingness-to-pay data.

These are the same results as before for our test, but now we keep the change in consumption in units of pounds and dollars, and use γ for currency conversion. Additionally, we assume our units of interest are PM10, so we do not need to convert pollution units, hence $\rho_0 = 0$ and $\rho = 1$.

Given this information, and given our formula earlier, we can solve for Λ and ϵ as follows:

$$P_{\text{mid1}} = (15.4 + 14.4)/2 = 14.9$$

$$P_{\text{mid2}} = (51.7 + 50.7)/2 = 51.2$$

$$\epsilon = \frac{\log(40.5) - \log(48) + \log\left(\frac{1/1}{0.75/1}\right)}{\log(14.9) - \log(51.2)} = 0.0955$$

$$\Lambda = \log(40.5) - (0.0955) \cdot \log(14.9) - \log(0.75) = 4.2466$$

Then $\exp(\Lambda) = \exp(4.2466) = 69.9$, and $1 + \epsilon = 0.9045$. Note, these are approximately the same as what we arrived at earlier. The numbers are not the same because our currency conversion factor is not exact.

B Data

B.1 AOD

Aerosol Optical Depth (AOD) is a satellite-based measure of the extent to which aerosols in a vertical column of the atmosphere scatter and absorb sunlight. Higher AOD values indicate a greater total aerosol load, which can be influenced by aerosol concentration, particle size distribution, and composition (Lenoble, Remer, and Tanre 2013). Typically, AOD measurements usually range from 0 to 1, but can span from -0.5 to 5. Negative values do not represent negative aerosol concentrations; rather, they indicate uncertainty in AOD retrieval. These negative values can be understood as very small positive AOD values which are attributed negatively due to measurement uncertainty. An AOD value less than 0.1 indicates clear skies and excellent satellite-to-surface visibility, while an AOD value near 1 indicates very hazy conditions. Values above 1 suggest thicker smoke in the atmosphere. Since values above 5 tend to be estimated with low confidence, the data is constrained to a maximum of 5 (NASA Earth Observatory 2024).

The NASA Aerosol Optical Depth (AOD) dataset is a publicly available collection of level-2 processed satellite images. Specifically, the AOD data is computed based on images collected by the TERRA satellite via MODIS instruments, and is accessible via NASA EarthData's Open-DAP protocol. (Cornillon, Gallagher, and Sgouros 2003; Xiong et al. 2020)

The AOD dataset has been continuously updated since 2002, with new satellite images regularly added. The satellite used to capture these images is TERRA, equipped with the MODIS (or Moderate Resolution Imaging Spectroradiometer) instrument, which provides a spatial resolution of 3km and a temporal resolution of 5 minutes. After capturing the images, a processing algorithm is used to extract information about the aerosol properties and produce the AOD measurement.

In our analysis, we collect AOD measurements for each 3km x 3km cell across the globe and aggregate them into 1-degree latitude and longitude combinations ($\sim 110\text{km} \times 110\text{km}$) . Figure E.1 illustrates the global availability of the AOD measures in 2010. This figure plots the frequency of AOD measures for 1-degree latitude-longitude combinations, showing that a considerable share of them are covered for more than a third of the year. However, in some places it is hard to process satellite images, such as deserts and ice coverage, leading to missing information.

The AOD measurement has been widely utilized in scientific research as a predictor of pollution, particularly in estimating PM_{2.5} levels(Chen et al. 2022; Fu et al. 2018; Yang et al. 2019). Documented evidence suggested that higher AOD values are positively correlated with higher levels of PM_{2.5}, which means more air pollution. (Bibi et al. 2015; Bright and Gueymard 2019; Chu et al. 2016)

The availability of this global dataset allows us to conduct comprehensive analyses of air pollution exposure on a global scale, as well as the ability to focus on specific regions or areas of interest.

B.1.1 Data download

To access the NASA EarthData, it is necessary to register a user and key in the Nasa EarthData website (Free registration). The key provided allows one to create a connection with OpenDAP servers, which is a extensively used cloud service that provides efficient access and storage to big datasets, as satellite iamges. In the case of NASA, creating an OpenDAP connection to make queries allows the user to access the AOD dataset at the daily level directly from your command prompt. This makes the process more efficient as the user does not need to download the datasets to process it.

B.1.2 Aggregation over space along satellite track

As mentioned before, the satellite data information collected from NASA has finer data as 3kmx3km. However, to merge the pollution information with the SEDAC population dataset, we aggregated the cells into one-degree combinations. The aggregation was done using a ceiling round method, which rounded all the latitude and longitude information to 1-degree (~ 110km). For instance, if one location is identified by latitude 49.568 and longitude -34.543, the aggregation method will transform this geo-location into 49 (lat) and -34 (long). After rounding latitude and longitude columns, we took the average AOD associated with a particular latitude-longitude 1-degree combination.

In figure E.4 we plot 1 degree x degree yearly measurements for 6 big cities in the world to illustrate how the cell annual average AOD is computed. On the x-axis we have the days within the months, which are plotted on the y-axis. For each combination of month-day we have either a missing (white cells) due to lack of observations in that particular day, or average AOD on that day (colorful cells). The cell average AOD is calculated by taking the mean of

these values.

In figure E.4, we can also see that the NASA AOD measures capture higher concentrations of pollution in cities well known for their higher concentration of pollutants, as Beijing and New Delhi. Comparing these two cities with other cities plotted in E.4, we can see that the frequency of darker colors is higher across and within months compared to other locations.

B.2 The location X day file

Using OpenDap we could access all days of the year 2010 and construct a dataset linking locations and days. The first column contains 1-degree combinations of latitude and longitude, where other columns correspond to AOD measures of these locations on each day of the year. Using this location day information, we can create our measure of average AOD concentration in each cell in the world. The number of observations per cell depends on the ability of the algorithm used by NASA to capture light, which is affected by some natural factors such as clouds, desert, and ice. To deal with potential lacking information, we use interpolation methods in our dataset.

B.2.1 Interpolation at time and location with missing information

The AOD dataset has global coverage but this coverage does not happen daily. Due to the satellite orbit, some cells are not covered every day, which creates potential missing daily information. Another issue is the incapacity of the algorithm to process images from deserts, oceans, or ice due to refraction, leading to missing values in the dataset. For example, the Sahara desert and Polars regions do not have much information due to the impossibility of processing the image in very reflective conditions (ice and sand). These issues lead to missings in two dimensions: time and location.

To test how sensitive our results are to these missing, we used interpolation methods to produce interpolated datasets based on the original AOD data. We used the Python package `numpy` which contains implemented interpolation functions that can be applied to our datasets. Additionally, we perform interpolation using one dimension (location) and two dimensions (location, time).

Figure E.1 illustrates the global availability of the AOD measures in 2010. This figure plots the frequency of AOD measures for 1-degree latitude-longitude combinations, where days are represented through shades of red from the darkest red (0 days) to the lightest red (all days

in the year). Our data shows that a considerable share of them are covered for more than a third of the year. However, some places where exacerbated reflexivity — such as deserts and ice coverage — makes satellite images hard to read, we do not have information.

On days in which we do not have available AOD information for a particular cell, we use information in neighboring locations and time periods to perform 3-dimensional—longitude, latitude, and time—interpolation and extrapolation to generate estimates for missing AOD data.

Given daily information, we compute annual average AOD exposures for each cell, first using only the raw data ignoring the days with missing values, and then separately using the raw data complemented with the interpolated and extrapolated estimates. Figure E.5 shows the distribution of our annual average AOD values at the cell level.

Due to the concentration of missing AOD data in regions with the least population, as shown in Figure E.2, our population-weighted AOD distributional results based on the raw data and interpolated and extrapolated data are very similar. Our global inequality results presented in the text are based on annual averages of the raw data.

B.3 SEDAC Population file

SEDAC stands for Socioeconomic Data and Applications Center and is a center that relates earth science data to socioeconomic data. Specifically, in this analysis, we are exploiting the Gridded Population of the World version 4 (GPWv4) (CIESIN Columbia University 2018) which presents the estimates of the global population by gender and by age groups. These estimates come from the Population census or each country’s population register. The data on the boundary comes from various sources including the GADM database of Global Administrative Areas, the Bureau of Statistics, the UN Office for the Coordination of Humanitarian Affairs, and the Center for International Earth Science Information Network (CIESIN) which hosts the SEDAC databases. Thus, the GPWv4 combines country-based administrative level data and administrative boundary data and distributes them into 30 arc-second grids (~1km at the equator) using a proportional allocation. The distribution by age and gender is done by using the proportion of males, females, and different age groups in each geographic unit and by applying those proportions to the 2010 estimates of the population in those same geographic units.

In our analysis, we used the 1-degree resolution (~110km) version of the data to create some

input files for further analysis. We use the geographic information available to create unique geo-code IDs that will allow us to uniquely identify each grid. We used the population data available by groups to create a unique category of population for each 1-degree combination grid. Figure E.6 illustrates the global population distribution based on the SEDAC dataset in 2010, we plot the share of the world's population per cell. Some locations well known for their population sizes, such as India and China appear as hot spots in the heat map.

B.4 Subnational GDP data

The gridded global GDP dataset used in this paper is a product from the Gridded global datasets for Gross Domestic Product (Kummu, Taka, and Guillaume 2018). This data is derived from subnational GDP per capita data from Gennaioli et al. 2013, with the GDP per capita values adjusted for purchasing price parity and based on 2005 international dollars.

B.4.1 Source of data for GDP and Pop

For GDP per capita at the country level, we are using the World Bank's publicly available databases. This database has information on countries' GDP and is linked with the ISOCODE and ISONAMES for each country. Using these codes, we can merge the GDP and the pollution measures by using our key location files, which are all linked through the 1-degree geolocation combinations.

To get the country population info, we aggregated all the cell information within a country to get its population estimation using SEDAC. However, this method may have issues due the size of the cells. which led us to use other population data sources as robustness.

B.5 Merging and National and subnational boundaries

We combine the 2010 annual average AOD across 1° cell with the cell-specific total population estimates from around 2010. Because cells without any population will not impact population weighted statistics, we select the subset of cells from the annual average AOD vector which has corresponding non-zero cell-specific population estimates. Additionally, to allow for the comparisons of population-weighted AOD distributions across and within countries and economies, we identify the subset of populated-cells that intersect with national-level boundary enclosures. To consider the relationship between population-weighted AOD distribution and GDP per capita at the subnational level, we also identify subsets of populated-cells

that intersect with subnational boundary data embedded in the subnational GDP data from (Kummu, Taka, and Guillaume 2018).

B.5.1 Country Boundaries and names

To identify which country is associated with the 1-degree latitude longitude combinations, we use SEDAC as the input data. The raster from SEDAC has two layers that inform the country in a particular degree combination. First, they inform the UNSDCODE, an international standardized code for each country defined by the United Nations Statistics Division (UNSD), also known as the M49 code. Two, they also inform the international standardized acronyms for these countries (ISOCODE). For example, Brazil's UNSDCODE is 076 and its ISOCODE is BRA. To add country and region names, we merge the Standard country or area codes for statistical use (M49) dataset from United Nations using the ISOCODE column from SEDAC. This dataset contains geographical units's names and codes for different administrative levels, as continents, subregions, and countries. For example, the ISOCODE BRA is associated to Brazil (country name), South America (Region name) and Latin America and the Caribbean (Subregion name). With this, we can create our country key file linking degree combinations and country information, as region and subregion. The input data used by SEDAC to categorize these boundaries are the censuses.

The fact that we are using 1-degree latitude longitude combinations can lead to imprecise borders due to the size of the cells. 1 degree corresponds to approximately 110 km, which can incorporate full cities. For example, figure E.3 shows how the cells are allocated to different countries in the world. We can see that the size of the cell allocates some land to countries that it is not actually precise. For example, SEDAC categorizes part of Peru, Bolivia, Paraguay, and Uruguay to Brazil. This can impact the measurements if it includes major cities or populated areas. A specific case is Santiago in Chile, which is allocated to Argentina due to the size of the cells. Because of this, an important part of Chile that concentrates 40 % of its population and the most polluted region is allocated to Argentina. This can impact the inequality and mean measures of countries depending on their size and shape.

B.5.2 How do we use it, matching of coordinates to boundaries

To match these coordinates, we created a file called skeleton, which includes all the 1-degree combinations in the world. Using SEDAC, we can build a dataset with three columns, latitude

and longitude combination (one degree), ISOCODE, and UNSDCODE. After merging these files, we can use it to merge with our geographical units, population and pollution datasets also linked using the latitude-longitude combinations and ISOCODES.

C Integrating Climatic and Population Data

C.1 Program and Framework for analysis

The key file inputs make possible the merge between the geocoded pollution, population, and country datasets. In our analysis, we used two file inputs:

1. key_loc.csv
2. key_country_code_finer_subregions.csv.

The first key file has an id for every latitude-longitude combination at 1 degree level. The IDs were constructed using the following pattern. The latitude and longitude numbers were transformed into strings and concatenated (using "_" to separate the numbers) into one string called "geo_id ". For example, the location defined by latitude 45 and longitude -67 has the geo_id as "45_-67". After constructing all the possible geo_ids combinations, we sorted the location by latitude and longitude and assigned a number to each geo_id following the ascending order. This new column is called id_location and it is used to merge locations across different datasets, such as the pollution and the population geocoded information.

The second key file has the id_location and geo_id columns associated with geographical locations in the world. four layers of location: continent, subregion, and country. For instance, we know what are the latitude and longitude combinations that are associated with specific continents, sub-regions, and countries, which makes it possible to merge geocoded information from other datasets.

D Additional Results on heat exposure for children

D.1 Overall global distribution

D.1.1 Global country-level distribution

Figure E.7 and E.8 present histograms for the global relative distribution of air pollution by aerosols as measured by Aerosol Optical Depth (AOD). The x-axis is in units of global excess aerosol burdens. For the weighted distributions, we compute annual average AOD for each $1^\circ \times 1^\circ$ longitude–latitude grid (cell) and generate country-specific AOD measures as cell-population weighted averages. The country-based distribution in Panel (a) uses country-specific AOD, weighted by aggregate population estimates for each country. The cell-based distribution in Panel (b) uses cell-specific AOD, weighted by cell-specific population estimates. The population weights are important because distributions where national or subnational units have equal weights mask the heterogeneous population burdens of exposure across geographical units.^{D.1}

The variance for the cell-based distribution of in Panel (b) is 1.7 times larger than the country-based distribution in Panel (a), illustrating the wider distribution at the cell level. Moreover, Panel (a)'s country-level distribution of global excess aerosol burden ranges from -0.81 to 1.18, and has an 80th percentile that is 1.44 times larger relative to its 20th percentile. In contrast, Panel (b)'s cell level distribution of global excess aerosol burden ranges from approximately -1.0 to 10.06, and has an 80th percentile that is 3.62 times more exposed than the 20th percentile.

Comparisons between panels demonstrate that country-level information masks inequalities across cells within countries. Our analysis in the following sections will focus on population-weighted cell-based distributions.

D.1.2 Global cell-level distribution

Panel (a) of Figure 1 presents a global map of the relative distribution of air pollution by aerosols - calculated according to equation (??) - matching cell-specific AOD to cell locations. The colors correspond to levels of global excess aerosol burdens—darker shades of green (red) represent greater magnitudes of negative (positive) excess burdens.

D.1. In Appendix Figure E.8, we present un-weighted histograms. Comparing the distributions with and without weights, we can see a shift of the weighted distributions to the right. These shifts highlight the importance of considering the population weights, as our interest is how individuals in countries are exposed to air pollution.

The map shows that Asia and Africa have relatively higher levels of air pollution by aerosols. Focusing on countries, India, China, and Pakistan stand out as large countries with areas experiencing high levels of excess aerosol burdens. In contrast, Australia, Mexico, and Argentina are also large economies but have relatively lower levels of excess aerosol burdens. Additionally, there are variations in the within-country heterogeneities of exposures. For example, locations in the southeastern and northwestern regions of China have high excess burdens, but areas in northern and southwestern China have relatively lower levels of excess burdens. In contrast, countries within Western Europe and North America tend to have limited variations concentrated around lower levels of excess burdens.

D.2 Regional distribution

D.2.1 Africa

The most populous African country, Nigeria, has an annual average AOD of 0.56 ($\approx 28.98 \mu\text{g}/\text{m}^3$ of PM_{2.5}), which is behind WHO interim target 2. Nigeria's average exposure level corresponds to a global excess aerosol burden of 0.24, meaning that Nigeria's global share of air pollution by aerosols is 24% larger than its population share. Exposure inequalities are significant within Nigeria—Nigerian population at the 80th (90th) percentile of aerosol distribution are 77% (106%) more exposed than those at the 20th (10th) percentile. One of the least populous countries in Africa, São Tome and Principe, has an average annual AOD of 0.47 ($\approx 24.65 \mu\text{g}/\text{m}^3$ of PM_{2.5}), just passing WHO interim target 2. In contrast to Nigeria, relative population exposure percentiles are close to 1 due to the small size of the country.

D.2.2 Americas

South America has the highest average annual AOD at 0.22 ($\approx 12.93 \mu\text{g}/\text{m}^3$ of PM_{2.5}). Central America has the lowest average annual AOD at 0.19 ($\approx 11.65 \mu\text{g}/\text{m}^3$ of PM_{2.5}). All regions in the Americas, on average, have reached WHO interim targets 3.

The most populous country in the Americas, the United States of America, has an annual average AOD of 0.19 ($\approx 11.67 \mu\text{g}/\text{m}^3$ of PM_{2.5}), close to reach WHO interim target 4. The US's average exposure level corresponds to a global excess aerosol burden of -0.56, meaning that the US's global share of air pollution by aerosols is 56% smaller than its population share. Exposure inequalities are important but limited in the US—Americans population at the 80th

(90th) percentile of aerosol distribution are 36% (71%) more exposed than those at the 20th (10th) percentile. One of the least populous countries in the Americas, Saint Lucia, has an average annual AOD of 0.21 ($\approx 12.49 \mu\text{g}/\text{m}^3$ of PM_{2.5}). Relative population exposure percentiles is equal to 1 in Saint Lucia. Not all countries with low population have no within-country exposure variabilities. Suriname, which is another low population country in the Americas, has a similar AOD level as Saint Lucia, but greater within-country variabilities—Surinamese population at the 20th percentile of aerosol distribution are 36% more exposed than those at the 80th percentile.

D.2.3 Asia

The most populous Asian country, China, has an annual average AOD of 0.7 ($\approx 35.58 \mu\text{g}/\text{m}^3$ of PM_{2.5}), which is behind WHO interim target 1, indicating very hazardous levels of average air pollution by aerosols. China's average exposure level corresponds to a global excess aerosol burden of 0.55, meaning that China's global share of air pollution by aerosols is 55% larger than its population share. Exposure inequalities are large within China—the Chinese population at the 80th (90th) percentile of aerosol distribution are 111% (216%) more exposed than those at the 20th (10th) percentile. One of the least populous countries in Asia, Qatar, has an average annual AOD of 0.60, which is similar to the level in China. Relative population exposure percentiles are equal to 1 due to the geographical confines of Qatar.

D.2.4 Europe

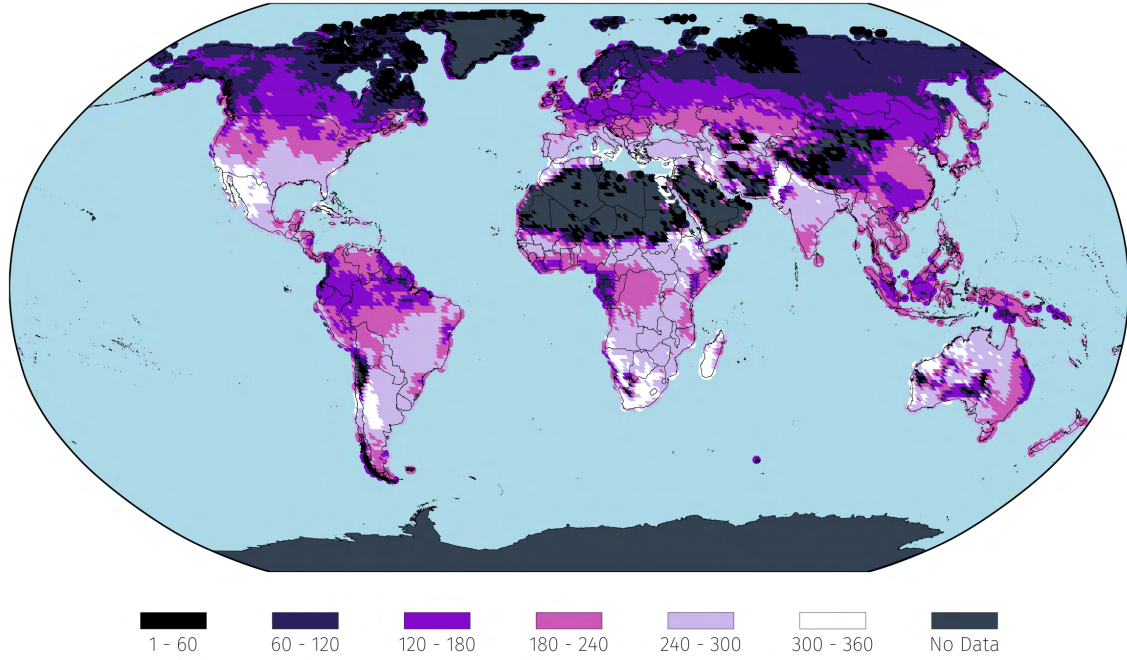
The most populous European country, Russia, has an annual average AOD of 0.29 ($\approx 16.39 \mu\text{g}/\text{m}^3$ of PM_{2.5}), which is behind WHO interim target 3. Russia's average exposure level corresponds to a global excess aerosol burden of -0.34, meaning that Russia's global share of air pollution by aerosols is 34% smaller than its population share. Exposure inequalities are significant within Russia—Russian population at the 80th (90th) percentile of aerosol distribution are 67% (130%) more exposed than those at the 20th (10th) percentile. One of the least populous countries in Europe, Iceland, has an average annual AOD of 0.21 ($\approx 12.68 \mu\text{g}/\text{m}^3$ of PM_{2.5}), close to reaching WHO interim target 4. Despite its limited population, there are exposure variabilities in Iceland due to its large geography—Icelandic population at the 80th (90th) percentile of aerosol distribution are 39% (49%) more exposed than those at the 20th (10th) percentile.

D.2.5 Oceania

Australia is the most populated country in the Oceania region and the least populated is Palau. In AOD terms, the mean exposure to pollution in Australia is 0.11, whereas the inequality measured using the ratio between 80th and the 20th percentiles indicates 29% more exposure to pollution to the upper side of the distribution. If we consider the extremes percentiles ratios, the 90th percentile is 48% more exposed to pollution in comparison to the 10th percentile. For Palau, the mean AOD exposure is 0.13, whereas the inequality using the percentile ratios in 1.03 and 1.03 for both ratios, indicates 3% more exposure faced by the upper part of the distribution. In PM_{2.5} terms, the mean exposure faced by Australia is 21.23, higher than the third worse level recommendation by WHO, and the inequality measure for the 80th measure is 19% and 30% for the 90th percentile ratio. For Palau, the pm is 2.5. measures imply a mean exposure of 8.89 (below WHO guidelines) and the ratio for both inequality measures is 1.02, i.e., 2% more exposure faced by the upper part of the population distribution.

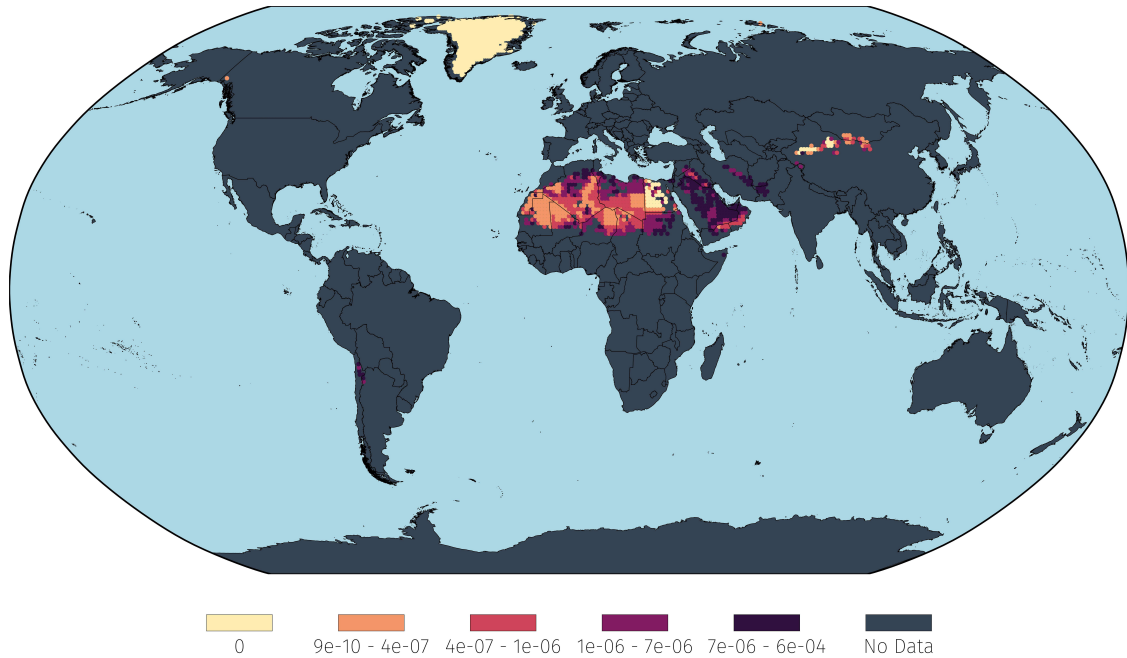
E Additional Figures and Tables

Figure E.1: Number of days with AOD data available for each $1^\circ \times 1^\circ$ longitude–latitude grid, 2010



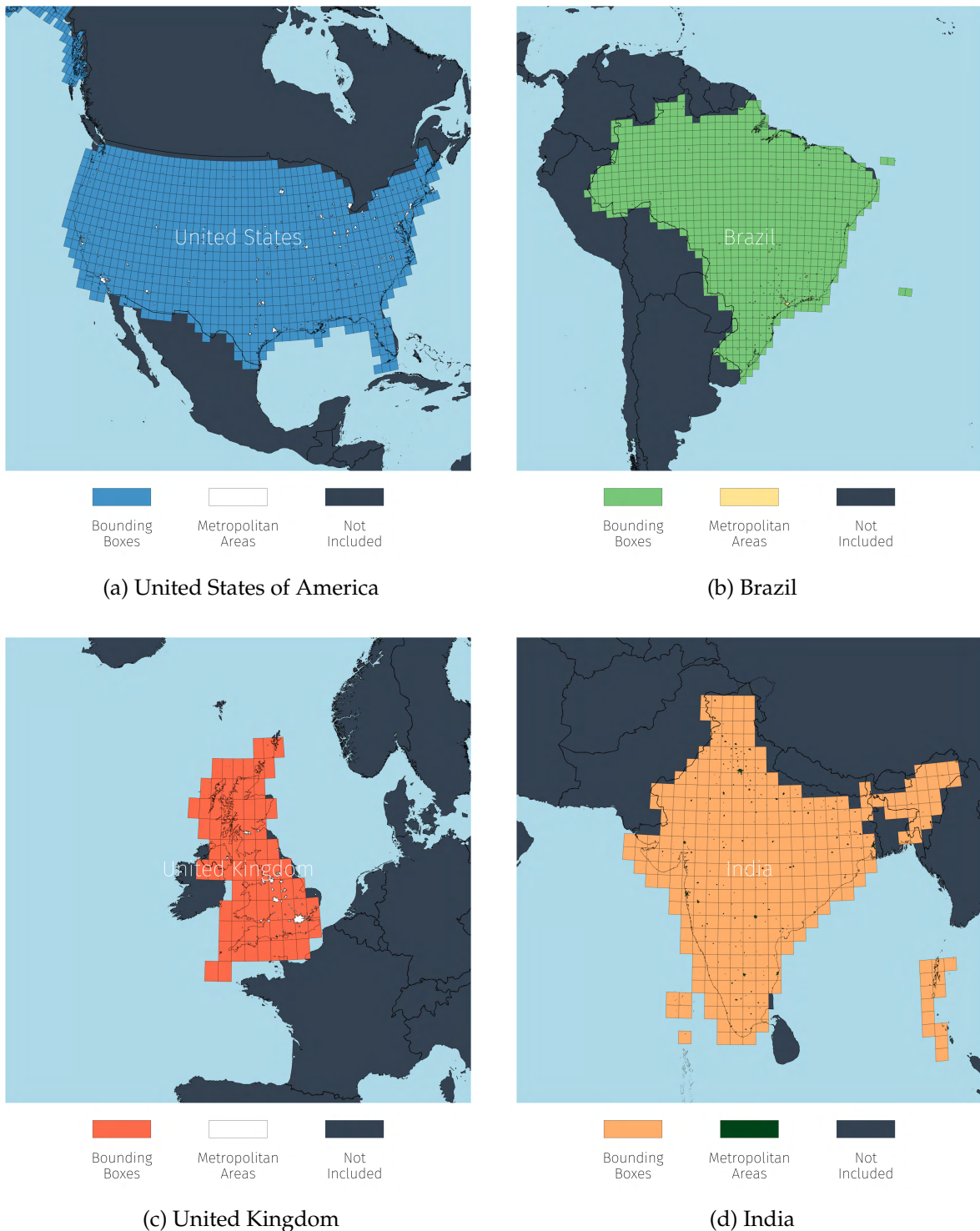
Notes: The figure presents the geographical and temporal availability of Aerosol Optical Depth (AOD) data, our global proxy for ambient particulate matter pollution exposures. For our analysis, we download raw AOD data available at $3\text{km} \times 3\text{km}$ resolution and compute average daily AOD on each day of the year with available AOD measurements for each $1^\circ \times 1^\circ$ longitude–latitude grid (cell). The figure shows the number of days in 2010 during which AOD data was available within each cell. The days are represented through shades of purple and pink from the darkest purple (1 day) to the lightest pink (almost all days in the year); days with zero data are represented by a gray color. Due to the concentration of missing AOD data in regions with the least population, our population-weighted AOD distributional results based on the raw data and interpolated and extrapolated data are very similar. Our global inequality results presented in the text are based on annual averages of the raw data.

Figure E.2: Population shares in areas with no raw AOD measurements $1^\circ \times 1^\circ$ longitude–latitude grid, 2010



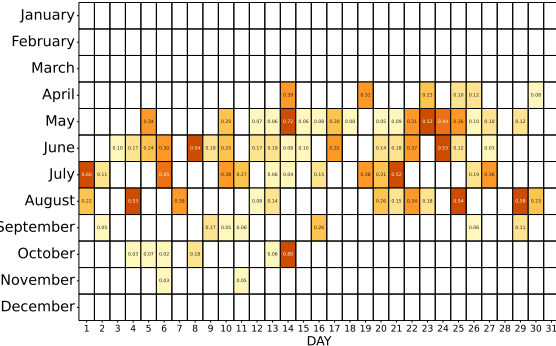
Notes: The figure plots the population shares of areas for which no AOD measurements exist. The share of global population represented by all colored areas amounts to just 0.00602 with 99.8% of cells in this section having a population share below the mean population share (0.000128) in areas with existing AOD measurements. Similarly, 85.8% of cells in this area have values below the median population measure (0.0000069) in areas for which AOD values exist. This means that above-global-average AOD measurements would have to had existed in these areas for our global population-weighted AOD mean to remain the same, otherwise our global mean would be lower than what was calculated meaning relative burden measures can be considered conservative estimates.

Figure E.3: $1^\circ \times 1^\circ$ longitude–latitude grids over select countries

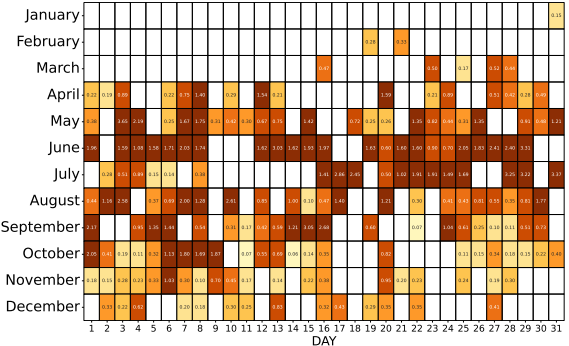


Notes: These plots display $1^\circ \times 1^\circ$ cells over select countries along a spherical surface. These boxes serve as a visual illustration of the area along which we aggregate our AOD data for a given day; the average AOD in a given $1^\circ \times 1^\circ$ area for a given day is then associated to the new $1^\circ \times 1^\circ$ coordinate point. The classification of a given coordinate as belonging to a given country was determined by NASA's SEDAC population layer.

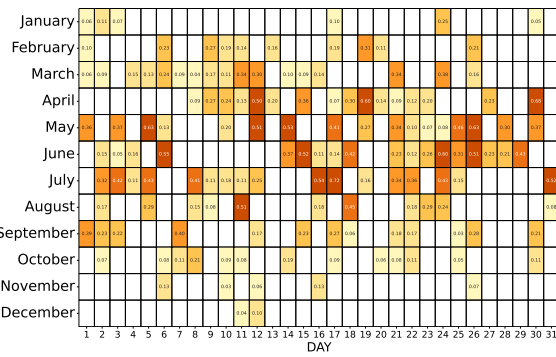
Figure E.4: AOD measurement heatmaps for major cities by $1^\circ \times 1^\circ$ longitude–latitude grids, 2010



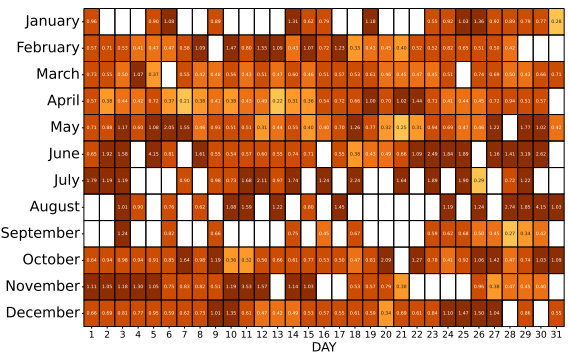
(a) New York City, United States



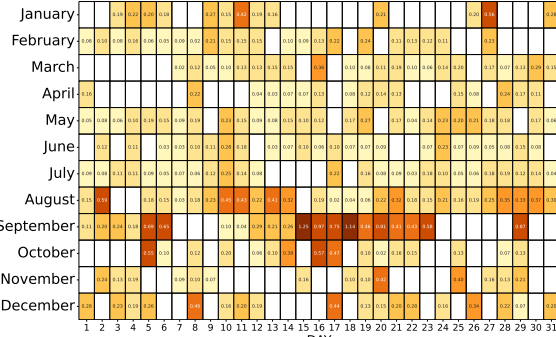
(b) Beijing, China



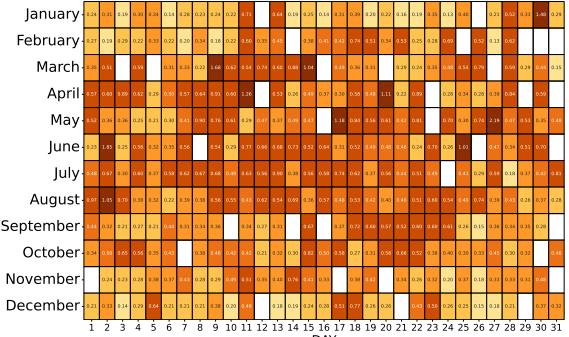
(c) London, United Kingdom



(d) New Dehli, India



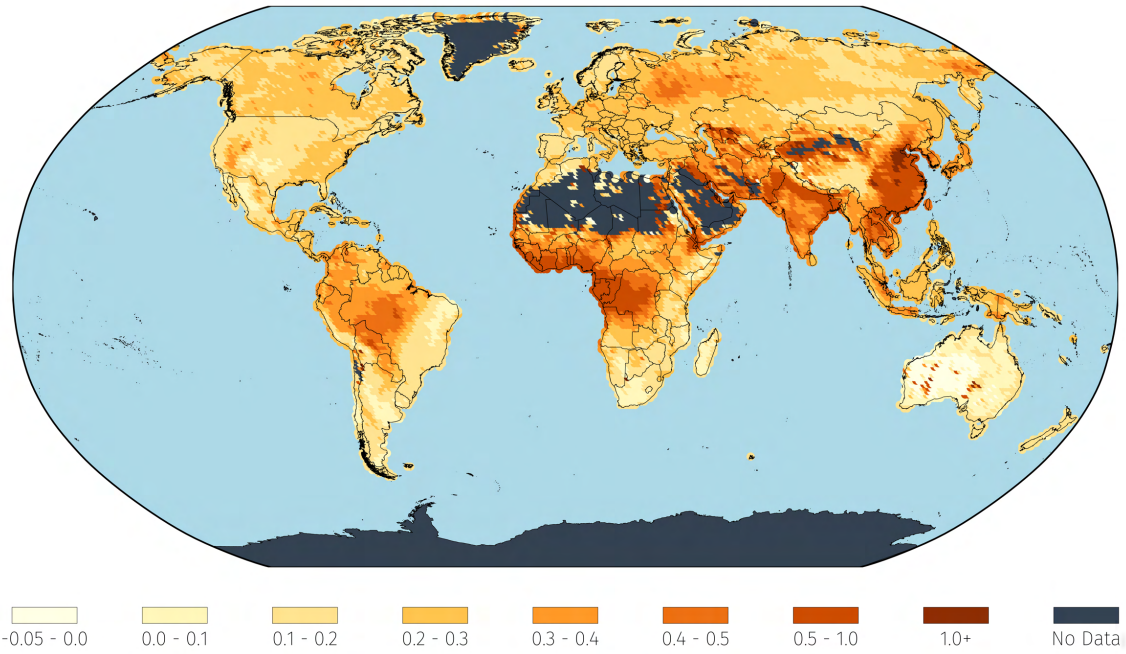
(e) São Paulo, Brazil



(f) Cairo, Egypt

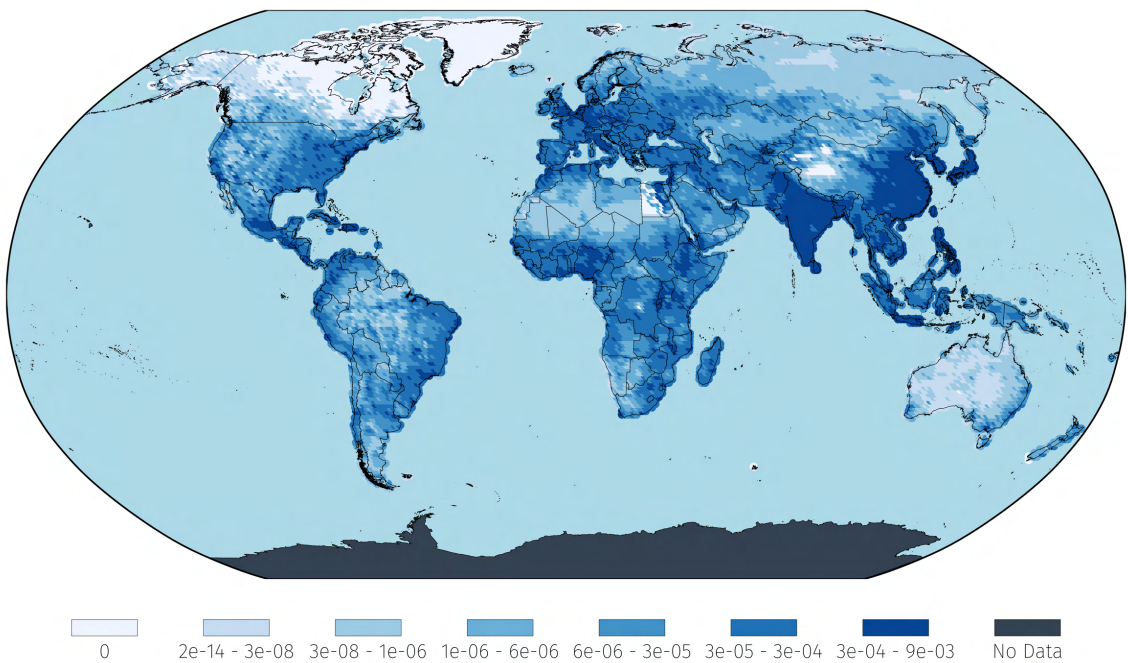
Notes: Daily Aerosol Optical Depth (AOD) measurements for the year 2010, displayed as calendar heatmaps for selected major global cities: São Paulo, New York City, New Delhi, London, Cairo, and Beijing. Each heatmap represents AOD values captured over a $1^\circ \times 1^\circ$ grid centered on the city, with darker colors indicating higher AOD values. Empty cells denote days with no available data. The coordinate grids were determined by applying the ceiling function to the longitude and latitude of each city's central coordinates. These visualizations highlight temporal variations in atmospheric aerosol loading, with notable peaks often associated with seasonal pollution events, such as biomass burning or dust storms.

Figure E.5: Daily-averaged-then-annualized AOD values for each $1^\circ \times 1^\circ$ longitude–latitude grid, 2010



Notes: The figure presents the Aerosol Optical Depth (AOD) values for each coordinate grid, globally, as computed by first averaging collected values in a given day for a given coordinate, for each day, then annualized across daily data, for 2010. Darker shades of orange indicate higher levels of AOD

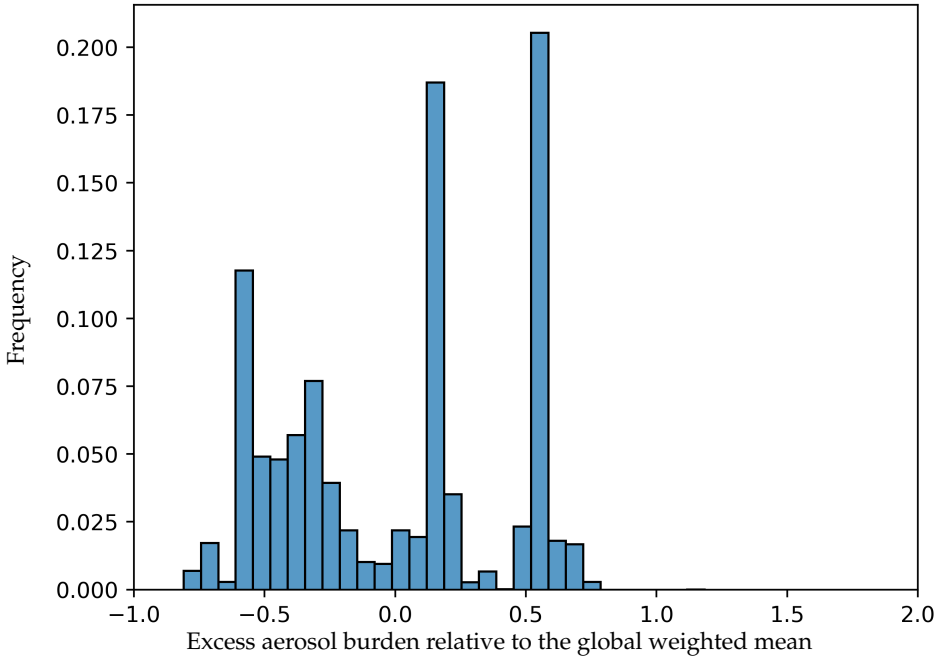
Figure E.6: GPWv4 population shares for each $1^\circ \times 1^\circ$ longitude–latitude grid, 2010



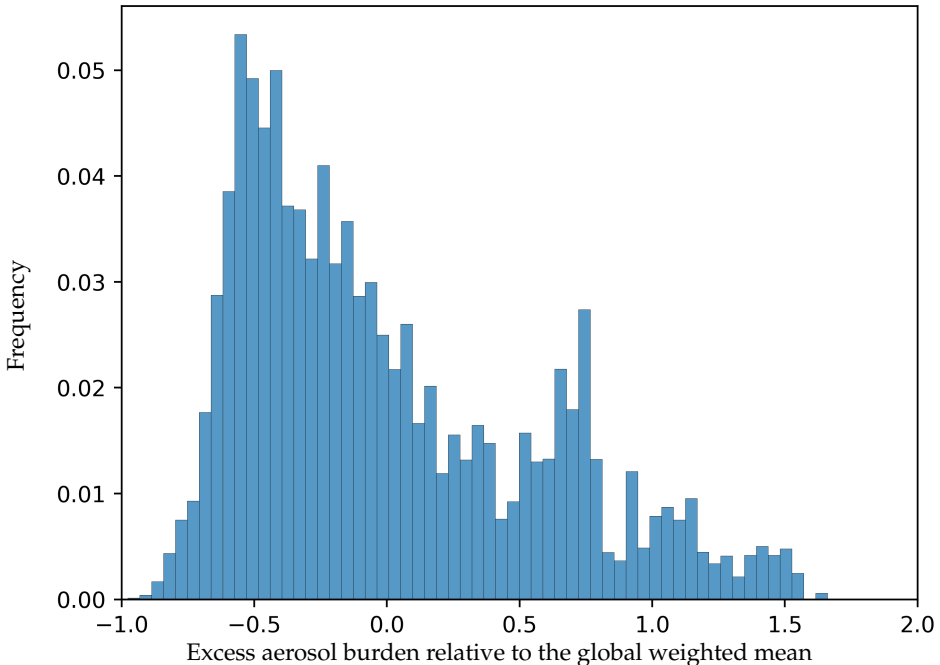
Notes: The figure presents raw population figures as part of SEDAC's GPWv4 population data collection, for 2010. The units of measurements are cell-level global population shares for every $1^\circ \times 1^\circ$ grid. Darker shades of blue indicate a higher population share.

Figure E.7: Population weighted Global dispersion of air pollution by aerosols, 2010

(a) Country as the unit of observation (population weight for each country)



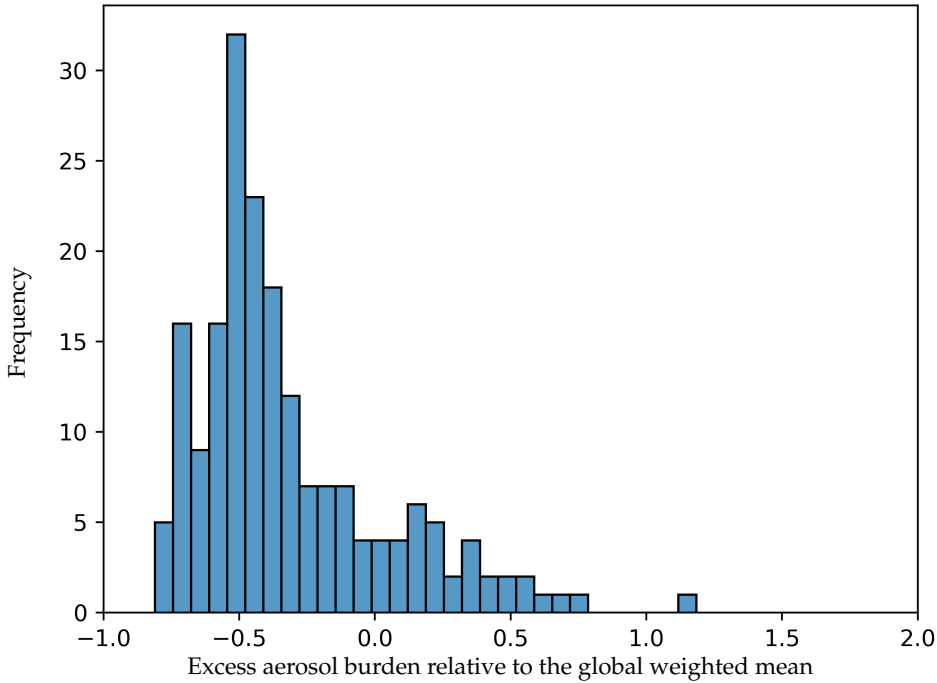
(b) 1° cell as the unit of observation (population weight for each cell)



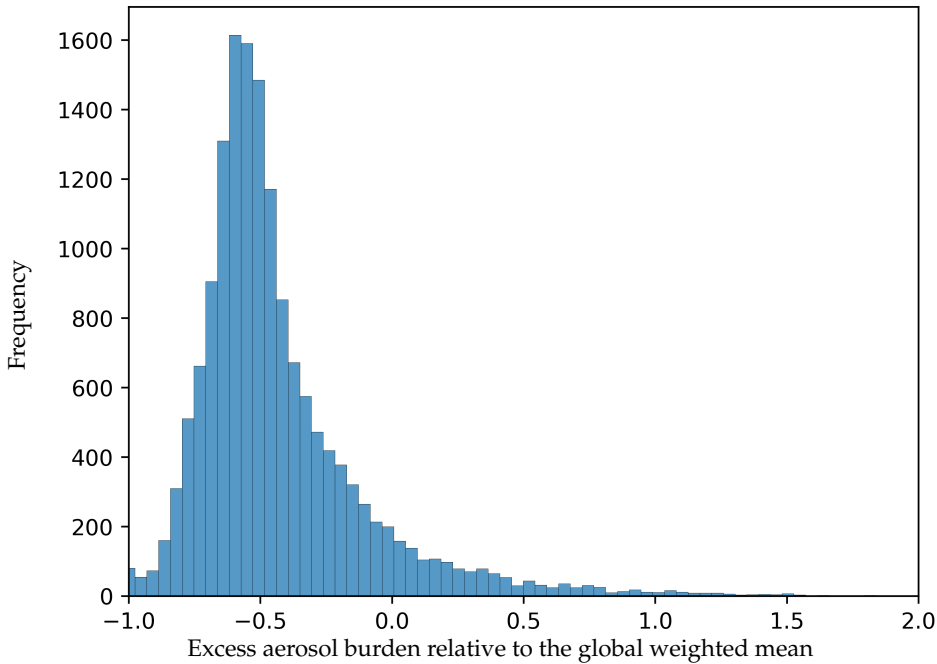
Notes: The panels present the population weighted global relative dispersion of air pollution by aerosols as measured by Aerosol Optical Depth (AOD). We compute annual average AOD for each cell ($1^\circ \times 1^\circ$ longitude–latitude grid) and then generate country-specific AOD as cell-population weighted averages. The y-axis shows frequencies, counting the number of countries or cells. The x-axis is in units of what we call global excess population-pollution burden (EPB): A value of 0.5 (-0.5) indicates that a country or cell's AOD measure is 50 percent greater (smaller) than the global weighted mean.

Figure E.8: Unweighted Global dispersion of air pollution by aerosols, 2010

(a) Country as the unit of observation (equal weight for each country)



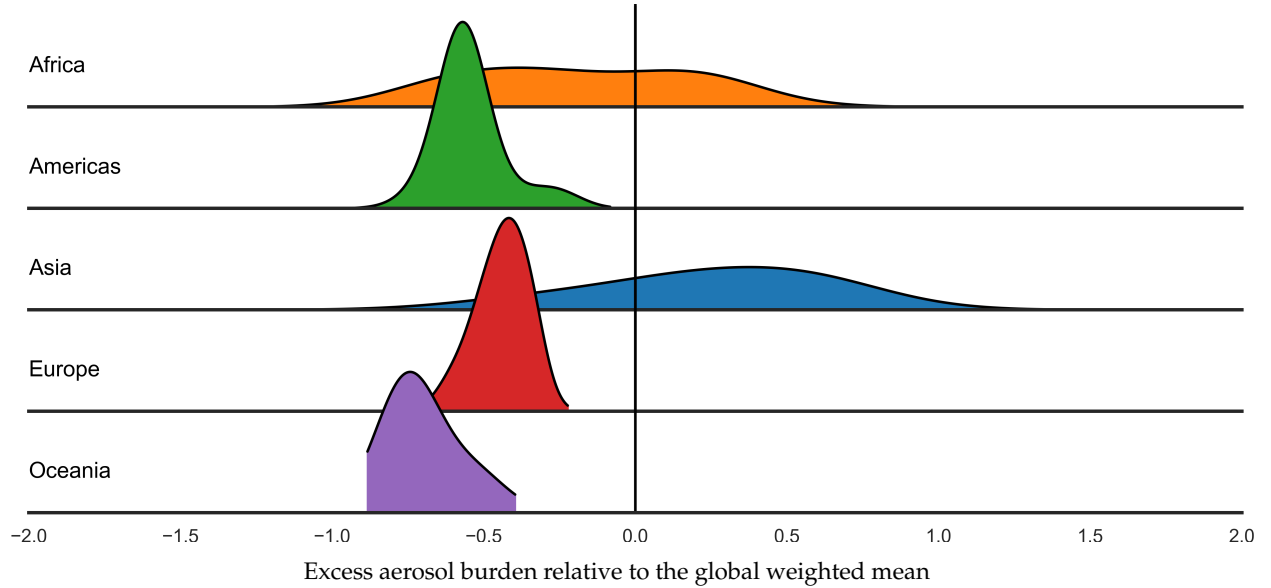
(b) 1° cell as the unit of observation (equal weight for each cell)



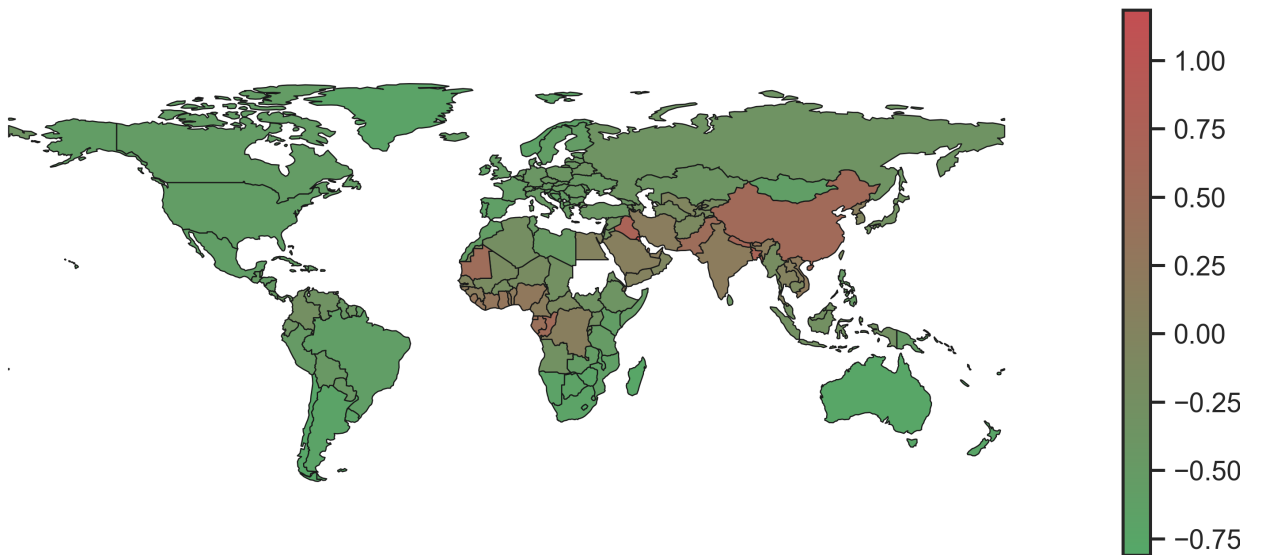
Notes: The panels present the global relative dispersion of air pollution by aerosols as measured by Aerosol Optical Depth (AOD). In contrast to Figure E.7, Panel (a) and (b) here treat each country or cell as a unit of observation with equal weights. The y-axis shows frequencies, counting the number of countries or cells. The x-axis is in units of what we call global excess population-pollution burden (EPB): A value of 0.5 (-0.5) indicates that a country or cell's AOD measure is 50 percent greater (smaller) than the global weighted mean.

Figure E.9: Continental dispersion of air pollution by aerosols, 2010

(a) Country as the unit of observation (weighted by country-population), by continents

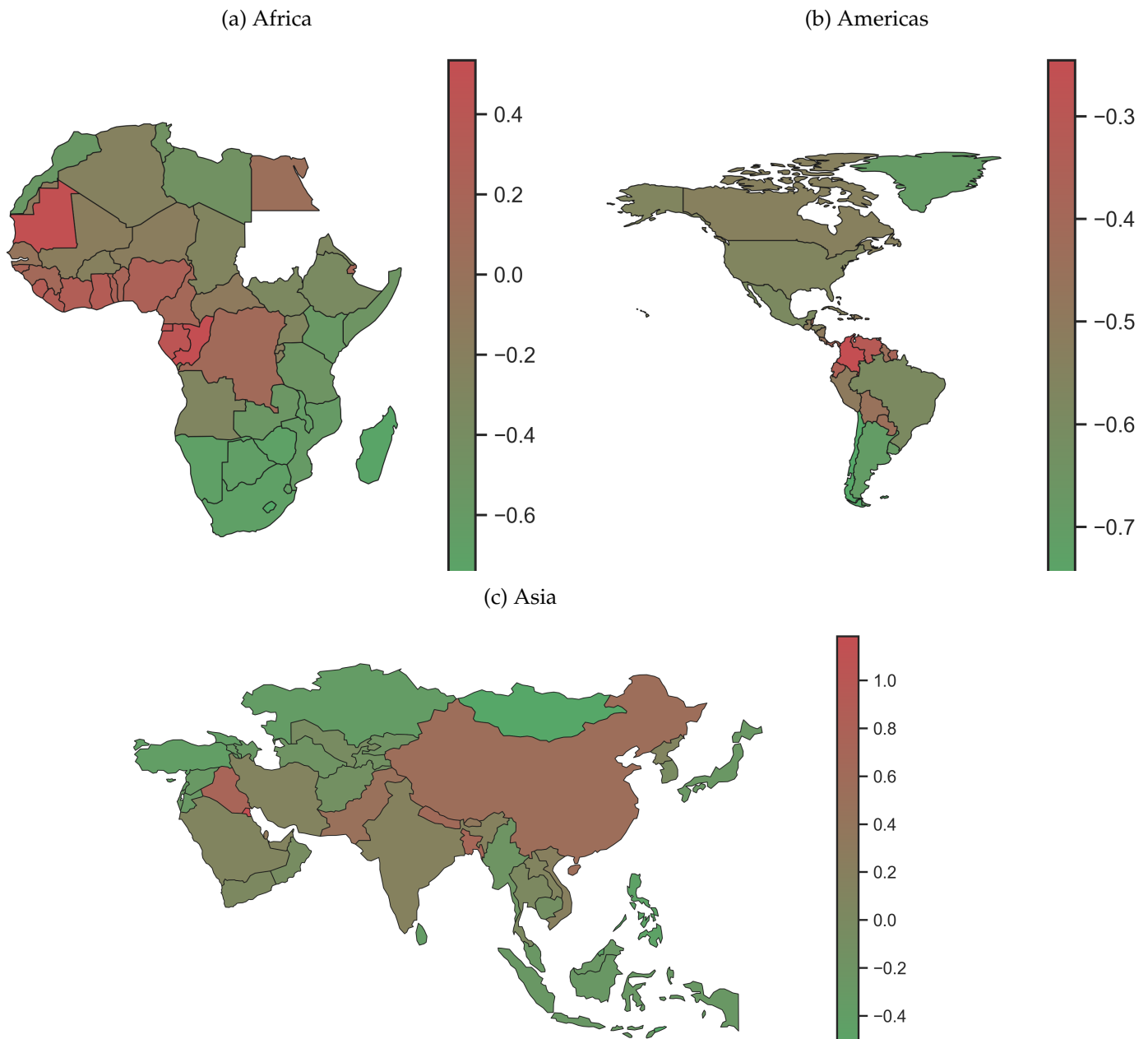


(b) Country as the unit of observation map



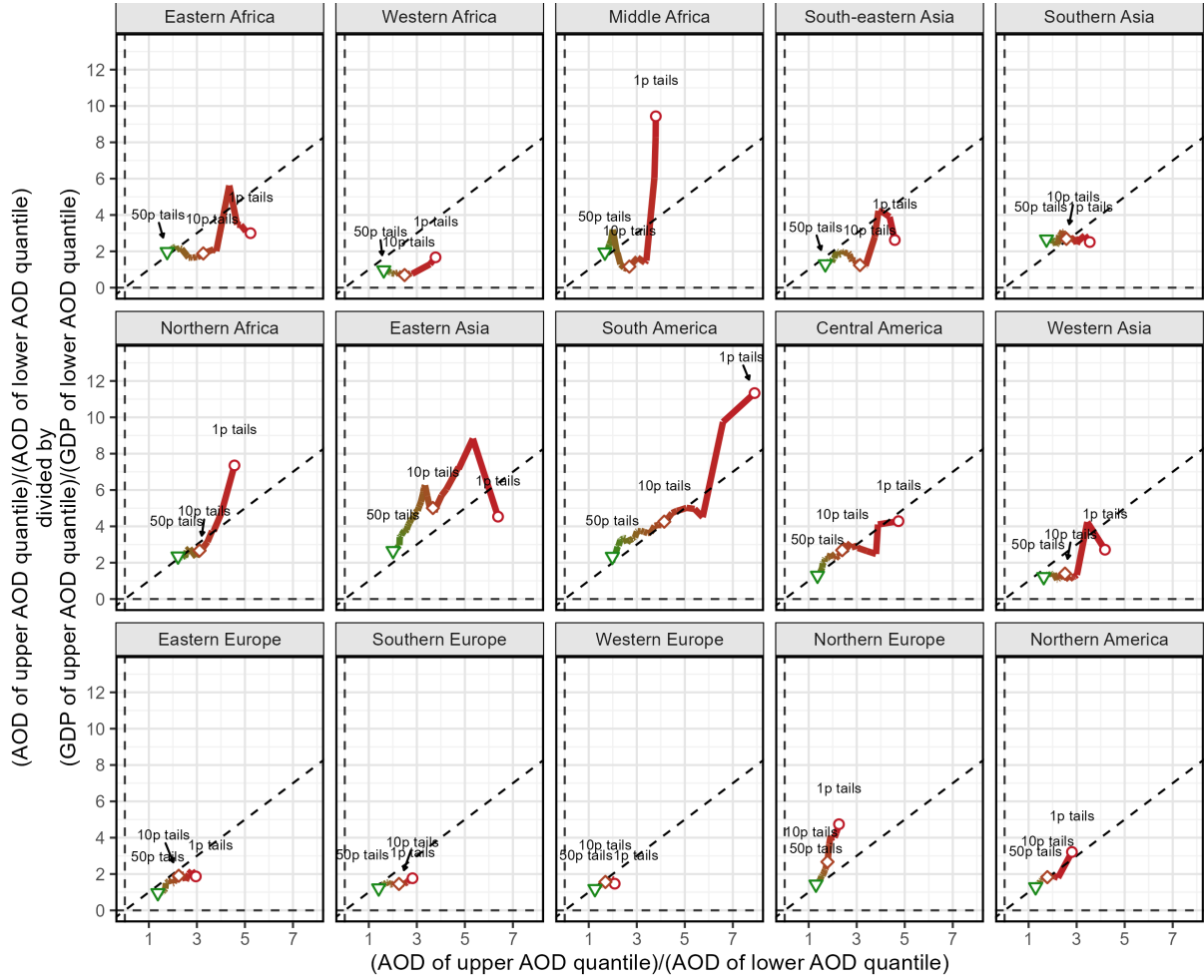
Notes: The panels present the global relative dispersion of air pollution by aerosols as measured by Aerosol Optical Depth (AOD). We compute annual average AOD for each cell ($1^\circ \times 1^\circ$ longitude–latitude grid) and then generate country-specific AOD as cell-population weighted averages. In contrast to Figure 1, Panel (a) treats each country as the unit of observation, weighted by aggregate population estimates for each country, and Panel (b) matches country-specific AOD to country locations. In Panel (a), the y-axis shows country population weighted density approximations. The x-axis in Panel (a) and colors in Panel (b) correspond to what we call global excess population-pollution burden (EPB): A value of 0.5 (-0.5) indicates that a country's AOD measure is 50 percent greater (smaller) than the global weighted mean. In Panel (b), darker shades of green (red) correspond to greater magnitudes of negative (positive) excess burdens.

Figure E.10: Continental dispersion of air pollution by aerosols, relative to continent-specific weighted means, 2010



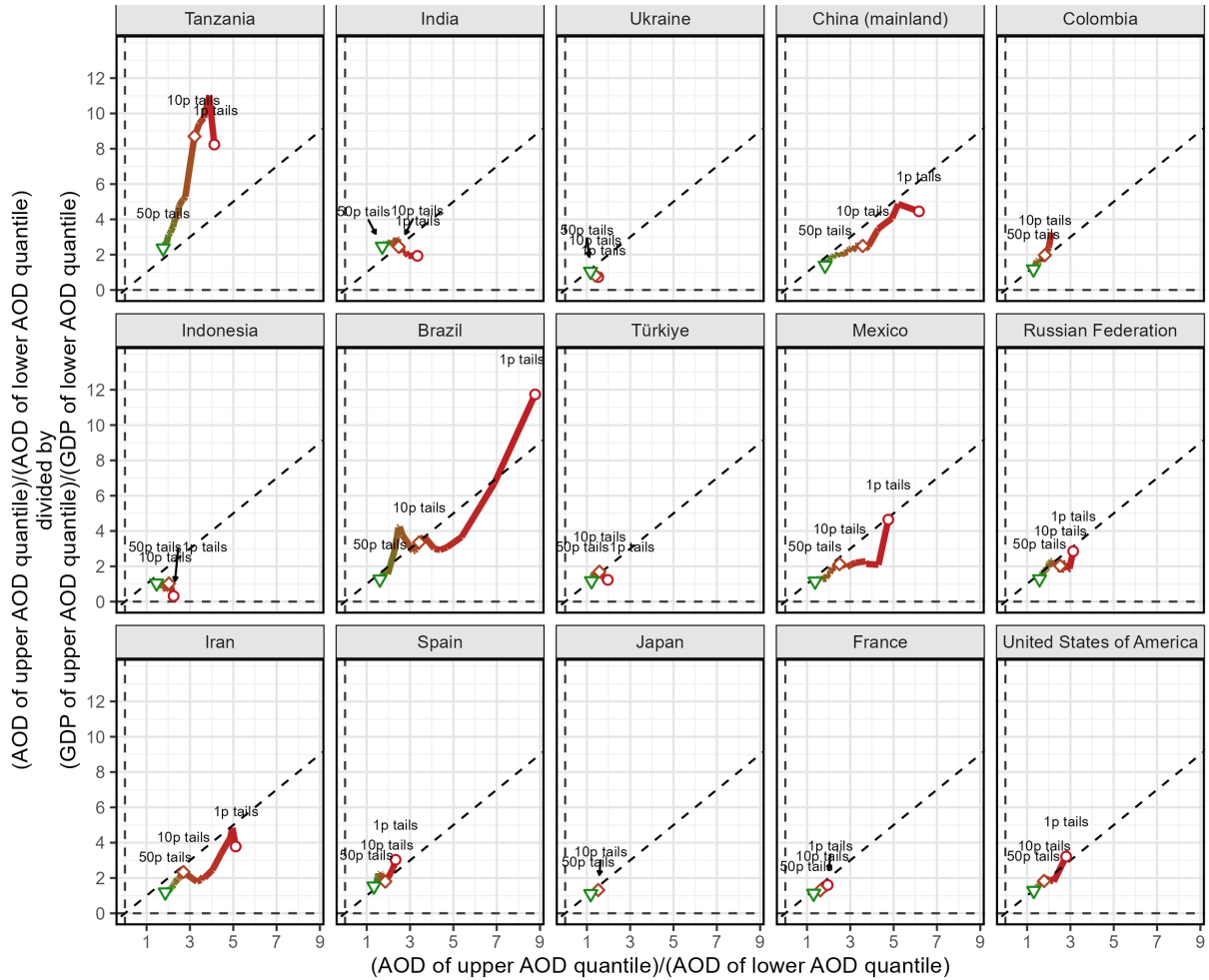
Note: The panels present the continent-specific relative dispersion of air pollution as measured by Aerosol Optical Depth (AOD). We compute annual average AOD for each cell ($1^\circ \times 1^\circ$ longitude–latitude grid) and then generate country-specific AOD as cell-population weighted averages. The colors in each Panel correspond to levels of what we call continental excess population-pollution burden (EPB): A value of 0.5 (-0.5) indicates that a country's AOD measure is 50 percent greater (smaller) than the continental weighted mean. In all Panels, darker shades of green (red) correspond to greater magnitudes of negative (positive) excess burdens.

Figure E.11: African subregional scatter plot, subnational population weighted bivariate and quadratic regression line



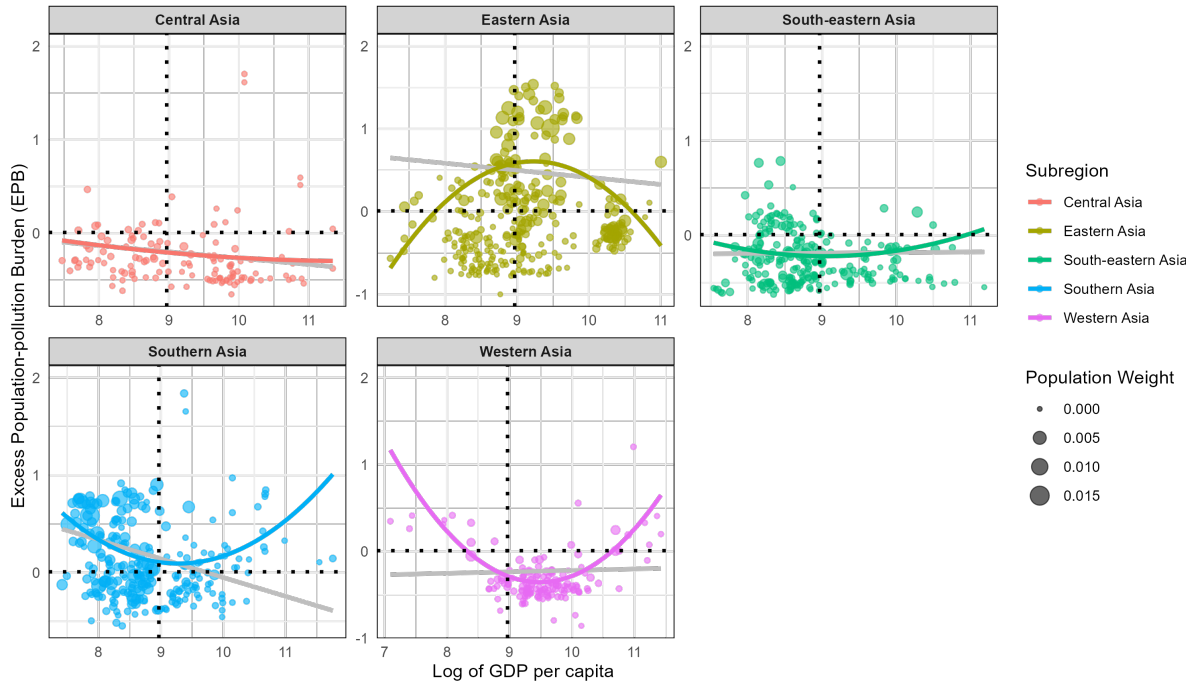
Notes: The figure presents subnational—first-level subnational administrative division—results. Across the panels, the x-axes correspond to levels of economic development as measured by GDP (Purchasing Price Parity adjusted) per capita in log base e units, and the y-axes correspond to relative exposures to air pollution by aerosols as measured by Aerosol Optical Depth (AOD). The size of the scatter points is proportional to population sizes of each subnational unit. Colors distinguish subnational units by subregional groupings. Additionally, the black lines mark global weighted averages along each axis and divide subnational units into four quadrants for relative comparisons: upper-right, higher GDP per capita and AOD; upper-left, lower GDP per capita and higher AOD; bottom-left, lower GDP per capita and AOD; and bottom-right, higher GDP per capita and lower AOD. The y-axes across panels are in units of what we call global excess population-pollution burden (EPB): A value of 0.5 (-0.5) indicates that a subnational unit's AOD measure is 50 percent greater (smaller) than the global weighted mean. We compute annual average AOD for each cell ($1^\circ \times 1^\circ$ longitude–latitude grid) and then generate subnational AOD as cell-population weighted averages. Subnational GDP and boundaries come from Kummu, Taka, and Guillaume (2018).

Figure E.12: African subregional scatter plot, subnational population weighted bivariate and quadratic regression line



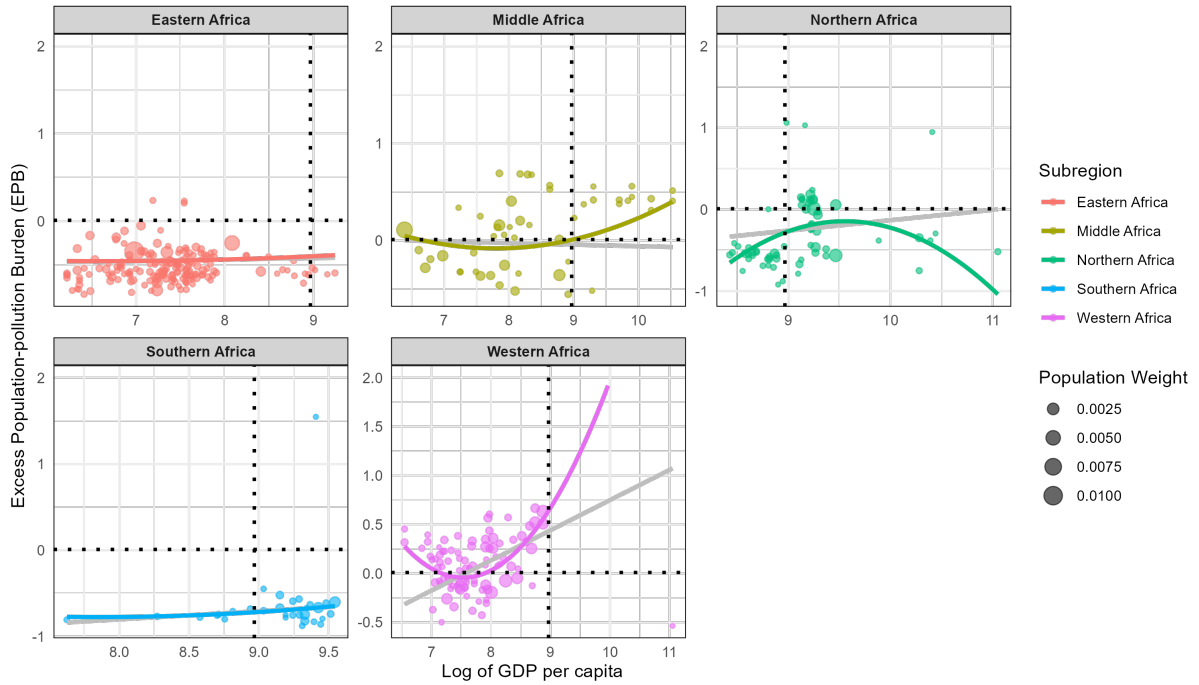
Notes: The figure presents subnational—first-level subnational administrative division—results. Across the panels, the x-axes correspond to levels of economic development as measured by GDP (Purchasing Price Parity adjusted) per capita in log base e units, and the y-axes correspond to relative exposures to air pollution by aerosols as measured by Aerosol Optical Depth (AOD). The size of the scatter points is proportional to population sizes of each subnational unit. Colors distinguish subnational units by subregional groupings. Additionally, the black lines mark global weighted averages along each axis and divide subnational units into four quadrants for relative comparisons: upper-right, higher GDP per capita and AOD; upper-left, lower GDP per capita and higher AOD; bottom-left, lower GDP per capita and AOD; and bottom-right, higher GDP per capita and lower AOD. The y-axes across panels are in units of what we call global excess population-pollution burden (EPB): A value of 0.5 (-0.5) indicates that a subnational unit's AOD measure is 50 percent greater (smaller) than the global weighted mean. We compute annual average AOD for each cell ($1^\circ \times 1^\circ$ longitude–latitude grid) and then generate subnational AOD as cell-population weighted averages. Subnational GDP and boundaries come from Kummu, Taka, and Guillaume (2018).

Figure E.13: Asian subregional scatter plot, subnational population weighted bivariate and quadratic regression line



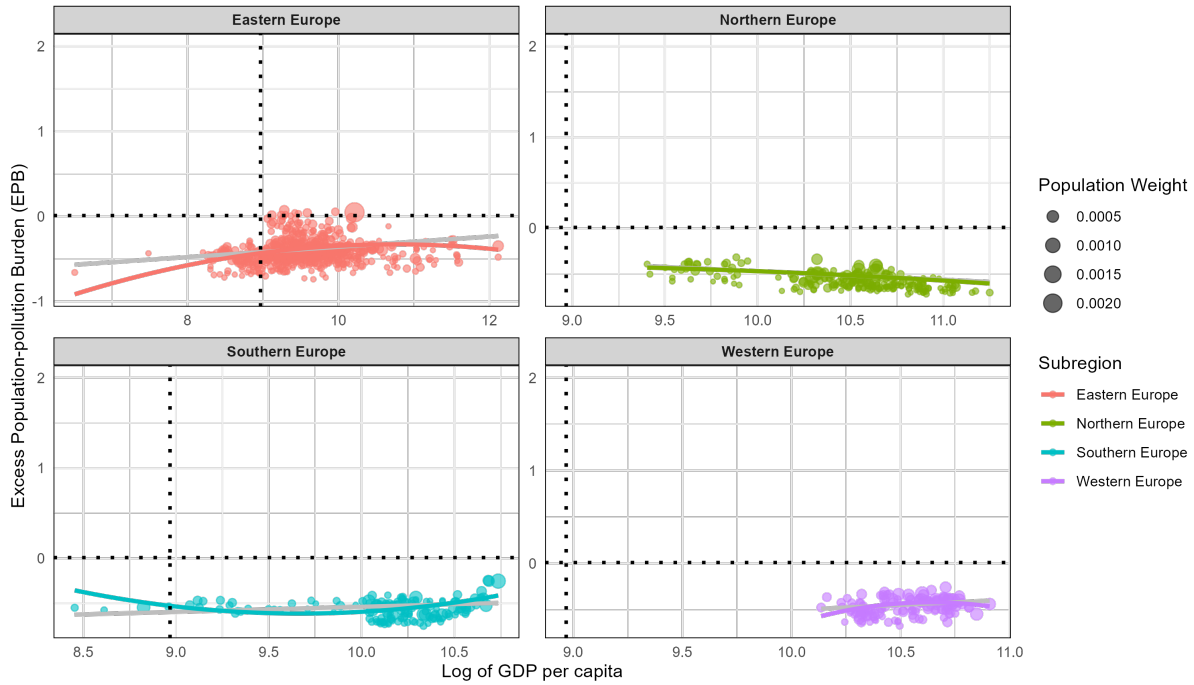
Notes: The figure presents subnational—first-level subnational administrative division—results. Across the panels, the x-axes correspond to levels of economic development as measured by GDP (Purchasing Price Parity adjusted) per capita in log base e units, and the y-axes correspond to relative exposures to air pollution by aerosols as measured by Aerosol Optical Depth (AOD). The size of the scatter points is proportional to population sizes of each subnational unit. Colors distinguish sub-national units by subregional groupings. Additionally, the black lines mark global weighted averages along each axis and divide subnational units into four quadrants for relative comparisons: upper-right, higher GDP per capita and AOD; upper-left, lower GDP per capita and higher AOD; bottom-left, lower GDP per capita and AOD; and bottom-right, higher GDP per capita and lower AOD. The y-axes across panels are in units of what we call global excess population-pollution burden (EPB): A value of 0.5 (-0.5) indicates that a subnational unit's AOD measure is 50 percent greater (smaller) than the global weighted mean. We compute annual average AOD for each cell ($1^\circ \times 1^\circ$ longitude–latitude grid) and then generate subnational AOD as cell-population weighted averages. Subnational GDP and boundaries come from Kummu, Taka, and Guillaume (2018).

Figure E.14: African subregional scatter plot, subnational population weighted bivariate and quadratic regression line



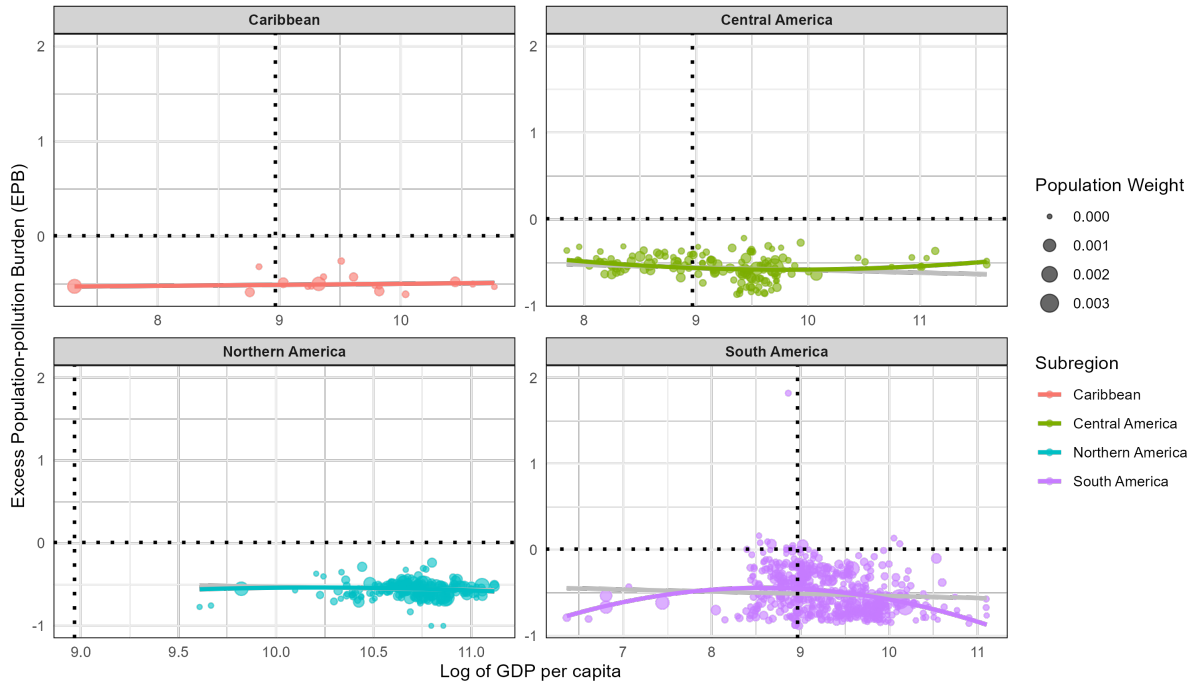
Notes: The figure presents subnational—first-level subnational administrative division—results. Across the panels, the x-axes correspond to levels of economic development as measured by GDP (Purchasing Price Parity adjusted) per capita in log base e units, and the y-axes correspond to relative exposures to air pollution by aerosols as measured by Aerosol Optical Depth (AOD). The size of the scatter points is proportional to population sizes of each subnational unit. Colors distinguish subnational units by subregional groupings. Additionally, the black lines mark global weighted averages along each axis and divide subnational units into four quadrants for relative comparisons: upper-right, higher GDP per capita and AOD; upper-left, lower GDP per capita and higher AOD; bottom-left, lower GDP per capita and AOD; and bottom-right, higher GDP per capita and lower AOD. The y-axes across panels are in units of what we call global excess population-pollution burden (EPB): A value of 0.5 (-0.5) indicates that a subnational unit's AOD measure is 50 percent greater (smaller) than the global weighted mean. We compute annual average AOD for each cell ($1^\circ \times 1^\circ$ longitude–latitude grid) and then generate subnational AOD as cell-population weighted averages. Subnational GDP and boundaries come from Kummu, Taka, and Guillaume (2018).

Figure E.15: European subregional scatter plot, subnational population weighted bivariate and quadratic regression line



Notes: The figure presents subnational—first-level subnational administrative division—results. Across the panels, the x-axes correspond to levels of economic development as measured by GDP (Purchasing Price Parity adjusted) per capita in log base e units, and the y-axes correspond to relative exposures to air pollution by aerosols as measured by Aerosol Optical Depth (AOD). The size of the scatter points is proportional to population sizes of each subnational unit. Colors distinguish subnational units by subregional groupings. Additionally, the black lines mark global weighted averages along each axis and divide subnational units into four quadrants for relative comparisons: upper-right, higher GDP per capita and AOD; upper-left, lower GDP per capita and higher AOD; bottom-left, lower GDP per capita and AOD; and bottom-right, higher GDP per capita and lower AOD. The y-axes across panels are in units of what we call global excess population-pollution burden (EPB): A value of 0.5 (-0.5) indicates that a subnational unit's AOD measure is 50 percent greater (smaller) than the global weighted mean. We compute annual average AOD for each cell ($1^\circ \times 1^\circ$ longitude–latitude grid) and then generate subnational AOD as cell-population weighted averages. Subnational GDP and boundaries come from Kummu, Taka, and Guillaume (2018).

Figure E.16: American subregional scatter plot, subnational population weighted bivariate and quadratic regression line



Notes: The figure presents subnational—first-level subnational administrative division—results. Across the panels, the x-axes correspond to levels of economic development as measured by GDP (Purchasing Price Parity adjusted) per capita in log base e units, and the y-axes correspond to relative exposures to air pollution by aerosols as measured by Aerosol Optical Depth (AOD). The size of the scatter points is proportional to population sizes of each subnational unit. Colors distinguish subnational units by subregional groupings. Additionally, the black lines mark global weighted averages along each axis and divide subnational units into four quadrants for relative comparisons: upper-right, higher GDP per capita and AOD; upper-left, lower GDP per capita and higher AOD; bottom-left, lower GDP per capita and AOD; and bottom-right, higher GDP per capita and lower AOD. The y-axes across panels are in units of what we call global excess population-pollution burden (EPB): A value of 0.5 (-0.5) indicates that a subnational unit's AOD measure is 50 percent greater (smaller) than the global weighted mean. We compute annual average AOD for each cell ($1^\circ \times 1^\circ$ longitude–latitude grid) and then generate subnational AOD as cell-population weighted averages. Subnational GDP and boundaries come from Kummu, Taka, and Guillaume (2018).

Table E.1: Global quadratic association between population-weighted air pollution by aerosol and GDP per capita (PPP, 2010 US Dollars) at regional, subregional, country, and subnational aggregations.

	Dependent variable: air pollution by aerosol.			
	Region	Subregion	Country	Subnational
	(1)	(2)	(3)	(4)
Log gdp per capita	9.416* (2.567)	3.537** (1.382)	2.770*** (0.446)	2.105*** (0.115)
Log gdp per capita squared	-0.534* (0.141)	-0.204** (0.076)	-0.162*** (0.025)	-0.124*** (0.006)
Constant	-41.253* (11.624)	-15.190** (6.246)	-11.630*** (2.005)	-8.794*** (0.512)
GDP turning point	\$6,727	\$5,897	\$5,037	\$4,948
Turning point 95 CI	[\$5,315 \$8,513]	[\$3,563 \$9,761]	[\$3,982 \$6,371]	[\$4,565 \$5,363]
Observations	5	22	170	3,712
R ²	0.917	0.351	0.298	0.140
Adjusted R ²	0.833	0.283	0.289	0.139

Note:

*p<0.1; **p<0.05; ***p<0.01

Table E.2: Asia, GDP per capita (PPP) in 2010 U.S. dollars, population-weighted air pollution by aerosol (AOD) distributions: mean, excess population-pollution burden (EPB), interquintile and interdecile ranges and ratios (2010).

Economies	GDP/capita	Mean (EPB)	AOD-population distributional statistics			
			Percentile ranges		Percentile ratios	
			Interquintile = 80th - 20th	Interdecile = 90th - 10th	80th to 20th	90th to 10th
Panel A: Central Asia						
Kazakhstan	18,642	0.29 (-37%)	0.11 = 0.33 - 0.22	0.12 = 0.33 - 0.21	1.47	1.63
Kyrgyzstan	3,076	0.38 (-16%)	0.20 = 0.49 - 0.29	0.23 = 0.49 - 0.26	1.69	1.88
Tajikistan	2,291	0.39 (-14%)	0.13 = 0.46 - 0.33	0.15 = 0.47 - 0.32	1.39	1.46
Turkmenistan	8,972	0.37 (-19%)	0.12 = 0.43 - 0.31	0.14 = 0.43 - 0.29	1.39	1.46
Uzbekistan	5,505	0.44 (-4%)	0.12 = 0.49 - 0.37	0.20 = 0.51 - 0.31	1.33	1.62
Panel B: Eastern Asia						
China (mainland)	9,256	0.71 (+55%)	0.50 = 0.96 - 0.46	0.73 = 1.07 - 0.34	2.12	3.16
DPR Korea		0.51 (+12%)	0.23 = 0.60 - 0.37	0.27 = 0.60 - 0.33	1.63	1.84
Japan	35,335	0.33 (-27%)	0.04 = 0.35 - 0.31	0.07 = 0.36 - 0.29	1.13	1.23
Mongolia	7,532	0.19 (-59%)	0.15 = 0.26 - 0.11	0.20 = 0.31 - 0.11	2.27	2.71
Republic of Korea	31,737	0.44 (-3%)	0.11 = 0.48 - 0.37	0.15 = 0.52 - 0.37	1.27	1.39
Taiwan	33,962	0.4 (-12%)	0.20 = 0.49 - 0.29	0.20 = 0.49 - 0.29	1.70	1.70
Panel C: South-eastern Asia						
Brunei Darussalam	79,543	0.23 (-50%)	0.00 = 0.23 - 0.23	0.00 = 0.23 - 0.23	1.00	1.00
Cambodia	2,989	0.4 (-12%)	0.09 = 0.46 - 0.37	0.09 = 0.46 - 0.37	1.24	1.24
Indonesia	8,353	0.33 (-28%)	0.15 = 0.39 - 0.24	0.22 = 0.43 - 0.21	1.60	2.01
Laos	3,772	0.51 (+12%)	0.05 = 0.54 - 0.49	0.11 = 0.55 - 0.44	1.10	1.25
Malaysia	20,193	0.34 (-26%)	0.13 = 0.39 - 0.26	0.15 = 0.39 - 0.24	1.47	1.64
Myanmar	3,348	0.36 (-21%)	0.07 = 0.39 - 0.32	0.20 = 0.50 - 0.30	1.23	1.65
Philippines	5,489	0.24 (-48%)	0.06 = 0.27 - 0.21	0.07 = 0.27 - 0.20	1.24	1.32
Thailand	12,932	0.47 (+ 2%)	0.19 = 0.56 - 0.37	0.26 = 0.56 - 0.30	1.52	1.90
Timor-Leste	1,955	0.18 (-61%)	0.02 = 0.19 - 0.17	0.03 = 0.20 - 0.17	1.13	1.17
Viet Nam	5,389	0.55 (+21%)	0.40 = 0.80 - 0.40	0.50 = 0.81 - 0.31	1.98	2.62
Panel D: Southern Asia						
Afghanistan	1,766	0.4 (-12%)	0.06 = 0.40 - 0.34	0.12 = 0.44 - 0.32	1.20	1.39
Bangladesh	2,834	0.77 (+69%)	0.02 = 0.79 - 0.77	0.09 = 0.79 - 0.70	1.02	1.12
Bhutan	7,246	0.61 (+34%)	0.03 = 0.62 - 0.59	0.03 = 0.62 - 0.59	1.06	1.06
India	4,206	0.53 (+17%)	0.35 = 0.74 - 0.39	0.42 = 0.77 - 0.35	1.93	2.20
Iran	17,866	0.52 (+13%)	0.23 = 0.59 - 0.36	0.50 = 0.82 - 0.32	1.66	2.56
Maldives	12,816	0.26 (-44%)	0.08 = 0.30 - 0.22	0.08 = 0.30 - 0.22	1.36	1.36
Nepal	2,139	0.74 (+62%)	0.11 = 0.80 - 0.69	0.27 = 0.87 - 0.60	1.16	1.45
Pakistan	3,786	0.68 (+49%)	0.40 = 0.84 - 0.44	0.48 = 0.85 - 0.37	1.90	2.32
Sri Lanka	8,234	0.29 (-37%)	0.02 = 0.30 - 0.28	0.03 = 0.31 - 0.28	1.10	1.12

Continued on next page

Table E.2: Asia, GDP per capita (PPP) in 2010 U.S. dollars, population-weighted air pollution by aerosol (AOD) distributions: mean, excess population-pollution burden (EPB), interquintile and interdecile ranges and ratios (2010).

Economies	GDP/capita	Mean (EPB)	AOD-population distributional statistics				
			Percentile ranges		Percentile ratios		
			Interquintile = 80th - 20th	Interdecile = 90th - 10th	80th to 20th	90th to 10th	
Panel E: Western Asia							
Armenia	7,095	0.32 (-29%)	0.05 = 0.35 - 0.30	0.05 = 0.35 - 0.30	1.19	1.19	
Azerbaijan	14,681	0.33 (-28%)	0.07 = 0.37 - 0.30	0.15 = 0.38 - 0.23	1.22	1.66	
Cyprus	33,506	0.29 (-37%)	0.02 = 0.29 - 0.27	0.02 = 0.29 - 0.27	1.09	1.09	
Georgia	7,712	0.27 (-40%)	0.10 = 0.31 - 0.21	0.11 = 0.31 - 0.20	1.44	1.51	
Iraq	12,186	0.79 (+72%)	0.08 = 0.75 - 0.67	0.19 = 0.76 - 0.57	1.12	1.32	
Israel	29,362	0.35 (-24%)	0.00 = 0.35 - 0.35	0.00 = 0.35 - 0.35	1.00	1.00	
Jordan	9,417	0.32 (-29%)	0.30 = 0.42 - 0.12	0.30 = 0.42 - 0.12	3.51	3.51	
Kuwait	75,184	1 (+118%)	0.00 = 1.00 - 1.00	0.00 = 1.00 - 1.00	1.00	1.00	
Lebanon	14,704	0.32 (-31%)	0.00 = 0.32 - 0.32	0.00 = 0.32 - 0.32	1.00	1.00	
Oman	55,667	0.43 (-5%)	0.14 = 0.49 - 0.35	0.21 = 0.49 - 0.28	1.38	1.75	
Qatar	151,646	0.61 (+34%)	0.04 = 0.64 - 0.60	0.04 = 0.64 - 0.60	1.06	1.06	
Saudi Arabia	58,884	0.5 (+10%)	0.23 = 0.60 - 0.37	0.40 = 0.70 - 0.30	1.61	2.34	
Syria		0.32 (-29%)	0.08 = 0.35 - 0.27	0.14 = 0.41 - 0.27	1.29	1.54	
Türkiye	17,344	0.27 (-40%)	0.06 = 0.30 - 0.24	0.09 = 0.32 - 0.23	1.23	1.42	
United Arab Emirates	83,671	0.52 (+13%)	0.05 = 0.54 - 0.49	0.13 = 0.54 - 0.41	1.10	1.33	
Yemen	3,603	0.47 (+ 3%)	0.08 = 0.51 - 0.43	0.17 = 0.58 - 0.41	1.21	1.42	

Note: Table statistics are computed based on the distribution of AOD and population across cells ($1^\circ \times 1^\circ$ longitude–latitude grid). The interpretation of AOD is that < 0.1 indicates crystal clear sky and AOD of 1 indicates very hazy conditions. For excess population-pollution burden (EPB), a value of +50% (-50%) indicates that a geographical unit's's AOD measure is 50 percent greater (smaller) than the global population-weighted mean.

Table E.3: Africa, GDP per capita (PPP) in 2010 U.S. dollars, population-weighted air pollution by aerosol (AOD) distributions: mean, excess population-pollution burden (EPB), interquintile and interdecile ranges and ratios (2010).

Economies	GDP/capita	Mean (EPB)	AOD-population distributional statistics				
			Percentile ranges		Percentile ratios		
			Interquintile = 80th - 20th	Interdecile = 90th - 10th	80th to 20th	90th to 10th	
Panel A: Eastern Africa							
Burundi	614	0.37 (-19%)	0.05 = 0.41 - 0.36	0.05 = 0.41 - 0.36	1.15	1.15	
Djibouti		0.53 (+16%)	0.07 = 0.55 - 0.48	0.07 = 0.55 - 0.48	1.15	1.15	
Eritrea	1,599	0.32 (-31%)	0.03 = 0.30 - 0.27	0.07 = 0.34 - 0.27	1.10	1.26	
Ethiopia	996	0.29 (-36%)	0.07 = 0.33 - 0.26	0.13 = 0.35 - 0.22	1.24	1.59	
Kenya	2,635	0.2 (-57%)	0.05 = 0.21 - 0.16	0.11 = 0.26 - 0.15	1.30	1.70	
Madagascar	1,464	0.11 (-75%)	0.09 = 0.16 - 0.07	0.13 = 0.19 - 0.06	2.16	3.36	
Malawi	1,458	0.17 (-63%)	0.03 = 0.18 - 0.15	0.05 = 0.20 - 0.15	1.20	1.31	
Mozambique	1,000	0.18 (-60%)	0.09 = 0.23 - 0.14	0.12 = 0.24 - 0.12	1.67	2.02	
Rwanda	1,314	0.38 (-17%)	0.03 = 0.40 - 0.37	0.03 = 0.40 - 0.37	1.09	1.09	
Seychelles	18,982	0.15 (-67%)	0.00 = 0.15 - 0.15	0.00 = 0.15 - 0.15	1.00	1.00	
Somalia	815	0.22 (-51%)	0.16 = 0.30 - 0.14	0.20 = 0.30 - 0.10	2.17	2.91	
South Sudan	2,948	0.3 (-33%)	0.06 = 0.34 - 0.28	0.11 = 0.36 - 0.25	1.22	1.46	
Tanzania	2,069	0.22 (-51%)	0.14 = 0.30 - 0.16	0.24 = 0.38 - 0.14	1.86	2.73	
Uganda	2,092	0.33 (-28%)	0.15 = 0.40 - 0.25	0.19 = 0.43 - 0.24	1.61	1.79	
Zambia	3,098	0.21 (-53%)	0.04 = 0.23 - 0.19	0.07 = 0.25 - 0.18	1.17	1.42	
Zimbabwe	1,734	0.14 (-70%)	0.03 = 0.15 - 0.12	0.06 = 0.17 - 0.11	1.28	1.61	
Panel B: Middle Africa							
Angola	6,607	0.32 (-29%)	0.27 = 0.48 - 0.21	0.31 = 0.50 - 0.19	2.32	2.61	
Cameroon	2,914	0.52 (+15%)	0.38 = 0.69 - 0.31	0.45 = 0.76 - 0.31	2.21	2.44	
Central African Republic	936	0.4 (-12%)	0.07 = 0.43 - 0.36	0.11 = 0.45 - 0.34	1.18	1.30	
Chad	1,767	0.33 (-28%)	0.15 = 0.41 - 0.26	0.27 = 0.51 - 0.24	1.55	2.11	
Congo (DRC)	597	0.51 (+11%)	0.20 = 0.63 - 0.43	0.29 = 0.63 - 0.34	1.48	1.87	
Equatorial Guinea	26,168	0.65 (+42%)	0.00 = 0.65 - 0.65	0.00 = 0.65 - 0.65	1.00	1.00	
Gabon	14,015	0.65 (+43%)	0.07 = 0.69 - 0.62	0.10 = 0.72 - 0.62	1.12	1.16	
Republic of Congo	5,125	0.7 (+53%)	0.10 = 0.76 - 0.66	0.15 = 0.78 - 0.63	1.15	1.23	
Sao Tome and Principe	2,859	0.48 (+ 4%)	0.00 = 0.48 - 0.48	0.00 = 0.48 - 0.48	1.00	1.00	
Panel C: Northern Africa							
Algeria	14,201	0.35 (-23%)	0.05 = 0.20 - 0.15	0.08 = 0.21 - 0.13	1.38	1.60	
Egypt	8,838	0.47 (+ 4%)	0.05 = 0.50 - 0.45	0.12 = 0.54 - 0.42	1.11	1.27	
Libya	30,234	0.24 (-47%)	0.30 = 0.39 - 0.09	0.33 = 0.39 - 0.06	4.60	7.03	
Morocco	6,849	0.2 (-56%)	0.03 = 0.21 - 0.18	0.07 = 0.24 - 0.17	1.21	1.38	
Tunisia	10,555	0.24 (-47%)	0.06 = 0.26 - 0.20	0.10 = 0.28 - 0.18	1.33	1.56	
Western Sahara		0.4 (-13%)	0.15 = 0.46 - 0.31	0.18 = 0.46 - 0.28	1.46	1.63	

Continued on next page

Table E.3: Africa, GDP per capita (PPP) in 2010 U.S. dollars, population-weighted air pollution by aerosol (AOD) distributions: mean, excess population-pollution burden (EPB), interquintile and interdecile ranges and ratios (2010).

Economies	GDP/capita	Mean (EPB)	AOD-population distributional statistics				
			Percentile ranges		Percentile ratios		
			Interquintile = 80th - 20th	Interdecile = 90th - 10th	80th to 20th	90th to 10th	
Panel D: Southern Africa							
Botswana	12,491	0.15 (-66%)	0.06 = 0.17 - 0.11	0.11 = 0.20 - 0.09	1.53	2.09	
Eswatini	7,156	0.17 (-63%)	0.00 = 0.17 - 0.17	0.00 = 0.17 - 0.17	1.00	1.00	
Lesotho	2,153	0.09 (-81%)	0.00 = 0.09 - 0.09	0.03 = 0.09 - 0.06	1.00	1.41	
Namibia	8,538	0.14 (-69%)	0.14 = 0.23 - 0.09	0.17 = 0.26 - 0.09	2.59	2.92	
South Africa	12,637	0.14 (-69%)	0.08 = 0.18 - 0.10	0.10 = 0.19 - 0.09	1.72	2.10	
Panel E: Western Africa							
Benin	2,220	0.54 (+19%)	0.11 = 0.60 - 0.49	0.14 = 0.60 - 0.46	1.24	1.29	
Burkina Faso	1,449	0.36 (-22%)	0.11 = 0.41 - 0.30	0.11 = 0.41 - 0.30	1.34	1.39	
Cabo Verde	6,039	0.41 (-11%)	0.02 = 0.42 - 0.40	0.03 = 0.42 - 0.39	1.05	1.08	
Côte d'Ivoire	3,361	0.59 (+30%)	0.06 = 0.62 - 0.56	0.09 = 0.64 - 0.55	1.11	1.18	
Ghana	3,855	0.6 (+33%)	0.07 = 0.65 - 0.58	0.16 = 0.68 - 0.52	1.12	1.30	
Guinea	1,622	0.52 (+13%)	0.06 = 0.54 - 0.48	0.21 = 0.63 - 0.42	1.12	1.51	
Guinea-Bissau	1,370	0.55 (+21%)	0.00 = 0.55 - 0.55	0.00 = 0.55 - 0.55	1.00	1.00	
Liberia	980	0.59 (+30%)	0.00 = 0.60 - 0.60	0.01 = 0.60 - 0.59	1.00	1.02	
Mali	1,687	0.38 (-17%)	0.08 = 0.41 - 0.33	0.16 = 0.44 - 0.28	1.24	1.61	
Mauritania	3,178	0.69 (+50%)	0.29 = 0.52 - 0.23	3.49 = 3.69 - 0.20	2.28	18.19	
Niger	1,058	0.38 (-17%)	0.14 = 0.44 - 0.30	0.21 = 0.48 - 0.27	1.47	1.76	
Nigeria	4,475	0.57 (+25%)	0.32 = 0.73 - 0.41	0.38 = 0.73 - 0.35	1.77	2.06	
Senegal	2,663	0.44 (-4%)	0.11 = 0.50 - 0.39	0.26 = 0.51 - 0.25	1.26	2.02	
Sierra Leone	1,828	0.6 (+32%)	0.01 = 0.61 - 0.60	0.01 = 0.61 - 0.60	1.02	1.02	
Togo	1,537	0.56 (+23%)	0.19 = 0.60 - 0.41	0.20 = 0.61 - 0.41	1.46	1.47	

Note: Table statistics are computed based on the distribution of AOD and population across cells ($1^\circ \times 1^\circ$ longitude–latitude grid). The interpretation of AOD is that < 0.1 indicates crystal clear sky and AOD of 1 indicates very hazy conditions. For excess population-pollution burden (EPB), a value of +50% (-50%) indicates that a geographical unit's AOD measure is 50 percent greater (smaller) than the global population-weighted mean.

Table E.4: Europe, GDP per capita (PPP) in 2010 U.S. dollars, population-weighted air pollution by aerosol (AOD) distributions: mean, excess population-pollution burden (EPB), interquintile and interdecile ranges and ratios (2010).

Economies	GDP/capita	Mean (EPB)	AOD-population distributional statistics			
			Percentile ranges		Percentile ratios	
			Interquintile = 80th - 20th	Interdecile = 90th - 10th	80th to 20th	90th to 10th
Panel A: Eastern Europe						
Belarus	15,339	0.3 (-35%)	0.04 = 0.32 - 0.28	0.05 = 0.32 - 0.27	1.13	1.17
Bulgaria	14,956	0.24 (-47%)	0.04 = 0.26 - 0.22	0.06 = 0.28 - 0.22	1.20	1.26
Czechia	28,157	0.27 (-40%)	0.01 = 0.28 - 0.27	0.02 = 0.29 - 0.27	1.02	1.10
Hungary	21,739	0.26 (-43%)	0.03 = 0.27 - 0.24	0.04 = 0.28 - 0.24	1.14	1.18
Poland	20,993	0.28 (-39%)	0.03 = 0.29 - 0.26	0.04 = 0.29 - 0.25	1.12	1.17
Republic of Moldova	6,323	0.25 (-46%)	0.00 = 0.25 - 0.25	0.00 = 0.25 - 0.25	1.00	1.00
Romania	17,357	0.26 (-44%)	0.03 = 0.27 - 0.24	0.04 = 0.28 - 0.24	1.14	1.19
Russian Federation	20,490	0.3 (-34%)	0.15 = 0.38 - 0.23	0.26 = 0.47 - 0.21	1.68	2.30
Slovakia	25,384	0.26 (-43%)	0.00 = 0.26 - 0.26	0.00 = 0.26 - 0.26	1.02	1.03
Ukraine	8,453	0.25 (-46%)	0.05 = 0.27 - 0.22	0.06 = 0.28 - 0.22	1.20	1.30
Panel B: Northern Europe						
Denmark	43,042	0.24 (-48%)	0.04 = 0.26 - 0.22	0.05 = 0.26 - 0.21	1.20	1.28
Estonia	21,617	0.23 (-50%)	0.02 = 0.24 - 0.22	0.05 = 0.25 - 0.20	1.10	1.24
Faroe Islands	39,767	0.14 (-70%)	0.00 = 0.14 - 0.14	0.00 = 0.14 - 0.14	1.00	1.00
Finland	38,951	0.21 (-54%)	0.02 = 0.22 - 0.20	0.05 = 0.24 - 0.19	1.12	1.27
Iceland	39,768	0.22 (-52%)	0.07 = 0.24 - 0.17	0.08 = 0.24 - 0.16	1.40	1.50
Ireland	43,217	0.18 (-60%)	0.03 = 0.19 - 0.16	0.07 = 0.23 - 0.16	1.18	1.43
Latvia	17,343	0.27 (-41%)	0.04 = 0.29 - 0.25	0.05 = 0.29 - 0.24	1.15	1.21
Lithuania	19,828	0.27 (-41%)	0.01 = 0.28 - 0.27	0.06 = 0.29 - 0.23	1.05	1.25
Norway	58,220	0.16 (-66%)	0.03 = 0.17 - 0.14	0.04 = 0.17 - 0.13	1.21	1.31
Sweden	41,956	0.2 (-56%)	0.04 = 0.22 - 0.18	0.06 = 0.22 - 0.16	1.25	1.40
United Kingdom	36,488	0.22 (-51%)	0.06 = 0.25 - 0.19	0.10 = 0.27 - 0.17	1.28	1.53
Panel C: Southern Europe						
Albania	9,627	0.21 (-53%)	0.05 = 0.24 - 0.19	0.05 = 0.24 - 0.19	1.23	1.26
Bosnia and Herzegovina	9,087	0.19 (-58%)	0.01 = 0.20 - 0.19	0.01 = 0.20 - 0.19	1.06	1.06
Croatia	20,144	0.21 (-54%)	0.03 = 0.22 - 0.19	0.05 = 0.24 - 0.19	1.15	1.24
Greece	27,842	0.25 (-45%)	0.02 = 0.26 - 0.24	0.03 = 0.26 - 0.23	1.10	1.13
Italy	35,298	0.25 (-44%)	0.13 = 0.34 - 0.21	0.14 = 0.34 - 0.20	1.60	1.68
Montenegro	13,634	0.2 (-56%)	0.00 = 0.20 - 0.20	0.00 = 0.20 - 0.20	1.00	1.00
North Macedonia	11,994	0.23 (-50%)	0.02 = 0.24 - 0.22	0.02 = 0.24 - 0.22	1.11	1.11
Portugal	27,295	0.17 (-63%)	0.01 = 0.18 - 0.17	0.02 = 0.18 - 0.16	1.10	1.14
Serbia	13,322	0.22 (-52%)	0.04 = 0.24 - 0.20	0.05 = 0.24 - 0.19	1.22	1.28
Slovenia	27,582	0.22 (-52%)	0.00 = 0.22 - 0.22	0.02 = 0.22 - 0.20	1.00	1.09

Continued on next page

Table E.4: Europe, GDP per capita (PPP) in 2010 U.S. dollars, population-weighted air pollution by aerosol (AOD) distributions: mean, excess population-pollution burden (EPB), interquintile and interdecile ranges and ratios (2010).

Economies	GDP/capita	Mean (EPB)	AOD-population distributional statistics				
			Percentile ranges		Percentile ratios		
			Interquintile = 80th - 20th	Interdecile = 90th - 10th	80th to 20th	90th to 10th	
Spain	31,808	0.18 (-60%)	0.04 = 0.20 - 0.16	0.09 = 0.23 - 0.14	1.30	1.66	
Panel D: Western Europe							
Austria	41,740	0.24 (-47%)	0.08 = 0.30 - 0.22	0.08 = 0.30 - 0.22	1.35	1.35	
Belgium	39,844	0.28 (-39%)	0.02 = 0.30 - 0.28	0.10 = 0.30 - 0.20	1.07	1.49	
France	35,912	0.22 (-52%)	0.07 = 0.26 - 0.19	0.09 = 0.26 - 0.17	1.41	1.55	
Germany	39,730	0.27 (-41%)	0.04 = 0.29 - 0.25	0.06 = 0.30 - 0.24	1.18	1.29	
Netherlands	45,306	0.26 (-42%)	0.05 = 0.28 - 0.23	0.09 = 0.30 - 0.21	1.21	1.47	
Switzerland	54,432	0.26 (-42%)	0.12 = 0.34 - 0.22	0.12 = 0.34 - 0.22	1.55	1.55	

Note: Table statistics are computed based on the distribution of AOD and population across cells ($1^\circ \times 1^\circ$ longitude–latitude grid). The interpretation of AOD is that < 0.1 indicates crystal clear sky and AOD of 1 indicates very hazy conditions. For excess population-pollution burden (EPB), a value of +50% (-50%) indicates that a geographical unit's AOD measure is 50 percent greater (smaller) than the global population-weighted mean.

Table E.5: The Americas, GDP per capita (PPP) in 2010 U.S. dollars, population-weighted air pollution by aerosol (AOD) distributions: mean, excess population-pollution burden (EPB), interquintile and interdecile ranges and ratios (2010).

Economies	GDP/capita	Mean (EPB)	AOD-population distributional statistics				
			Percentile ranges		Percentile ratios		
			Interquintile = 80th - 20th	Interdecile = 90th - 10th	80th to 20th	90th to 10th	
Panel A: Caribbean							
Anguilla		0.23 (-49%)	0.00 = 0.23 - 0.23	0.00 = 0.23 - 0.23	1.00	1.00	
Antigua and Barbuda	23,958	0.22 (-52%)	0.00 = 0.22 - 0.22	0.00 = 0.22 - 0.22	1.00	1.00	
Bahamas	30,126	0.23 (-50%)	0.08 = 0.26 - 0.18	0.08 = 0.26 - 0.18	1.39	1.39	
British Virgin Islands		0.22 (-52%)	0.00 = 0.22 - 0.22	0.00 = 0.22 - 0.22	1.00	1.00	
Cuba		0.21 (-54%)	0.02 = 0.22 - 0.20	0.05 = 0.24 - 0.19	1.14	1.26	
Dominican Republic	11,268	0.23 (-50%)	0.04 = 0.25 - 0.21	0.04 = 0.25 - 0.21	1.20	1.20	
Grenada	10,344	0.26 (-43%)	0.00 = 0.26 - 0.26	0.00 = 0.26 - 0.26	1.00	1.00	
Haiti	2,695	0.22 (-53%)	0.00 = 0.22 - 0.22	0.03 = 0.22 - 0.19	1.02	1.17	
Jamaica	8,080	0.23 (-50%)	0.00 = 0.23 - 0.23	0.00 = 0.23 - 0.23	1.00	1.00	
Martinique		0.22 (-53%)	0.00 = 0.22 - 0.22	0.00 = 0.22 - 0.22	1.00	1.00	
Montserrat		0.21 (-54%)	0.00 = 0.21 - 0.21	0.00 = 0.21 - 0.21	1.00	1.00	
Netherlands Antilles		0.29 (-36%)	0.00 = 0.29 - 0.29	0.00 = 0.29 - 0.29	1.00	1.00	
Puerto Rico	30,933	0.24 (-46%)	0.00 = 0.24 - 0.24	0.00 = 0.24 - 0.24	1.00	1.00	
Saint Lucia	12,718	0.22 (-53%)	0.00 = 0.22 - 0.22	0.00 = 0.22 - 0.22	1.00	1.00	
Trinidad and Tobago	30,778	0.28 (-40%)	0.05 = 0.31 - 0.26	0.08 = 0.34 - 0.26	1.19	1.29	
Turks and Caicos Islands		0.18 (-61%)	0.00 = 0.18 - 0.18	0.00 = 0.18 - 0.18	1.00	1.00	
Panel B: Central America							
Belize	9,735	0.27 (-40%)	0.02 = 0.29 - 0.27	0.04 = 0.29 - 0.25	1.08	1.15	
Costa Rica	12,928	0.25 (-46%)	0.00 = 0.25 - 0.25	0.00 = 0.25 - 0.25	1.00	1.00	
Guatemala	6,510	0.22 (-51%)	0.04 = 0.26 - 0.22	0.09 = 0.26 - 0.17	1.20	1.56	
Honduras	3,758	0.2 (-55%)	0.05 = 0.23 - 0.18	0.06 = 0.24 - 0.18	1.26	1.34	
Mexico	15,909	0.19 (-59%)	0.04 = 0.20 - 0.16	0.10 = 0.24 - 0.14	1.28	1.73	
Nicaragua	4,042	0.23 (-50%)	0.07 = 0.27 - 0.20	0.07 = 0.27 - 0.20	1.33	1.33	
Panama	15,573	0.28 (-38%)	0.09 = 0.33 - 0.24	0.09 = 0.33 - 0.24	1.36	1.40	
Panel C: Northern America							
Canada	40,098	0.21 (-54%)	0.04 = 0.23 - 0.19	0.06 = 0.24 - 0.18	1.19	1.36	
Greenland	49,864	0.14 (-69%)	0.03 = 0.16 - 0.13	0.07 = 0.18 - 0.11	1.28	1.71	
United States of America	48,651	0.2 (-56%)	0.06 = 0.23 - 0.17	0.10 = 0.24 - 0.14	1.37	1.71	
Panel D: South America							
Argentina	17,848	0.14 (-70%)	0.06 = 0.16 - 0.10	0.10 = 0.19 - 0.09	1.68	2.14	
Bolivia	5,101	0.25 (-46%)	0.36 = 0.47 - 0.11	0.41 = 0.50 - 0.09	4.35	5.36	
Brazil	14,452	0.19 (-59%)	0.05 = 0.20 - 0.15	0.15 = 0.27 - 0.12	1.36	2.21	
Chile	17,918	0.1 (-77%)	0.03 = 0.11 - 0.08	0.04 = 0.12 - 0.08	1.35	1.57	

Continued on next page

Table E.5: The Americas, GDP per capita (PPP) in 2010 U.S. dollars, population-weighted air pollution by aerosol (AOD) distributions: mean, excess population-pollution burden (EPB), interquintile and interdecile ranges and ratios (2010).

Economies	GDP/capita	Mean (EPB)	AOD-population distributional statistics				
			Percentile ranges		Percentile ratios		
			Interquintile = 80th - 20th	Interdecile = 90th - 10th	80th to 20th	90th to 10th	
Colombia	10,841	0.34 (-25%)	0.08 = 0.37 - 0.29	0.15 = 0.44 - 0.29	1.29	1.55	
Ecuador	8,969	0.3 (-35%)	0.09 = 0.34 - 0.25	0.09 = 0.34 - 0.25	1.36	1.37	
Falkland Islands		0.11 (-76%)	0.01 = 0.12 - 0.11	0.02 = 0.12 - 0.10	1.08	1.15	
French Guiana		0.25 (-45%)	0.02 = 0.26 - 0.24	0.02 = 0.26 - 0.24	1.08	1.08	
Guyana	9,337	0.26 (-44%)	0.02 = 0.26 - 0.24	0.04 = 0.27 - 0.23	1.11	1.20	
Paraguay	10,893	0.26 (-44%)	0.02 = 0.26 - 0.24	0.08 = 0.30 - 0.22	1.06	1.34	
Peru	9,713	0.23 (-50%)	0.16 = 0.31 - 0.15	0.20 = 0.33 - 0.13	2.04	2.51	
Suriname	13,039	0.28 (-38%)	0.08 = 0.32 - 0.24	0.08 = 0.32 - 0.24	1.36	1.37	
Uruguay	17,873	0.14 (-69%)	0.03 = 0.15 - 0.12	0.05 = 0.15 - 0.10	1.23	1.47	
Venezuela	16,528	0.31 (-31%)	0.12 = 0.38 - 0.26	0.19 = 0.41 - 0.22	1.44	1.84	

Note: Table statistics are computed based on the distribution of AOD and population across cells ($1^\circ \times 1^\circ$ longitude–latitude grid). The interpretation of AOD is that < 0.1 indicates crystal clear sky and AOD of 1 indicates very hazy conditions. For excess population-pollution burden (EPB), a value of +50% (-50%) indicates that a geographical unit's AOD measure is 50 percent greater (smaller) than the global population-weighted mean.

Table E.6: Oceania, GDP per capita (PPP) in 2010 U.S. dollars, population-weighted air pollution by aerosol (AOD) distributions: mean, excess population-pollution burden (EPB), interquintile and interdecile ranges and ratios (2010).

Economies	GDP/capita	Mean (EPB)	AOD-population distributional statistics			
			Percentile ranges		Percentile ratios	
			Interquintile = 80th - 20th	Interdecile = 90th - 10th	80th to 20th	90th to 10th
Panel A: Australia and New Zealand						
Australia	39,373	0.11 (-76%)	0.03 = 0.13 - 0.10	0.04 = 0.13 - 0.09	1.30	1.49
New Zealand	31,214	0.12 (-74%)	0.03 = 0.13 - 0.10	0.04 = 0.13 - 0.09	1.30	1.44
Panel B: Melanesia						
Fiji	7,476	0.14 (-70%)	0.02 = 0.15 - 0.13	0.02 = 0.15 - 0.13	1.15	1.22
New Caledonia		0.14 (-70%)	0.00 = 0.13 - 0.13	0.02 = 0.15 - 0.13	1.00	1.13
Papua New Guinea	2,912	0.22 (-52%)	0.03 = 0.23 - 0.20	0.06 = 0.25 - 0.19	1.17	1.32
Solomon Islands	2,182	0.18 (-61%)	0.01 = 0.18 - 0.17	0.02 = 0.19 - 0.17	1.05	1.15
Vanuatu	2,733	0.21 (-53%)	0.01 = 0.22 - 0.21	0.01 = 0.22 - 0.21	1.02	1.02
Panel C: Micronesia						
Kiribati	1,724	0.14 (-69%)	0.00 = 0.14 - 0.14	0.00 = 0.14 - 0.14	1.00	1.00
Marshall Islands	3,473	0.18 (-60%)	0.01 = 0.19 - 0.18	0.01 = 0.19 - 0.18	1.03	1.05
Micronesia	3,126	0.18 (-61%)	0.01 = 0.18 - 0.17	0.03 = 0.18 - 0.15	1.07	1.20
Northern Mariana Is.		0.15 (-67%)	0.02 = 0.16 - 0.14	0.02 = 0.16 - 0.14	1.13	1.13
Palau	13,449	0.14 (-70%)	0.00 = 0.14 - 0.14	0.00 = 0.14 - 0.14	1.04	1.04
Panel D: Polynesia						
Cook Islands		0.12 (-73%)	0.00 = 0.12 - 0.12	0.00 = 0.12 - 0.12	1.00	1.00
French Polynesia		0.12 (-74%)	0.01 = 0.12 - 0.11	0.01 = 0.12 - 0.11	1.05	1.12
Tonga	4,465	0.13 (-73%)	0.00 = 0.13 - 0.13	0.00 = 0.13 - 0.13	1.00	1.00
Wallis and Futuna Is.		0.13 (-72%)	0.00 = 0.13 - 0.13	0.00 = 0.13 - 0.13	1.00	1.00

Note: Table statistics are computed based on the distribution of AOD and population across cells ($1^\circ \times 1^\circ$ longitude-latitude grid). The interpretation of AOD is that < 0.1 indicates crystal clear sky and AOD of 1 indicates very hazy conditions. For excess population-pollution burden (EPB), a value of +50% (-50%) indicates that a geographical unit's AOD measure is 50 percent greater (smaller) than the global population-weighted mean.